

UNIVERSITÀ DEGLI STUDI  
DI MILANO



UNIVERSITÀ DEGLI STUDI  
DI NAPOLI FEDERICO II



PhD degree in Systems Medicine (curriculum in Human Genetics)

European School of Molecular Medicine (SEMM),

University of Milan and University of Naples “Federico II”

Settore disciplinare: BIO/18

# **The centrosomal OFD1 protein regulates autophagy induction**

*Umberto Formisano*

TIGEM, Pozzuoli

Matricola n. R11143

*Supervisor:* Prof. Brunella Franco  
TIGEM, Pozzuoli

*Internal Supervisor:* Dr. Carmine Settembre  
TIGEM, Pozzuoli

*External Supervisor:* Dr. Alessandra Boletta  
IRCCS Ospedale San Raffaele, Milano

Anno accademico 2017-2018

## Table of Contents

List of abbreviations .....	4
Figures index .....	7
Abstract .....	9
Introduction.....	10
1. Cilia: structure and biomedical relevance .....	10
1.1 Cilia and centrosomes .....	10
1.2 Ciliopathies.....	16
1.3 The oral facial digital type I syndrome .....	20
2. The OFD1 protein.....	22
2.1 Localization and functional studies .....	22
2.2 Animal models.....	25
3. Autophagy .....	29
3.1 The role of autophagy .....	29
3.2 The autophagic machinery .....	31
3.3 The regulation of autophagy .....	34
3.4 Selective autophagy .....	37
3.5 Primary cilia control autophagy.....	39
3.6 Does Autophagy influences ciliogenesis?.....	41
3.7 Autophagy and the centrosome.....	42
3.8 The impact of autophagy in kidney function.....	44
Results .....	46
1. OFD1 is required for autophagy inhibition.....	46

2. OFD1 regulates autophagy in a cilia independent manner.....	50
3. The role of OFD1 in autophagy is mTOR independent .....	51
4. OFD1 interacts with the ULK1 complex and controls its stability .....	53
5. Analysis of ULK1 and ATG13 ubiquitination in KO-OFD1 cells .....	58
6. ULK1 and ATG13 are degraded through different mechanisms .....	61
7. Is OFD1 a novel selective autophagy receptor? .....	63
8. Loss of <i>Ofd1</i> enhances autophagy <i>in vivo</i> .....	66
9. Inhibition of autophagy reduces renal cysts formation in <i>Ofd1</i> mutant mice ..	68
Discussion .....	71
Materials & Methods .....	78
Cell culture, treatments and transfection.....	78
Plasmids and siRNAs .....	78
Western blot and co-immunoprecipitation .....	79
Antibodies .....	80
Ubiquitination assays.....	81
GST pull-down assay .....	81
Histological and immunofluorescence analysis.....	82
Real-time PCR and Primers .....	82
Animal models.....	83
Contributions .....	84
References .....	85

## List of abbreviations

<b>AMPK</b>	AMP-activated protein kinase
<b>AQP11</b>	Aquaporin-11
<b>Atg</b>	Autophagy related gene
<b>ADPKD</b>	Autosomal dominant polycystic kidney disease
<b>ARPKD</b>	Autosomal recessive polycystic kidney disease
<b>Baf</b>	Bafilomycin
<b>BNIP3L</b>	BCL2 Interacting Protein 3 Like
<b>BECN1</b>	Beclin1
<b>CEP63</b>	Centrosomal protein of 63 kDa
<b>Cq</b>	Chloroquine
<b>Co-IP</b>	Co-immunoprecipitation
<b>cAMP</b>	Cyclic adenosine monophosphate
<b>CHX</b>	Cycloheximide
<b>Cul3</b>	E3 ligase Cullin-3
<b>E</b>	Embryonic day
<b>ER</b>	Endoplasmic reticulum
<b>eIF</b>	Eukaryotic Initiation Factor
<b>FBS</b>	Fetal bovine serum
<b>FIP200</b>	Focal adhesion kinase family interacting protein of 200 kDa
<b>GABARAP</b>	Gamma-aminobutyric acid receptor-associated protein
<b>GST</b>	Glutathione S-transferase
<b>HBSS</b>	Hanks' Balanced Salt Solution
<b>Hh</b>	Hedgehog
<b>HK2</b>	Human Kidney 2
<b>IP</b>	Immunoprecipitation

<b>IFT</b>	Intra-flagellar transport
<b>KLHL20</b>	Kelch-like family member 20
<b>KO</b>	Knock Out
<b>LC3</b>	Microtubule-associated protein light chain 3
<b>LIR</b>	LC3-Interacting Region
<b>LisH</b>	LIS1 homology domain
<b>mTOR</b>	Mammalian target of rapamycin
<b>MTOC</b>	Microtubule-organizing center
<b>MEF</b>	Mouse embryonic fibroblast
<b>mTORC1</b>	mTOR complex 1
<b>mTORC2</b>	mTOR complex 2
<b>NBR1</b>	Neighbour of BRCA1 gene 1
<b>NEDD4L</b>	Neural precursor cell-expressed developmentally down-regulated 4-like
<b>OFD</b>	Oral facial digital
<b>OFD1</b>	Oral facial digital 1 protein
<b>OFDI</b>	Oral facial digital type I syndrome
<b>PCM</b>	Pericentriolar material
<b>PCM1</b>	Pericentriolar material 1 protein
<b>PE</b>	Phosphatidylethanolamine
<b>PI3K</b>	Phosphatidylinositol 3-kinase
<b>PI3P</b>	Phosphatidylinositol-3-phosphate
<b>PCP</b>	Planar-cell-polarity
<b>PDGF</b>	Platelet-derived growth factor
<b>PKD</b>	Polycystic kidney disease
<b>PC1</b>	Polycystin 1

<b>PC2</b>	Polycystin 2
<b>P</b>	Post-natal day
<b>PCD</b>	Primary ciliary dyskinesia
<b>RAPTOR</b>	Regulatory-associated protein of mTOR
<b>RPE</b>	Retinal pigmented epithelium
<b>RPGRIP1L</b>	RPGRIP1-like
<b>SAOS</b>	Sarcoma osteogenic cells
<b>Shh</b>	Sonic Hedgehog
<b>SEM</b>	Standard error mean
<b>NDP52</b>	The nuclear dot protein 52 kDa
<b>TRAF6</b>	TNF receptor associated factor 6
<b>UBL</b>	Ubiquitin-like
<b>ULK1</b>	Unc-51-like kinase 1
<b>UVRAG</b>	UV irradiation resistance-associated gene
<b>VPS34</b>	Vacuolar protein sorting 34
<b>WB</b>	Western blot
<b>WT</b>	Wild type
<b>Wnt</b>	Wingless/Integrated

## Figures index

Figure 1. Ciliary structure.....	12
Figure 2. Ciliary signaling.....	14
Figure 3. Centrosomes structure.....	15
Figure 4. Organs affected in human ciliopathies. ....	18
Figure 5. Clinical signs of OFDI syndrome.....	21
Figure 6. Subcellular localization of the endogenous OFD1 protein. ....	24
Figure 7. Characterization of <i>Ofd1<sup>fl</sup>;Cre<sup>Ksp</sup></i> mutant animals. ....	28
Figure 8. The autophagic machinery.....	34
Figure 9. Regulation of the ULK1 complex.....	37
Figure 10. Autophagy-related proteins associate with ciliary structures. ....	40
Figure 11. OFD1 interacts with LC3 and is degraded through autophagy. ....	43
Figure 12. Loss of OFD1 enhances LC3-II protein levels.....	47
Figure 13. Loss of OFD1 promotes p62 degradation. ....	48
Figure 14. OFD1 over-expression inhibits autophagy. ....	49
Figure 15. Increased autophagy in lymphoblasts from OFDI patients. ....	50
Figure 16. OFD1 regulates autophagy in a cilia independent manner. ....	51
Figure 17. The role of OFD1 in autophagy is mTOR independent.....	52
Figure 18. OFD1 interacts with components of the ULK1 complex. ....	53
Figure 19. Loss of OFD1 enhances the ULK1 kinase activity.....	54
Figure 20. OFD1 does not influence ULK1 complex formation.....	55
Figure 21. Impaired degradation of ULK1 and ATG13 in KO-OFD1 cells.....	56
Figure 22. FIP200, ULK1 and ATG13 transcripts are not regulated by OFD1. ....	56
Figure 23. OFD1 promotes ULK1 and ATG13 degradation.....	57
Figure 24. Analysis of ULK1 and ATG13 ubiquitination levels.....	59
Figure 25. OFD1 interacts with KLHL20.....	60
Figure 26. ULK1 is mainly degraded by proteasome.....	61

Figure 27. ATG13 degradation is impaired in autophagy-deficient cells. ....	62
Figure 28. Autophagy inhibition upregulates ATG13 and OFD1. ....	63
Figure 29. OFD1 protein contains putative LIR motifs. ....	64
Figure 30. OFD1 interacts with LC3. ....	65
Figure 31. OFD1 binds LC3 through the N-terminal and C-terminal regions of the protein. ....	66
Figure 32. Kidneys from <i>Ofd1</i> -IND mice showed increased autophagy. ....	67
Figure 33. Kidneys from <i>Cre<sup>Ksp</sup>;Ofd1</i> mice showed increased autophagy. ....	67
Figure 34. ATG13 is increased in <i>Cre<sup>Ksp</sup>;Ofd1</i> mice. ....	68
Figure 35. Inhibition of autophagy reduces renal cysts formation in <i>Ofd1</i> mutant mice. ....	69
Figure 36. Chloroquine reduces cysts number in kidneys from <i>Ofd1</i> mutant mice. ....	70



## Abstract

The OFD1 protein is codified by the gene mutated in Oral facial digital syndrome type I, a rare developmental disorder ascribed to the growing number of diseases associated to cilia dysfunction. OFD1 encodes for a centrosomal/basal body protein required for formation of primary cilia, sensory organelles present on the cell surface of almost all mammalian cells. A cross talk between autophagy and primary cilia has recently emerged. By using a variety of *in vivo* and *in vitro* approaches, I demonstrated that, contrary to what shown for other cilioproteins, OFD1 depletion results in autophagy enhancement and increased autophagosomes biogenesis. In addition, the results obtained indicate that OFD1 acts by regulating the stability of the ULK1 complex which plays a critical role in autophagy initiation. Loss of OFD1 impairs degradation of ULK1 complex components (e.g. ULK1 and ATG13) thus promoting ULK1 kinase activity and enhancing autophagosome biogenesis. The identification of LC3 interacting regions (LIR) in the OFD1 protein sequence suggest that OFD1 may function as a selective autophagy receptor for ATG13 by mediating ATG13 degradation through LC3 interaction.

One of the main features of ciliopathies, including OFD type I syndrome, is the presence of renal cystic disease. Conditional renal inactivation of *Atg7*, an essential gene for autophagy, caused a significant reduction in the number of cysts in mutant kidneys of an *Ofd1* mouse model. In line with these observations, treatment with chloroquine, an autophagy inhibitor already used in clinical practice, showed a beneficial effect on the renal cystic phenotype observed in a murine *Ofd1* model, suggesting that increased autophagy might be associated to renal cystogenesis.

The modulation of autophagy, alone or combined with other treatments, could represent a therapeutic approach in renal cystic disease.

## **Introduction**

### **1. Cilia: structure and biomedical relevance**

#### **1.1 Cilia and centrosomes**

Over the past decades, cilia emerged as crucial organelles of growing biomedical importance for many tissues. Cilia protrude as filiform organelles from the plasma membrane of most vertebrate cell types (Satir and Christensen 2007). These evolutionarily-conserved organelles can be classified into two main functional groups: motile and non-motile cilia (also called primary cilia). Motile cilia are usually present on a cell's surface in large numbers and beat in coordinated waves to regulate fluid transport or cell motility. Motile cilia are present, for example, on the respiratory epithelium, along the female reproductive tract and on ependymal cells lining the ventricles of the brain (Stannard and O'Callaghan 2006). Conversely, primary cilia usually localize one per cell and are predominantly sensory organelles functioning as cells' antenna. Primary cilia are widespread in the organism, they are found on epithelial cells such as kidney tubules, bile ducts, endocrine pancreas, thyroid but also on non-epithelial cells such as chondrocytes, fibroblasts, smooth muscle cells, neurons, and Schwann cells (Singla and Reiter 2006).

Cilia consist of a microtubule-based cytoskeleton, the axoneme, composed of nine peripheral microtubule doublets arranged around a central core that may or may not contain a pair of singlet microtubules (9+2 or 9+0 pattern) (Fig. 1) (Satir and Christensen 2007). Motile cilia display the central pair of microtubules (9+2) and a complex motor machinery composed of dynein arms and radial spokes which permits the mechanical movement of the cilium (Fig. 1) (Roy 2009). Nodal cilia, localized at the embryonic node, are the unique motile cilia which lack the central microtubules doublet. Primary cilia also lack the central microtubule doublet (9+0) and the accessory motor machinery, in fact they do not actively move (Fig. 1) (Satir, Pedersen et al. 2010). Microtubules of ciliary axoneme undergo several types of

post-translational modifications, mainly acetylation and polyglutamylation of tubulin to increase their stability (Janke and Kneussel 2010).

The ciliary axoneme is covered by a specialized membrane, the ciliary membrane, which is continuous with the cell membrane but exhibits a distinct lipid and protein composition (Rohatgi and Snell 2010). This is made possible by the presence of a selective barrier at the base of the cilium: the transition zone, which controls the trafficking of essential ciliary components and signalling molecules in the cilium (Fig. 1). The transition zone is characterized by Y-shaped links between the ciliary membrane and the doublet microtubules of the axoneme (Fig. 1) (Czarnecki and Shah 2012). At the distal end of the cilium there is the ciliary tip, another specialized subdomain of the cilium. This subdomain can be dynamically remodelled: for example, proteins involved in signal transduction, such as mediators of Hedgehog (Hh) signaling, increase their localization to the ciliary tip in response to pathway activation (Chen, Yue et al. 2011).

Cilia assembly and maintenance requires a dedicated protein shuttle, the intra-flagellar transport (IFT) machinery, composed of two multiprotein complexes IFT-A and IFT-B, responsible, respectively, for anterograde and retrograde transport of cargoes along the axoneme (Fig. 1). The IFT particles and their associated cargo proteins are transported along axonemal microtubules by kinesin 2 motor proteins in the anterograde direction, and by cytoplasmic dynein 2 in the retrograde direction (Lechtreck 2015). Cilia are highly dynamic organelles, they are assembled and disassembled each time the cell divides. IFT mediates both assembly and resorption of the cilium, and processing of signaling molecules. Perturbation of ciliary trafficking by disruption of the IFT transport results in short or absent cilia (Lechtreck 2015).

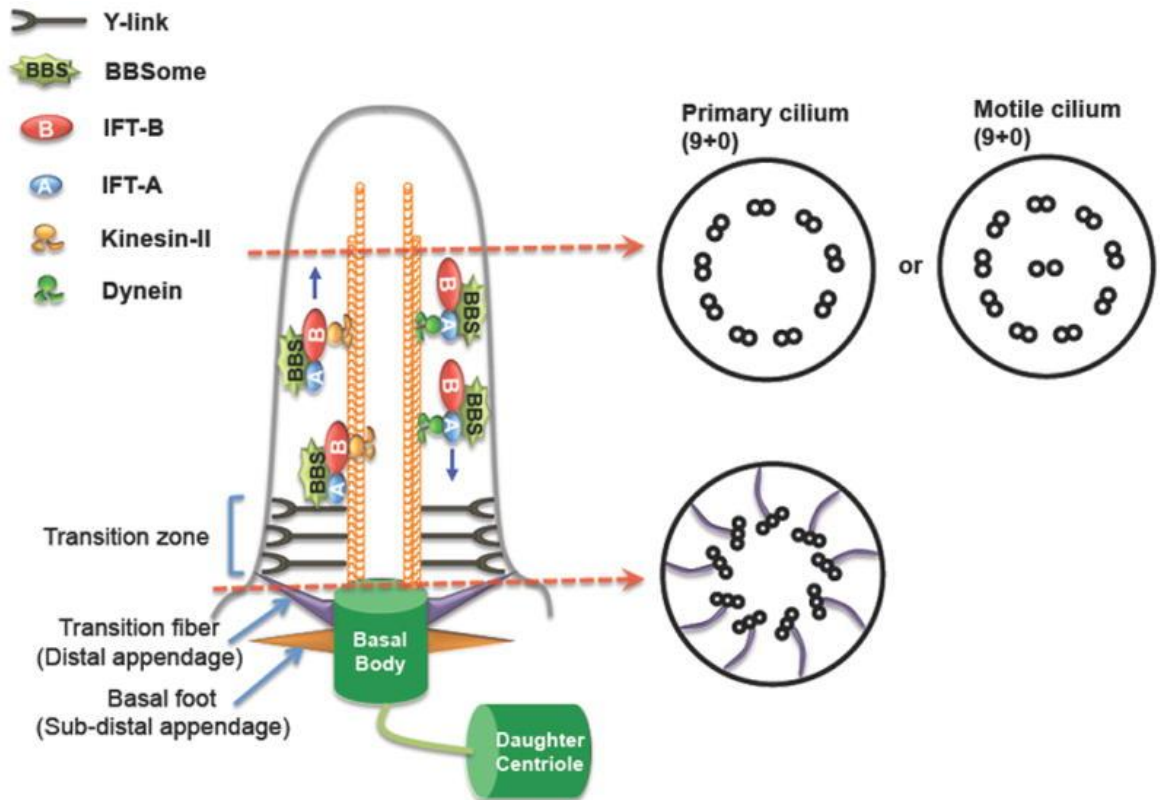


**Figure 1. Ciliary structure.**

The cilium is a membrane-bound organelle and contains nine outer doublet microtubules running along its axoneme. The two central singlet microtubules are present only in motile cilia. At its point of attachment to the cell, the axoneme connects with the basal body. The basal body is attached to the ciliary membrane through transition fibers. Above transition fibers, the transition zone is characterized by Y-shaped links connecting the axoneme to the ciliary membrane (Wei, Ling et al. 2015).

At the base of the axoneme, under the cell surface, is located the basal body, a structure derived from the mother centriole of the centrosome. The basal body contains a ring of nine microtubule triplets which represent the nucleation site for cilia growth (Fig. 1). The microtubule triplets protrude from the basal body to the transition zone and then they extend as doublets to form the ciliary axoneme. In quiescent cells, the mother centriole migrates to the apical surface of the cell and matures into the basal body, then it is tethered to the base of ciliary membrane by the distal appendages, also known as transition fibers (Fig. 1) (Kim and Dynlacht 2013). Once the basal body is docked, the axoneme begins to be assembled, incorporating tubulin at the distal end. Cilia typically form during G1 or G0 phases and disassemble during cell division. This cycle does not occur in multi-ciliated cells, which are terminally differentiated and do not undergo division. Typically, the length

of cilia and the percent of ciliated cells in a population of cells are increased in quiescent rather than cycling cells. In fact, serum starvation is a method widely used to promote cilia formation. Other stimuli which influence ciliogenesis are cell confluence, fluid flow and cell spreading (Plotnikova, Pugacheva et al. 2009, Pitaval, Tseng et al. 2010, Orhon, Dupont et al. 2016). Likewise, cilia are able to influence cell cycle progression, as it has been observed that loss of cilia is commonly associated with increased cell proliferation and loss of cell polarity, two features related to tumorigenesis (Izawa, Goto et al. 2015).

As stated above, primary cilia act as cell's antenna with a sensory role. A variety of receptors, ion channels and transporter proteins localize to cilia and allow the cell to sense and to respond to various external stimuli (Fig. 2) (Satir, Pedersen et al. 2010). Primary cilia are able to sense chemical signals, mechanical stress (Nauli, Alenghat et al. 2003), light and temperature (Prodromou, Thompson et al. 2012, Yildiz and Khanna 2012), depending on the cell type. Primary cilia transduce these signals to multiple cellular processes, such as proliferation, differentiation, migration, etc. (Fig. 2) (Clement, Kristensen et al. 2009, Plotnikova, Pugacheva et al. 2009, Christensen, Veland et al. 2013). Signaling pathways associated to primary cilia include the Sonic-Hedgehog (Shh) pathway (Goetz and Anderson 2010), the Wntless/Integrated (Wnt) pathway (Jackson 2018), the Platelet-derived growth factor (PDGF) signaling (Goetz and Anderson 2010), the Planar-cell-polarity (PCP) signaling (Jones and Chen 2008), the calcium signaling (Lee, Guevarra et al. 2015), the cyclic adenosine monophosphate (cAMP) signaling (Ye, Wang et al. 2017) and the mammalian target of rapamycin (mTOR) signaling (Boehlke, Kotsis et al. 2010) (Fig. 2).

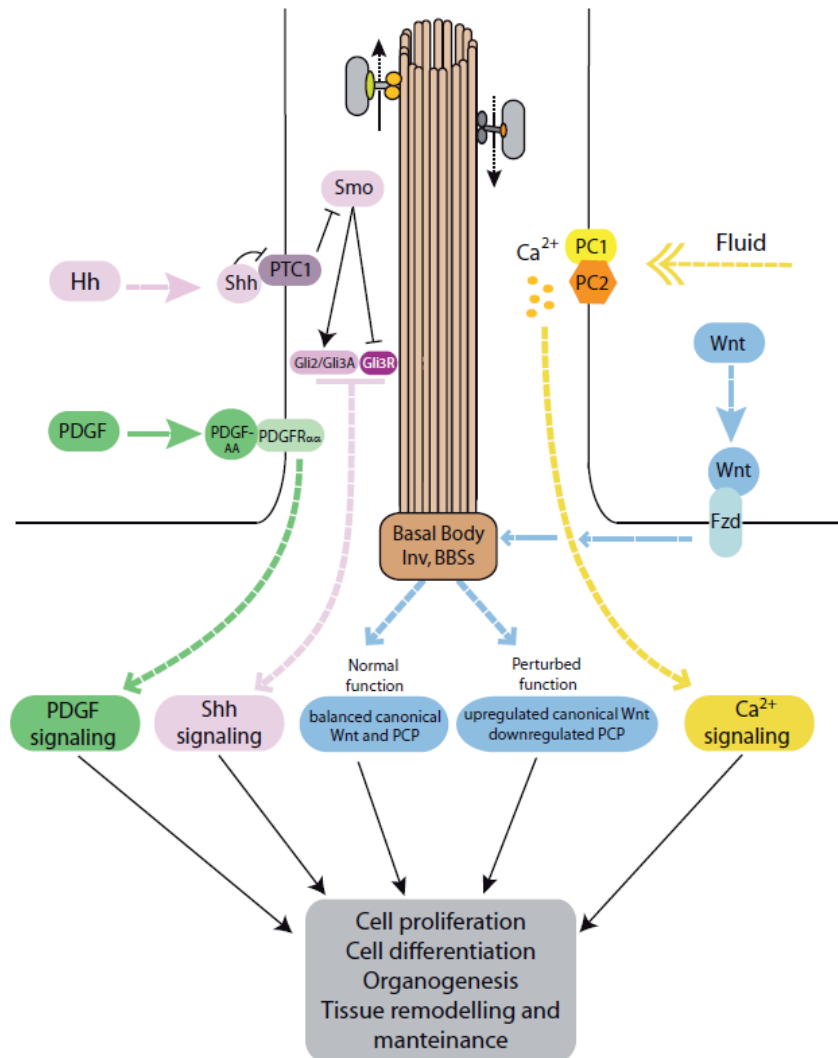


**Figure 2. Ciliary signaling.**

The primary cilium acts as an antenna for the cell and several important pathways are transduced through it. The cilium is an essential organelle regulating key developmental pathways such as Sonic Hedgehog (Shh) and Wnt (planar cell polarity (PCP) pathways). Cilia participate also to the regulation of intracellular Ca<sup>2+</sup> level, through its mechano-sensation capacity (Irigoien and Badano 2011).

As stated above the basal body derives from the mother centriole which is the older centriole present in the centrosome. The centrosome is a complex organelle that functions as the major microtubule-organizing center (MTOC) in animal cells. It is composed of mother and daughter centrioles arranged in orthogonal configuration, surrounded by an electron-dense area called pericentriolar material (PCM) (Fig. 3). Centrioles are cylindrical structures composed of nine microtubule triplets symmetrically arranged around a central core (Fig. 3) (Nigg and Stearns 2011).

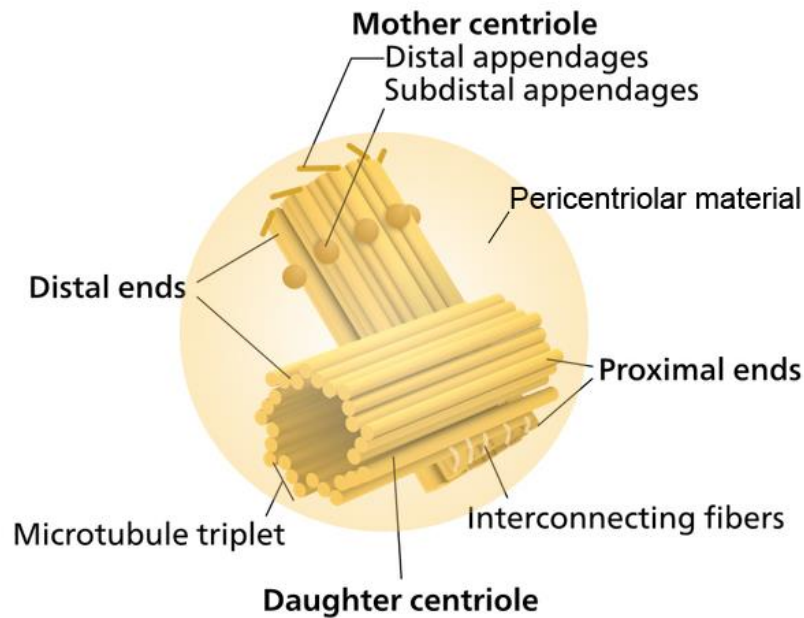


**Figure 3. Centrosomes structure.**

Centrosomes are composed of two perpendicular centrioles, mother and daughter, linked together by interconnecting fibres. Centrioles are surrounded by an amorphous pericentriolar matrix which contain also the centriolar satellites. Contrary to the daughter centriole, the mother centriole possesses the distal and subdistal appendages necessary for cilia assembly. Modified from (Wikipedia 2018).

The PCM is a scaffold for anchoring of numerous proteins required for microtubule nucleation, primary cilia formation and other cellular processes (Lopes, Prosser et al. 2011). In addition to these structures, some electron-dense spherical granules have been identified around the centrosome. These granules have been termed centriolar satellites and are marked by the pericentriolar material 1 protein (PCM1). The centriolar satellites function as shuttles that transport components from the cytoplasm to the centrosome and vice versa (Lopes, Prosser et al. 2011).

During the cell division cycle, a new centriole grows at the proximal end of both centrioles, then each pair segregate in new formed cells (Plotnikova, Pugacheva et al. 2009). Each daughter cell inherits two centrioles: one centriole derives from the mother cell and the other is replicated from the mother centriole during the cell cycle. Centrosome duplication is strictly regulated by cell cycle control, the dysregulation of centrosome number is implicated in chromosomal instability and carcinogenesis (Nigg and Stearns 2011).

Centrosomes function as centres for integration of different signalling pathways which regulate cell cycle progression, cell polarity, migration and mitosis (Arquint, Gabryjonczyk et al. 2014). The PCM contains many proteins with coiled-coil domains which represent a scaffold for different signaling proteins (Arquint, Gabryjonczyk et al. 2014). Many kinases and phosphatases, such as the cAMP-dependent kinases and DNA damage response proteins, have been associated with centrosomes (Mayor, Meraldi et al. 1999). Recent observations suggest that centrosomes are sites for accumulation of proteasome substrates. The proteasome is present in a functional and activated form at the centrosome and is responsible for degradation of several centrosome-associated proteins (Vora and Phillips 2016). The number of centrioles is tightly regulated by the amounts of centrosomal proteins mainly through the ubiquitin proteasome degradation system (Wojcik, Glover et al. 2000).

## **1.2 Ciliopathies**

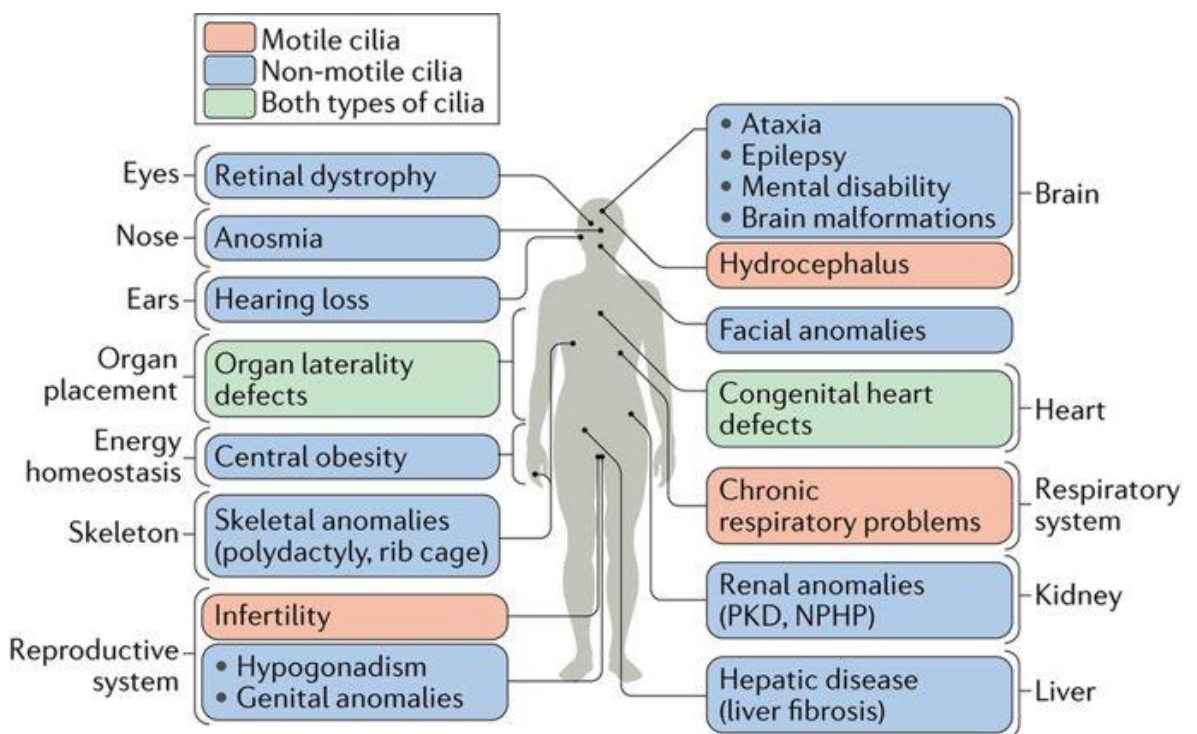
Cilia dysfunction is associated to numerous human genetic disorders known as ciliopathies. Genes mutated in ciliopathies codify for proteins located at cilia or basal bodies (Waters and Beales 2011). However, also proteins that do not specifically localize to cilia may influence ciliary functions and cause ciliopathies. For example, the X-prolyl aminopeptidase 3 (XPNPEP3) protein localizes to mitochondria, but mutations in its gene are associated with nephronophthisis-like phenotype (O'Toole, Liu et al. 2010). In addition, *in vivo* analyses revealed a likely cilia-related function; suppression of zebrafish *xpnpep3* phenocopied the developmental phenotypes of ciliopathy morphants and, consistent with a role for XPNPEP3 in ciliary function, several ciliary cystogenic proteins were found to be XPNPEP3 substrates (O'Toole, Liu et al. 2010). Ciliopathies can be caused by impaired cilium formation, maintenance, or function, abrogation of ciliary signaling molecules, or trafficking



defects from and to the cilia. Compromised cilium formation or function often result in ciliopathies characterized by developmental abnormalities including skeletal anomalies, abnormalities of the central nervous system, organ laterality defects, retinal dystrophies and so on (Fig. 4) (Cardenas-Rodriguez and Badano 2009). Due to the role of cilia in signal transduction, ciliary signaling is essential for normal development; for example deregulation of ciliary Hedgehog signalling due to cilia abnormalities or disruption of the IFT machinery is associated with skeletal abnormalities (e.g. polydactyly) and neural tube defects (Murdoch and Copp 2010, Noda, Kitami et al. 2016). However, the relationship between ciliary genes and phenotypes is complex. Many clinical features of ciliopathies still do not have a precise molecular cause and could be multifactorial. In some cases, mutations in the same gene can result in different ciliopathies with no, or limited, phenotypic overlap and this can be explained by the presence of protein isoforms with different function or expression (Reiter and Leroux 2017).

We can distinguish between ciliopathies caused by dysfunction of motile cilia (motile ciliopathies) and non-motile cilia (sensory ciliopathies) (Fig. 4). Primary ciliary dyskinesia (PCD) is the most classical example of motile ciliopathy and is characterized by respiratory problems, infertility and situs inversus (left–right patterning anomaly) (Praveen, Davis et al. 2015). Defects in primary cilia lead to different physiological and developmental anomalies which include rare conditions such as: Bardet-Biedl (Hernandez-Hernandez, Pravincumar et al. 2013), Joubert (Doherty 2009), Meckel-Gruber (Barker, Thomas et al. 2014) and Oral-facial-digital type I syndrome (Ferrante, Zullo et al. 2006), Retinitis pigmentosa (Di Gioia, Letteboer et al. 2012), Nephronophthisis (Hildebrandt, Attanasio et al. 2009), and more common disorders such as the autosomal dominant and recessive forms of Polycystic kidney disease (ADPKD and ARPKD, respectively) (Ward, Yuan et al. 2003, Lee and Somlo 2014). In particular, Polycystic kidney disease is the

commonest monogenic kidney disease, with a prevalence of 1/500 to 1/1000 and the commonest hereditary cause of end stage renal failure (Ong and Sandford 2016). Ciliopathies share some clinical manifestations, such as cystic disease of kidneys, ovary and liver, retinal degeneration, obesity, defects of the central nervous system, abnormal bone growth, laterality defects and skeletal abnormalities (Fig. 4) (Waters and Beales 2011). The symptoms display different degrees of clinical severity, as the disease is more severe when the cilia architecture is compromised. Additionally, genetic modifiers can influence the clinical manifestation of ciliopathies, partially explaining their pleiotropy (Waters and Beales 2011). The number of reported ciliopathies is rapidly increasing, as well as the number of candidate ciliopathy-associated genes.



Nature Reviews | Molecular Cell Biology

**Figure 4. Organs affected in human ciliopathies.**

Ciliopathies are different human diseases resulting from cilia dysfunction. Most ciliopathies have overlapping clinical features in multiple organs. Sensory ciliopathies show more mixed features in several vital organs, including the brain, kidney, liver, the eye and digits (Reiter and Leroux 2017).

Among the many clinical features of sensory ciliopathies, a major hallmark is renal cystic disease (Avasthi, Maser et al. 2017). Ciliary dysfunction may represent a common etiological event for renal cystogenesis, however it is not entirely clear how aberrant and/or malfunctioning cilia promotes the disease. Many cellular processes such as: cell dedifferentiation, increased cell proliferation, loss of cell polarity, increased fluid secretion, high intracellular cAMP levels and low intracellular calcium are deregulated in renal cystogenesis, (Winyard and Jenkins 2011). ADPKD is the commonest monogenic kidney disease, with a prevalence of 1/500 to 1/1000 and the commonest hereditary cause of end stage renal failure (Ong and Sandford 2016). It is caused by mutations in PKD1 and PKD2, which codify respectively for polycystin-1 (PC1) and polycystin-2 (PC2), two transmembrane proteins, which form a receptor-channel complex at primary cilia (Lee and Somlo 2014). Cysts appear like fluid-filled spherical structure lined by a single layer of tubular cells. They can originate from every segment of the nephron, although are usually more commonly observed in collecting ducts, then close off from the nephron and become separated (Verani and Silva 1988). Renal cysts then continue to enlarge by increased cell proliferation, fluid secretion and changes of the extracellular matrix. Cysts progressively grow leading to a massive enlargement of kidneys and replacement of the normal parenchyma ultimately leading to end stage renal failure which eventually requires dialysis and/or renal transplantation (Harris and Torres 2009). Our understanding of PKD basic disease mechanisms have led to the identification of novel or re-purposed drugs that target key signaling pathways involved in renal cysts growth. So far, PKD clinical trials performed with rapamycin analogues, which are inhibitors of the mTOR pathway, gave disappointing results and other clinical trial are ongoing.

### 1.3 The oral facial digital type I syndrome

The oral facial digital type I (OFDI) syndrome is an X-linked dominant disorder which belongs to the heterogeneous group of developmental disorders known as Oral facial digital (OFD) syndromes which affect the mouth, the face and the digits. Most forms are associated with brain abnormalities and intellectual disability, while the other clinical features help distinguish the different types of the disorder (Franco and Thauvin-Robinet 2016, Bruel, Franco et al. 2017). OFD type I, the most common type, occurs between in 1:50000 and 1:250.000 live births, and is transmitted as an X-linked dominant trait with male lethality (Macca and Franco 2009). Almost all individuals with OFDI are female, however exceptional cases of affected males have been described (Thauvin-Robinet, Thomas et al. 2013, Wentzensen, Johnston et al. 2016). The majority of cases (~75 %) represent sporadic, *de novo* mutations although pedigrees with the typical X-linked dominant inheritance can be observed thus clarifying the diagnosis of the disease. Female patients present anomalies of the face, oral cavity, and digits with high phenotypic variability even within the same family (Fig. 5) (Prattichizzo, Macca et al. 2008). Dysmorphic features affecting the head and face include facial asymmetry, hypertelorism, micrognathia, broadened nasal ridge, hypoplasia of the malar bone and of the nasal cartilage, and frontal bossing (Fig. 5). The digital abnormalities, which affect prevalently the hands, include syndactyly, brachydactyly, clinodactyly, unilateral duplication of the hallux and more rarely, polydactyly (Fig. 5) (Ferrante, Feather et al. 2001, Thauvin-Robinet, Cossée et al. 2006, Bisschoff, Zeschnigk et al. 2013). Central nervous system malformations also are relatively common (~65%) and comprise a variable spectrum of defects, including agenesis of the corpus callosum, intracerebral single or multiple epithelial or arachnoid cysts and porencephaly, heterotopia of grey matter, cerebellar malformations, abnormal gyrations, and microcephaly. Half of

individuals with OFD type I have some degree of intellectual deficit or learning disability (Del Giudice, Macca et al. 2014).

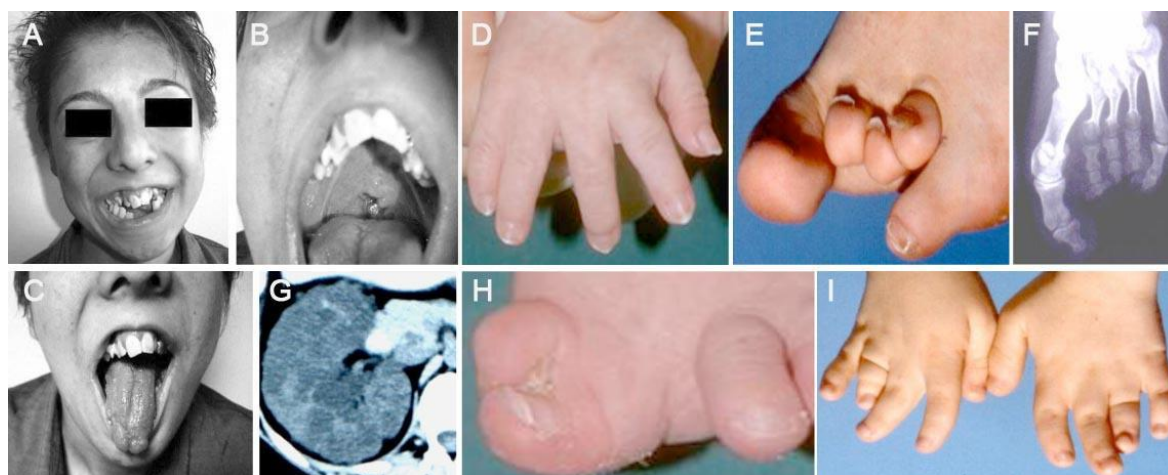


**Figure 5. Clinical signs of OFDI syndrome.**

**(A)** Peculiar face of an OFD type I patient and tooth abnormalities, **(B)** cleft palate, **(C)** tongue abnormalities (lobulated tongue), **(D)** clinodactyly, **(E and F)** Brachydactyly of the feet, **(G)** Cystic kidney, **(H)** Hallux duplication, **(I)** Brachydactyly and syndactyly observed in upper limbs. Modified from (Toprak, Uzum et al. 2006, Macca and Franco 2009)

These clinical features overlap with those reported in the other forms of OFD syndromes, however OFDI can be easily distinguished for the presence of the renal cystic disease and in familiar cases for the typical pattern of inheritance (Fig. 5) (Feather, Winyard et al. 1997). The renal impairment can be present at birth or develops later on, with reports of patients in which the renal involvement completely dominates the clinical course of the disease (Feather, Woolf et al. 1997). The overall incidence of renal cystic disease in this condition is around 40%, however, it is more frequently observed (60%) in cases >18 years (Prattichizzo, Macca et al. 2008). Histochemical analysis showed that most of the cysts have a glomerular origin, and only a small percentage are derived from renal tubules (Feather, Winyard et al. 1997). Moreover, pancreatic, ovarian and liver cysts have also been described in OFDI patients (Kennedy, Hashida et al. 1991).

OFDI syndrome is caused by mutations in the *OFD1* gene, which was identified through a positional candidate gene approach in 2001 (Ferrante, Feather et al. 2001). *OFD1* has 23 exons and is located on a region of the X chromosome where

transcripts frequently escape X-chromosome inactivation. Skewed X-inactivation may play a role in the extensive clinical variability observed in the disease (Morleo and Franco 2008). To date, more than 120 different mutations have been identified, the majority (58%) are small insertions or deletions resulting in frameshifts, with missense and nonsense mutations accounting for only 23% of cases. Interestingly, most mutations are in the first part of the gene (exons 3, 8, 9, 13), no mutations were identified beyond exon 17. This highlights the functional importance of the N-terminal region of the protein, which is also the most conserved part of the protein among homolog vertebrates (Thauvin-Robinet, Cossée et al. 2006, Prattichizzo, Macca et al. 2008). Mutations in the OFD1 transcript have been reported also in Joubert syndrome, Simpson–Golabi–Behmel syndrome type 2 and Retinitis Pigmentosa (Budny, Chen et al. 2006, Webb, Parfitt et al. 2012, Wentzensen, Johnston et al. 2016) thus highlighting the complexity of ciliopathies and of cilioproteins function and regulation.

The OFD1 transcript is expressed in all tissues affected by the disorder from early stages of development to adulthood. In particular, it is highly expressed during human organogenesis in the metanephros, gonads, brain, tongue, and limbs, and at lower levels in pancreas, kidneys, skeletal muscle, liver, lung, placenta, brain, and heart and maintain an abundant and almost ubiquitous expression in adult tissues (de Conciliis, Marchitello et al. 1998, Ferrante, Feather et al. 2001).

## **2. The OFD1 protein**

### **2.1 Localization and functional studies**

*OFD1* encodes for a 1012 amino acids protein, named OFD1 displaying five predicted coiled-coil motifs and a LIS1 homology domain (LisH) (de Conciliis, Marchitello et al. 1998). A coiled coil domain is a structural motif in which 2 or more alpha-helices are coiled together, this is a highly versatile folding motif

necessary for oligomerization or scaffold large macromolecular complexes (Truebestein and Leonard 2016). The LisH domain is located in N-terminal region of OFD1, its disruption leads to a reduced protein half-life (Gerlitz, Darhin et al. 2005). Interestingly, many missense mutations fall within the LisH domain (Macca and Franco 2009). The function of the LisH domain has not been completely clarified although it has been reported to be involved in microtubules dynamics, chromosome segregation and cell migration (Emes and Ponting 2001).

OFD1 is a centrosomal/basal body protein, it is associated with the distal ends of the centrioles and the pericentriolar material, as different studies have demonstrated that colocalizes with  $\gamma$ -Tubulin and PCM1 (Fig. 6) (Romio, Fry et al. 2004, Giorgio, Alfieri et al. 2007). The centrosomal localization is dependent on the coiled coil domains of OFD1, which are frequently missing in OFD1 patients. Previous studies have demonstrated that the LisH domain is not required for centrosomal localization of the protein (Romio, Fry et al. 2004). In post-mitotic ciliated cells OFD1 localizes at the basal body of primary cilia (Fig. 6) (Romio, Fry et al. 2004). Moreover, cell biology studies demonstrated that OFD1 is necessary for distal appendages' formation and centrosomal recruitment of IFT88, two processes essential for cilia formation. Indeed, mutations of the OFD1 protein result in centriole length defects and impaired ciliogenesis (Singla, Romaguera-Ros et al. 2010). In particular, mutations in the LisH domain blocks ciliogenesis, whereas carboxy-terminal mutations cause decreased ciliogenesis (Singla, Romaguera-Ros et al. 2010).

OFD1 localizes not only to centrosomes and basal bodies, but also to centriolar satellites. Immunofluorescence analysis demonstrated that OFD1 colocalizes with a key centriolar satellite component, PCM1. Moreover, biochemical analysis demonstrated that PCM1 binds to OFD1, and that the coiled coil domains of OFD1 are crucial for this interaction (Lopes, Prosser et al. 2011). The pool of OFD1 localized at centriolar satellites (Fig. 6) has an opposite role on ciliogenesis as it has

been demonstrated that the selective degradation of OFD1 in this specific location promotes primary cilia formation (Tang, Lin et al. 2013). Thus, while the pool of OFD1 at centrosomes is essential for ciliogenesis, that associated with centriolar satellites inhibits this process.

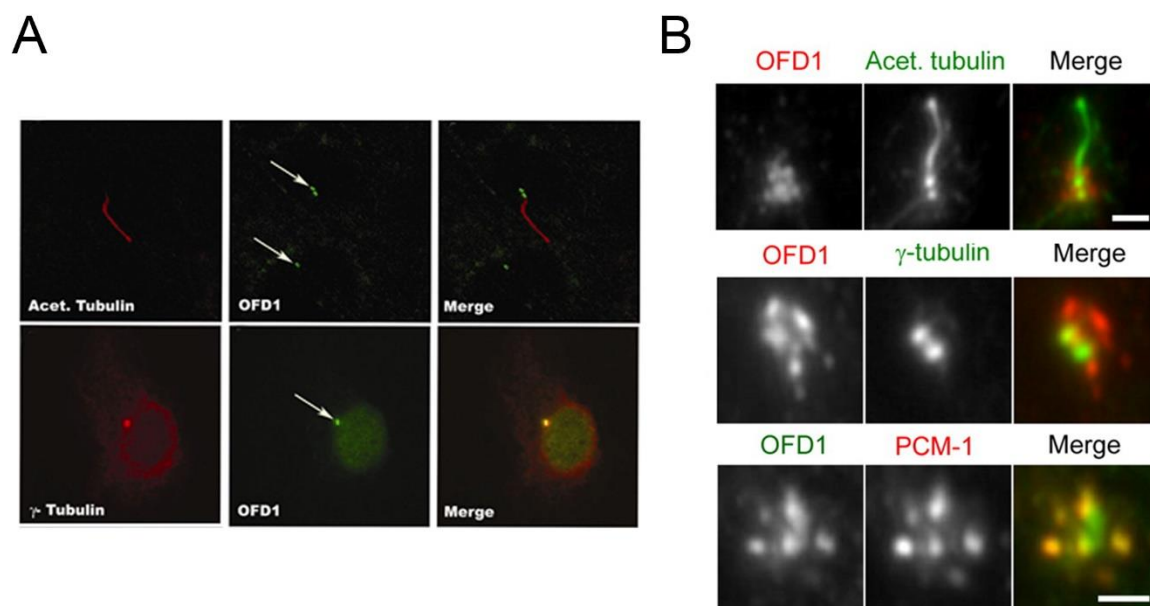


**Figure 6. Subcellular localization of the endogenous OFD1 protein.**

**(A)** Staining with OFD1 and Acetylated tubulin to detect cilia and  $\gamma$ -Tubulin to detect centrosomes, respectively. Modified from (Giorgio, Alfieri et al. 2007). **(B)** Staining with OFD1 and Acetylated tubulin to detect cilia,  $\gamma$ -Tubulin to detect centrosomes and PCM1 to detect pericentriolar material. Modified from (Lopes, Prosser et al. 2011).

OFD1 and Polycystins form a protein complex with EGFR and flotillins in primary cilia of odontoblasts and renal epithelial cells. This complex constitutes a ciliary signaling microdomain. When one of these proteins is mutated the stability of the entire ciliary signaling complex changes, for example the presence of a mutated form of Polycystin 1 (PC1) causes reduction of OFD1 and other key signaling proteins in primary cilia (Jerman, Ward et al. 2014).

Furthermore, previous studies also demonstrated that OFD1 displays a nuclear localization (Fig. 6) and interacts with RuvBI1, a protein belonging to the AAA<sup>+</sup> family of ATPase. In addition, OFD1 can dimerize through coiled coil domains and together with RuvBI1 interacts with subunits of the TIP60 histone acetyltransferase complex (Giorgio, Alfieri et al. 2007). This protein complex regulates transcription and cell



cycle progression, as well as the process of DNA repair and apoptosis (Doyon and Cote 2004).

In a recent work, produced in the laboratory where I performed my PhD training, the analysis of the OFD1 interactome revealed interesting findings about this protein. Some of the putative interactors were found to be involved in expected functions such as cilia assembly, cytoskeleton organization and chromatin remodelling, in line with previous observations (Iaconis, Monti et al. 2017). Other interactors were found to be associated to protein synthesis. Indeed, in the same laboratory it was demonstrated that OFD1 interacts with components of the Preinitiation complex of translation and of the eukaryotic Initiation Factor (eIF)4F complex and that OFD1 modulates the translation of specific mRNA targets in the kidney. The results suggest a possible role for the centrosome in protein synthesis regulation (Iaconis, Monti et al. 2017).

## **2.2 Animal models**

During the past 10 years in the laboratory of Prof. Franco where I did my PhD training a number of constitutional and conditional animal models have been created to better analyse and understand the pathogenetic mechanisms underlying OFDI syndrome. A murine animal model for this condition was generated using a Cre-loxP system (Nagy 2000, Ferrante, Zullo et al. 2006). Cre-mediated excision of exons 4 and 5 of *Ofd1* led to production of an aberrant mRNA encoding a truncated protein. Ubiquitous *Ofd1* inactivation obtained by crossing the *Ofd1* floxed line (*Ofd1<sup>fl</sup>*) with a transgenic line ubiquitously expressing the Cre from the 4 cells stage (pCX-NLS-Cre mice) thus from early stages of development causes male embryonic lethality, while female mice died at birth (Ferrante, Zullo et al. 2006). Heterozygous females (*Ofd1<sup>+/-</sup>*;pCX-NLS-Cre) reproduced the main features of the human disease, albeit with increased severity, probably due to differences between the X-inactivation

patterns observed between humans and mice (Ferrante, Barra et al. 2003, Morleo and Franco 2008). Heterozygous females were smaller than wild-type and showed craniofacial and limb abnormalities, including a severe cleft palate, which is the likely cause of the observed perinatal lethality in female mutants. Many other clinical features typical of ciliopathies were observed, such as: skeletal defects, disorganization of the brain, reduction of the lungs, defects in the great vessels and cystic kidney. Renal cysts have a glomerular origin in this model and cells lining the cysts do not display primary cilia. Conversely, cilia are present in non-cystic glomeruli and in normal tubules adjacent to the cysts, probably due to random X inactivation. The renal phenotype in these mutants is highly penetrant and 100% of females presented renal cystic disease which could not be further studied due to the perinatal lethality observed in female mice (Ferrante, Zullo et al. 2006). As stated above, the phenotype is more severe in male mutants and hemizygous knock-out (KO) males die by embryonic day (E) 12.5 for early developmental defects which affect neural tube, heart and left-right axis specification. Cilia were not present in the embryonic node of male embryos, confirming that absence of the OFD1 protein prevents assembly of primary cilia which is essential for normal development (Ferrante, Zullo et al. 2006).

Similar to other ciliopathies, OFD type I syndrome is characterized by the presence of neurological abnormalities (Waters and Beales 2011). Experimental evidence obtained by studying the *Ofd1*<sup>+/-</sup>;pCX-NLS-Cre demonstrated that *Ofd1* plays a crucial role in forebrain development, and in particular, in the control of dorso-ventral patterning and early corticogenesis. In *Ofd1* mutant male embryos, lack of cilia causes deregulation of the SHH pathway, a major pathway involved in brain development. Defects in cytoskeletal organization and apical-basal polarity in *Ofd1* mutant embryos lead to severe patterning and growth defects (D'Angelo, De Angelis et al. 2012).

Another mouse model with *Ofd1* limb-specific inactivation was generated to understand the role of *Ofd1* in development. *Ofd1* limb-specific inactivation resulted in polydactyly and shortened long bones, with progressive loss of Shh signal transduction and cilia malformation (Bimonte, De Angelis et al. 2011).

To study the role of *Ofd1* in the renal cystic disease, a conditional model in which *Ofd1* is specifically inactivated in the kidney was generated (Zullo, Iaconis et al. 2010). *Ofd1* floxed mice were crossed with the *Cre<sup>Ksp</sup>* mice, in which the *Cre* recombinase is expressed, starting from E15.5, predominantly in the medullary portion of the kidney. Renal inactivation of *Ofd1* leads to viable mice that develop cysts of tubular origin starting from postnatal day (P) 14 (Fig. 7). Cysts became progressively larger and more numerous leading to a severe impairment of the renal function at P28 (Fig. 7). By the stage of P90 mice are sacrificed since their condition is not compatible with life. Primary cilia initially form and then disappear after the development of cysts, suggesting that the absence of primary cilia is a consequence rather than a cause of renal cystic disease. The kidneys of *Ofd1<sup>fl</sup>;cre<sup>Ksp</sup>* mutants showed upregulation of the mTOR pathway, similarly to what observed in other models of polycystic kidney disease. Treatment with rapamycin, a specific inhibitor of the mTOR pathway, resulted in a significant reduction in the number and size of renal cysts (Zullo, Iaconis et al. 2010). mTOR represents a potentially interesting therapeutic target for cystic renal disease (Torres, Boletta et al. 2010), however different clinical trials with mTOR inhibitors have so far failed to be effective in clinical trials of PKD patients (Serra, Poster et al. 2010). In some cases mTOR inhibition slowed the increase in total kidney volume of patients but did not slow down the progression of renal impairment (Walz, Budde et al. 2010).

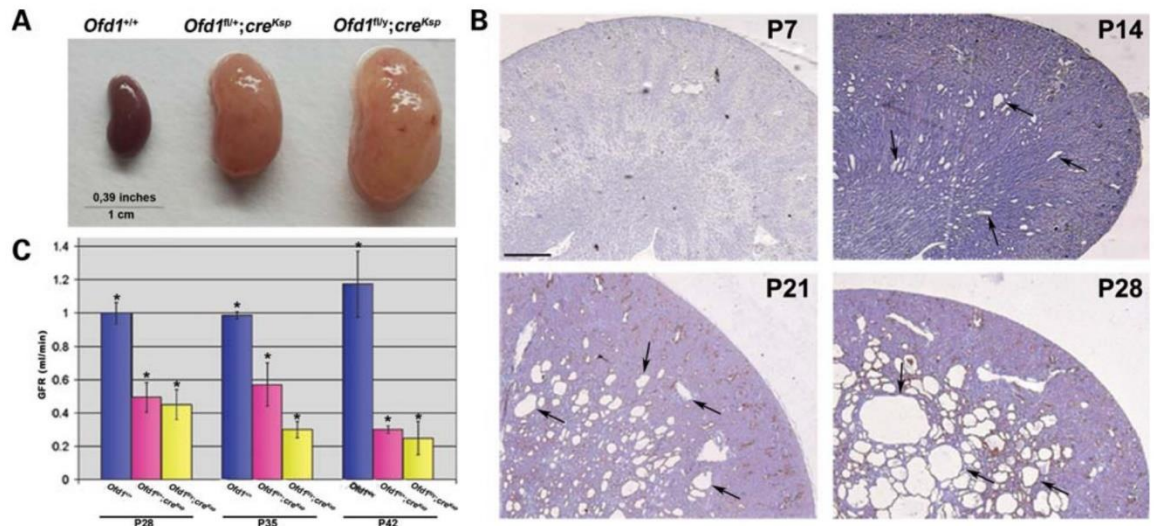


**Figure 7. Characterization of *Ofd1<sup>fl/y</sup>;Cre<sup>Ksp</sup>* mutant animals.**

**(A)** Gross appearance of kidneys from mice at P70. **(B)** Haematoxylin/eosin staining of kidney sections from *Ofd1<sup>fl/y</sup>;cre<sup>Ksp</sup>* mutants at different stages. At P7, no cysts are visible. Dilated tubules appeared at P14 and cysts (black arrows), rapidly increased in size and number. **(C)** Glomerular Filtration Rate (GFR) at different stages showed reduced renal function in kidneys from mutant males and females compared with control littermates. (Zullo, Iaconis et al. 2010)

Finally, an additional conditional null mouse model (*Ofd1*-IND) containing the *Ofd1* floxed alleles and the tamoxifen-inducible *Cre-recombinase* expressed from the actin promoter (CAGG-creER<sup>TM</sup>) has been generated (D'Angelo, De Angelis et al. 2012, Iaconis, Monti et al. 2017). In this model the activation of the Cre is achieved through tamoxifen administration at later stages to bypass the early stages of development during which the action of normally functioning cilia is required and to avoid the early male lethality and the perinatal lethality observed in female mutants. In this model efficient ubiquitous deletion of *Ofd1* is induced just before birth by injecting pregnant mothers at E18.5. The tamoxifen injection strongly downregulates *Ofd1* at P0 (80%). Interestingly, *Ofd1*-IND mice (both males and females) are viable 30 days after injection. These mutant mice (both males and females) show renal tubules dilation at P10, while at P18 the majority of the renal parenchyma is replaced by cysts. Similarly to *Ofd1<sup>fl/y</sup>;cre<sup>Ksp</sup>* model, an hyperactivation of the mTORC1 pathway in kidney is present starting from P10 (Iaconis, Monti et al. 2017).

### **3. Autophagy**

#### **3.1 The role of autophagy**

The term “autophagy” derives from the Greek meaning “self-eating”, it is a cellular catabolic process which degrades intracellular components, such as soluble proteins, aggregated proteins, organelles, macromolecular complexes, and infectious agents (Mizushima 2005). Autophagy delivers cytoplasmic contents to lysosomes via double-membrane organelles called autophagosomes. Following fusion with the lysosomes, the contents of the autophagosome are degraded by the lysosomal proteases. The primordial function of autophagy, which is conserved from yeast to humans, is to protect cells during starvation conditions (Moreau, Luo et al. 2010). Cells, through autophagy, degrade macromolecules into their building blocks, which can be used for protein synthesis and ATP energy production. Nutrient depletion in mice upregulate autophagy in almost all tissues with different degrees of intensity (Mizushima, Yamamoto et al. 2004). In the early neonatal period, neonates face severe starvation due to sudden termination of the placental nutrient supply. Autophagy is transiently upregulated in this period to protect neonates from nutrient deprivation (Kuma, Hatano et al. 2004).

Many studies have clearly demonstrated that the role of autophagy is not restricted to the response to starvation. Autophagy occurs constitutively at low levels even under normal growth conditions as quality control (Moreau, Luo et al. 2010). The most direct evidence is the accumulation of abnormal proteins and damaged organelles in autophagy-deficient cells (Komatsu, Waguri et al. 2005). Organelles such as peroxisomes, endoplasmic reticulum and ribosomes can be selectively degraded by autophagy. The turn-over of these organelles is fundamental to maintain cellular homeostasis. Damaged and dysfunctional mitochondria are removed by autophagy to protect cells from radical oxygen species. This selective mitochondrial autophagy is called mitophagy, and plays an important role in aging,

cancer and neurodegenerative diseases (Moreau, Luo et al. 2010). Moreover, mitophagy is also important to regulate the number of mitochondria to match metabolic demand. In most mammals, mature red blood cells lack mitochondria, and this is achieved by mitophagy during maturation of immature red blood cells.

Diverse neurodegenerative diseases, such as Parkinson, Alzheimer and Huntington, are characterized by protein inclusions and mitochondrial dysfunction which lead to cell death in neuronal tissues. Autophagy plays an important role in clearance of protein aggregates and damaged mitochondria to prevent these diseases (Ravikumar, Duden et al. 2002, Mizushima 2005). Genes associated with neurodegenerative diseases have been implicated in different steps of the autophagic process. For example, the mutant form of huntingtin, responsible for the Huntington disease, impairs through autophagosomes efficient cargo recognition (Rui, Xu et al. 2015). Moreover, two essential genes for mitophagy, encoding for the kinase PINK1 and the cytosolic E3 ubiquitin ligase parkin, are mutated in inherited forms of Parkinson's disease (Cookson 2012). Autophagic clearance of protein aggregates is also fundamental in other cell types, such as hepatocytes and cardiomyocytes (Nakai, Yamaguchi et al. 2007, Rautou, Mansouri et al. 2010)

Another important role of autophagy is the clearance of pathogens like viruses and bacteria in cells of the immune system. Recent studies also indicate that autophagy participates in the activation of innate and adaptive immunity (Levine and Deretic 2007).

Several studies showed a link between autophagy and cancer. The role of autophagy in tumour formation and progression is controversial. Autophagy defects are associated with increased tumorigenesis, but the mechanisms behind this has not been determined yet. Nevertheless, loss of the essential autophagy gene Beclin1 (BECN1) is found with high frequency in human cancers (Gong, Bauvy et al. 2012) and loss of autophagy induces genomic instability and necrosis with

inflammation in mouse tumour models (Karantza-Wadsworth, Patel et al. 2007). Conversely, in some cases autophagy helps cancer cells to maintain homeostasis and viability during periods of metabolic stress (Lu, Luo et al. 2008).

As stated above, the autophagy is mainly considered a protective mechanism required for cell survival, however excessive activation of this process can lead to cell death (Shi, Weng et al. 2012). Extensive autophagy is commonly observed in dying cells, leading to its classification as an alternative form of programmed cell death. Autophagic cell death is notable for the presence of autophagic vacuoles in the dying cell (Debnath, Baehrecke et al. 2005). The excessive activation of autophagy may increase the amount of cargo randomly sequestered by autophagosomes and the loss of selectivity leads to a complete self-digestion of the cell (Wong and Cuervo 2010).

### **3.2 The autophagic machinery**

The identification of the genes involved in autophagy mainly comes from studies in yeast. Most of these autophagy related genes (Atg) have orthologs in mammals with similar functions, revealing conservation of the autophagic machinery across species (Mizushima 2007). The most characteristic feature of the autophagic process is the formation of double-membraned vesicles known as autophagosomes, which correspond to the mature form of phagophores. The phagophore or isolation membrane is a cup-shaped double-membrane whose edges extend and fuse, trapping the engulfed cytosolic material as autophagic cargo (Fig. 8) (Mizushima 2007). Phagophores nucleate at endoplasmic reticulum (ER) membrane sub-domains termed “omegasomes” that are phosphatidylinositol-3-phosphate (PI3P) rich and marked with the DFCP1 and WIPI2 proteins (Fig. 8) (Axe, Walker et al. 2008). However, ER-mitochondria and ER-plasma membrane contact sites as well as other organelles, such as the Golgi complex and the plasma

membrane were described as sites for phagophore formation (Hamasaki, Furuta et al. 2013, Abada and Elazar 2014, Nascimbeni, Giordano et al. 2017).

The synthesis of PI3P by the vacuolar protein sorting 34 (VPS34), a class III phosphatidylinositol 3-kinase (PI3K), is critical for initial steps of autophagosome biogenesis (Fig. 8). VPS34 forms a core complex with its regulator, p150 and its accessory protein BECLIN1. BECLIN1 forms the scaffold for recruitment of additional proteins, such as ATG14L (yeast Atg14 ortholog) or UV irradiation resistance-associated gene (UVRAG). The binding of UVRAG and ATG14L to the core complex is mutually exclusive (Itakura, Kishi et al. 2008). In particular, ATG14L is responsible for recruitment of the PI3K class III complex on the ER membrane and nucleation of the phagophore (Matsunaga, Morita et al. 2010), while UVRAG is involved in the autophagosome maturation (Kim, Jung et al. 2015). The formation of PI3P at phagophore formation sites enables recruitment of PI3P-binding proteins WIPI2 and DFCP1, belonging to the WIPI family, and consequently allows the recruitment of the ATG12–ATG5–ATG16L complex (Fig. 8) (Dooley, Razi et al. 2014).

Subsequently, two conjugation systems involving ubiquitin-like (UBL) proteins contribute to expansion of the phagophore (Fig. 8). The first UBL protein conjugation system involves the formation of the ATG12–ATG5–ATG16L complex. Sequential reactions catalysed by the E1 enzyme ATG7 and the E2 enzyme ATG10 conjugate ATG12 to the lysine residue in ATG5, and the resulting ATG12-ATG5 conjugate forms a complex with ATG16L that associates with the extending phagophore (Ohsumi and Mizushima 2004). Once the autophagosome is formed, the ATG5–ATG12–ATG16L complex dissociates from the membrane. The second UBL protein conjugation system involves the modification of Atg8 orthologs: the microtubule-associated protein light chain 3 (LC3) and the gamma-aminobutyric acid receptor-associated protein (GABARAP). LC3 is cleaved by cysteine protease ATG4 and



then conjugated with phospholipid phosphatidylethanolamine (PE) by ATG7 and ATG3, a second E2-like enzyme (Ichimura, Kirisako et al. 2000). At this point LC3 is present in its lipidated form (LC3-II) which associates with newly forming autophagosome membranes and remains on mature autophagosomes until its fusion with lysosomes. Atg8-family proteins are the best-studied proteins of the core autophagic machinery. They are essential for elongation and closure of phagophore to form a proper autophagosome. LC3-II is attached to both outer and inner membranes of autophagosomes, and it is actively involved in sequestration of material in the growing phagophore. It has been demonstrated that Atg8-family proteins are crucial for selective autophagy through interaction with selective autophagy receptors. In addition to the crucial role of Atg8 proteins, ATG9 has been described to participate to phagophores expansion (Fig. 8). ATG9 is the only transmembrane protein in the autophagy core machinery and has been proposed to play a key role in directing membranes from donor organelles for autophagosome formation. However direct experimental evidence or a mechanistic explanation supporting the latter hypothesis are not available yet (Feng and Klionsky 2017). Once the autophagosome has formed, it fuses with lysosomes and delivers its contents for degradation. The resulting structures are called “autolysosomes” or “autophagolysosomes” (Fig. 8) (Mizushima 2007). The phagophore closure is a critical step for autophagosome maturation and for the successive fusion with lysosomes. The cleavage of LC3 and the removal of PI3Ps from the outer autophagosomal membrane facilitates the maturation into fusion-capable autophagosomes (Nair, Yen et al. 2012, Wu, Cheng et al. 2014).

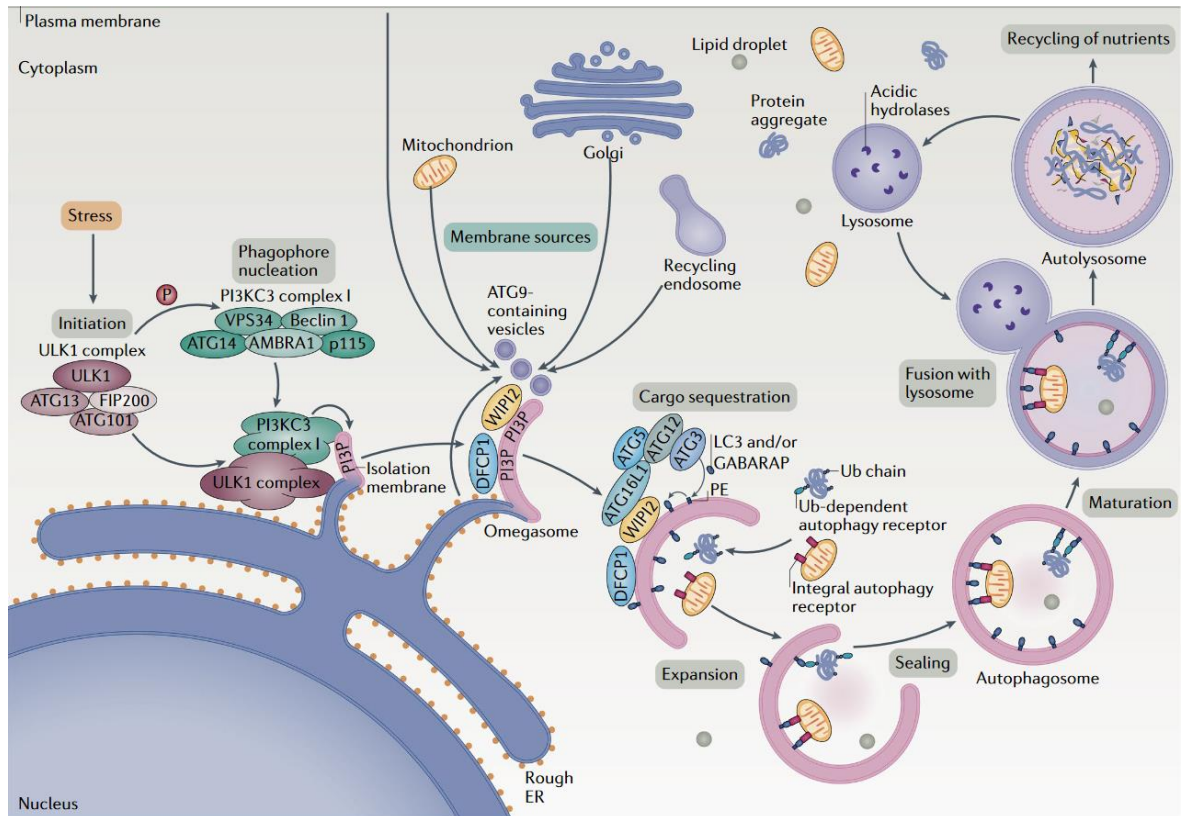


**Figure 8. The autophagic machinery.**

Autophagosome formation is controlled upstream by the Unc-51-like kinase 1 (ULK1) complex. This complex phosphorylates components of the PI3K class III complex which in turn produces local PI3Ps at a characteristic ER structure called omegasome. PI3P recruits the PI3P-binding proteins WIP2 and DFCP1. Expansion and closure of the autophagosomal membrane are dependent on the ATG5-ATG12-ATG16L complex and on the mammalian homologs of Atg8, which are LC3 and GABARAP. Cellular membranes, delivered by ATG9-containing vesicles, contribute to elongation of the autophagosomal membrane. Phagophore closure allows autophagosomes to fuse with lysosomes, generating autolysosomes in which enclosed cargoes are degraded (Dikic and Elazar 2018).

### 3.3 The regulation of autophagy

Basal autophagy is very low under normal conditions; therefore, an efficient mechanism to induce autophagy is crucial for cells to adapt to stress and extracellular cues when cells need to rapidly switch. In yeast, induction of autophagosome formation is regulated by the Atg1-Atg13-Atg17 complex (Kamada, Funakoshi et al. 2000). In mammalian cells, the very first autophagy-specific complex is the ULK1 complex, consisting of the unc-51-like kinase 1 (ULK1) itself, the focal adhesion kinase family interacting protein of 200 kDa (FIP200), ATG13 and ATG101 (Fig. 8) (Hosokawa, Hara et al. 2009, Hosokawa, Sasaki et al. 2009, Jung, Jun et al. 2009). ULK1 is a serine/threonine protein kinase and represents the

mammalian orthologue of the yeast Atg1, while FIP200 functions as the mammalian counterpart of Atg17 (Hara, Takamura et al. 2008). In contrast to the yeast Atg1 complex, ULK1, ATG13, FIP200, and ATG101 form a stable complex independent from nutritional conditions, thus, autophagy induction does not seem to be regulated at the level of assembly of the complex (Hosokawa, Hara et al. 2009). The kinase activity of ULK1 is essential for autophagy initiation: kinase-dead mutants of ULK1, as well as chemical inhibition of ULK1 kinase activity, block the autophagic response to starvation (Egan, Chun et al. 2015). FIP200 and ATG13, also, are essential for autophagy induction, as both proteins increase ULK1 kinase activity and stability (Ganley, Lam et al. 2009). In particular, the ATG13-ATG101 heterodimer mediates the interaction between FIP200 and ULK1 (Qi, Kim et al. 2015). Perturbation of these interactions leads to impaired autophagy, highlighting the importance of these protein–protein interactions. Lack of one or more components of the ULK1 complex results in reduced stability of the complex and impaired autophagy in response to starvation (Jung, Jun et al. 2009).

The exact localization of the ULK1 complex under normal conditions is unclear, but upon starvation the ULK1 complex forms punctate structures in proximity to the phagophore assembly sites on the ER (Karanasios, Stapleton et al. 2013). It has been showed that the ULK1 complex recruits other Atg proteins at these sites, including components of the VPS34 complex (Fig. 8). VPS34 and its interacting partners, BECLIN1 and ATG14L, are phosphorylated by ULK1, leading to enhanced VPS34 activity, in addition to PI3P production and autophagy initiation (Russell, Tian et al. 2013). ULK1 regulates the VPS34 complex also by AMBRA1, an interactor of BECLIN1 that functions as autophagy regulator. ULK1-mediated phosphorylation of AMBRA1 results in dissociation of the VPS34 complex from the cytoskeleton and in its translocation to autophagy initiation sites (Di Bartolomeo, Corazzari et al. 2010). In addition to VPS34 complex, ULK1 is also able to phosphorylate the initiation

complex members themselves, including ULK1 (autophosphorylation), ATG13, FIP200 and ATG101 (Ganley, Lam et al. 2009, Hosokawa, Hara et al. 2009).

The ULK1 complex integrates upstream nutrient and energy signals to coordinate the induction of autophagy. Different pathways converge on ULK1 through activatory/inhibitory post-translational modifications (Fig. 9). A master regulator of autophagy in response to nutrients is the mechanistic target of rapamycin (mTOR) protein, a serine/threonine kinase involved in cell growth and metabolism (Jung, Ro et al. 2010). mTOR is the catalytic subunit of two structurally distinct complexes: mTOR complex 1 (mTORC1) and mTOR complex 2 (mTORC2). mTORC1 functions as energy-sensor: in the presence of nutrients, mTORC1 is active and inhibits autophagy by phosphorylating ULK1 at a serine in position 757, as well as ATG13 at multiple residues (Fig. 9). Conversely, rapamycin and nutrient starvation reduce mTORC1 activity, thus both ULK1 and ATG13 are rapidly dephosphorylated, resulting in activation of the ULK1 kinase and consequent induction of autophagic processes (Ganley, Lam et al. 2009, Hosokawa, Hara et al. 2009).

Another important cellular energy sensor, the AMP-activated protein kinase (AMPK), plays an important role in autophagy induction. The increase in the AMP:ATP ratio leads to activation of AMPK, which inactivates mTORC1 through the phosphorylation of regulatory-associated protein of mTOR (RAPTOR), thus indirectly activating ULK1 activity (Kim, Kundu et al. 2011). However, AMPK can also directly phosphorylate and activate ULK1 at multiple serine residues in a nutrient dependent manner, thus leading to autophagy induction (Fig. 9) (Egan, Shackelford et al. 2011).

In addition to phosphorylation, ULK1 levels can also be regulated by ubiquitination which affects protein degradation (Fig. 9). For example, AMBRA1 and the E3-ligase TNF receptor associated factor 6 (TRAF6) promote ULK1 ubiquitination and subsequent stabilization, thus enhancing ULK1 activity (Nazio, Strappazzon et al.

2013). Conversely, the ubiquitination of ULK1 by the cullin E3 ligase complex, composed of the E3 ligase Cullin-3 (Cul3) and the adaptor kelch-like family member 20 (KLHL20) has been shown to promote ULK1 degradation in a proteasome-dependent manner (Liu, Lin et al. 2016). In the same report Liu et al., demonstrated that KLHL20-dependent ULK1 degradation restrains the amplitude and duration of autophagy. Apart from Cul3-KLHL20, the E3-ligase neural precursor cell-expressed developmentally down-regulated 4-like (NEDD4L) has also been demonstrated to regulate ULK1 degradation during prolonged starvation (Nazio, Carinci et al. 2016).

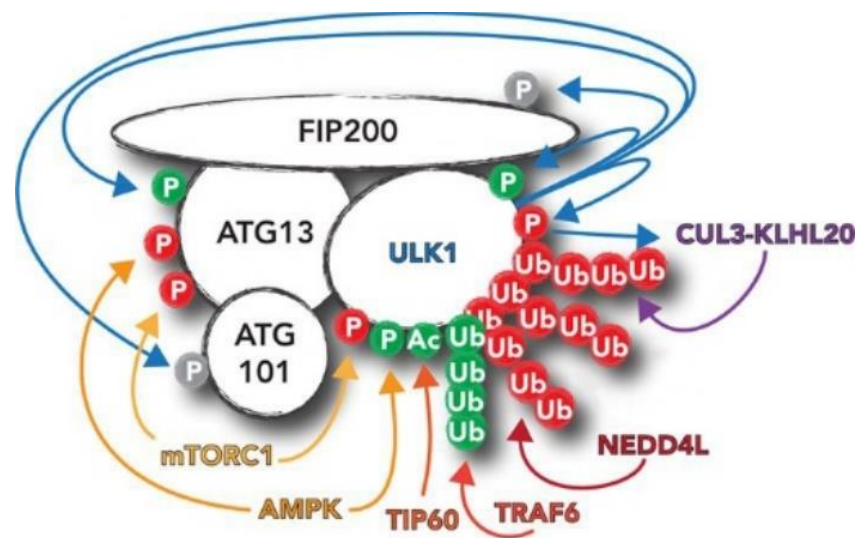


**Figure 9. Regulation of the ULK1 complex.**

The ULK1 complex undergoes multiple modifications: phosphorylation (P), acetylation (Ac) and ubiquitylation (Ub). Green modifications activate the complex whereas red modifications have an inhibitory effect. Modified from (Zachari and Ganley 2017)

### 3.4 Selective autophagy

Although autophagy has primarily been recognized as a non-selective degradation pathway, recent studies reveal that the autophagosomal membrane can selectively recognize specific cargos, a process named “selective autophagy”. Selective autophagy occurs to specifically remove damaged or excessive organelles or specific proteins even under nutrient-rich conditions (Zaffagnini and Martens 2016). Selectivity in autophagy is conferred by cargo receptor proteins, which are able to

tether a cargo to a nascent autophagosome by simultaneously binding cargoes and Atg8-family proteins on the isolation membrane. These proteins are called selective autophagy receptors and are themselves degraded by autophagy. The interaction between receptors and Atg8-family proteins is mediated by an **LC3-Interacting Region** called “LIR” characterized by a specific consensus sequence (Jacomin, Samavedam et al. 2016). This consensus sequence corresponds to the shortest sequence required for interaction with an Atg8-family protein. The consensus sequence is (ADEFGLPRSK)-(DEGMSTV)-(WFY)-(DEILQTV)-(ADEFHIKLMPSTV)-(ILV), where the aromatic residue in positions 3 and the hydrophobic residue in position 6 correspond to the most crucial amino acids for the interaction (Jacomin, Samavedam et al. 2016). In addition to the core motif, the importance of an acidic amino acid, either N- or C-terminal to the conserved aromatic residue, has been demonstrated (Jacomin, Samavedam et al. 2016).

The first selective autophagy receptor to be identified was sequestosome 1 (SQSTM1; also known as p62), that is able to bind polyubiquitinated proteins and mediate their autophagic degradation through the interaction with LC3 (Pankiv, Clausen et al. 2007). The LIR motif is absolutely required for targeting of receptors and bound cargoes into the lumen of autophagosomes. Following the discovery of p62, additional selective autophagy receptors have been identified. Similarly, to p62, the related neighbour of BRCA1 gene 1 (NBR1) was found to act as an aggrephagy receptor. NBR1 share a similar domain architecture with p62, characterized by a LIR and a ubiquitin-binding domain, important for the sequestration of misfolded and ubiquitinated proteins and their autophagic degradation (Lamark, Kirkin et al. 2009). Other important selective autophagy receptors are: the nuclear dot protein 52 kDa (NDP52) which functions as xenophagy receptor, the BCL2 Interacting Protein 3 Like (BNIP3L) and optineurin, which is important for clearance of damaged mitochondria (Birgisdottir, Lamark et al. 2013).

LIR containing proteins are not necessarily selective autophagy receptors. Indeed, many proteins of the core autophagic machinery have functional LIR motifs. The LIR motif in ULK1 is required for its starvation-induced association with autophagosomes but not for ULK1 degradation (Alemu, Lamark et al. 2012). Interestingly, in addition to the interaction with ULK1, ATG13 and FIP200 interact also with human Atg8 proteins through LIR domains. This interaction allow Atg8 proteins to act as scaffolds for assembly of the ULK complex at the phagophore (Alemu, Lamark et al. 2012).

In addition, LIR motifs are present in proteins involved in other autophagic functions such as autophagosomes maturation or vesicular transport (Birgisdottir, Lamark et al. 2013). Moreover, several signaling proteins, such as Dishevelled 2, have a functional LIR which is necessary for their autophagic degradation (Gao, Cao et al. 2010).

### **3.5 Primary cilia control autophagy**

Recently, emerging studies showed a bidirectional interaction between cilia and autophagy. It has been showed that primary cilia are able to influence autophagy and vice versa. The first connection between autophagy and primary cilia came from the observation that autophagy activation upon starvation requires the presence of a properly functional primary cilium (Pampliega, Orhon et al. 2013). Pampliega and co-authors demonstrated that loss of components of the IFT machinery (i.e. IFT88 and IFT20) impairs ciliogenesis and prevents a complete induction of autophagy. In addition, in the same paper the authors present data suggesting that defective Hedgehog ciliary signaling may be behind the impaired autophagy induction in cells with dysfunctional cilia (Pampliega, Orhon et al. 2013). However, the molecular mechanisms connecting the ciliary Hedgehog signaling with autophagy is/are still poorly understood. In addition to these observations, several components of the

autophagic machinery have been localized at the axoneme and/or the basal body of the cilium (Fig. 10). In particular, the presence of Atg proteins in these structures suggests that the ciliary base with the adjacent plasma membrane could be a new site for autophagosome formation (Pampliega, Orhon et al. 2013).

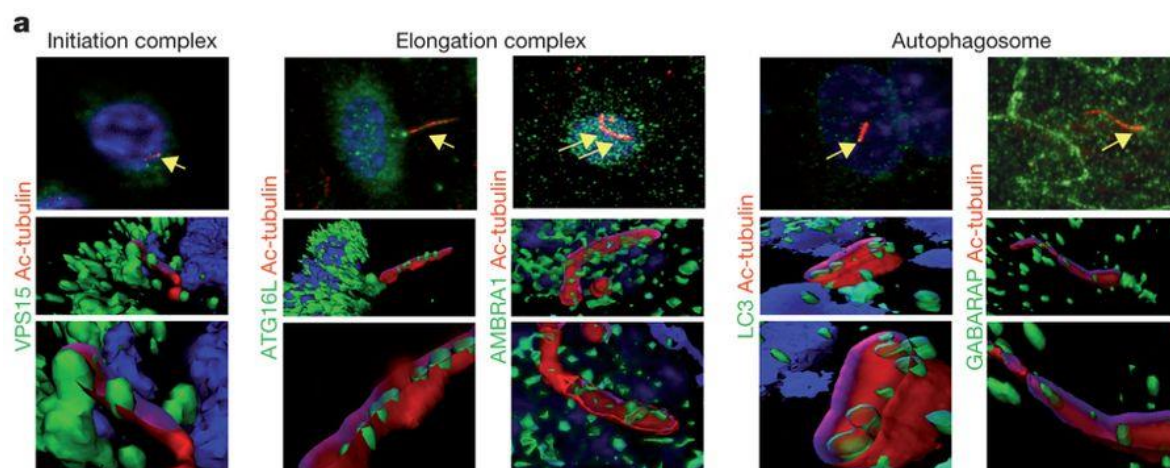


**Figure 10. Autophagy-related proteins associate with ciliary structures.**

Co-immunostaining (top) and 3D reconstruction (middle and bottom) for the indicated autophagy-related proteins (green) and acetylated tubulin (red) in kidney epithelial cells after 24 hours of serum-starvation. The analysed Atg proteins associated with the basal body and the ciliary axoneme. Modified from (Pampliega, Orhon et al. 2013).

Moreover, another paper showed that the crosstalk between primary cilia and autophagy involves the mTOR pathway. In this paper the data presented indicate that primary cilia depletion inhibits autophagy through activation of the mTOR signaling pathway. On the other hand, treatment with rapamycin is able to restore autophagy in cells with compromised cilia (Wang, Livingston et al. 2015). The involvement of mTOR in cilia-mediated autophagy has been showed also in RPGRIP1-like (RPGRIP1L) KO cells. Mutations in RPGRIP1L cause ciliary dysfunctions and reduced autophagic activity due to an increased activation of MTORC1. Application of the MTORC1 inhibitor rapamycin rescued dysregulated MTORC1, autophagic activity and cilia length (Struchtrup, Wiegering et al. 2018). In line with these data, primary cilia have been demonstrated to be necessary for activation of autophagy during neuroectoderm differentiation. In this model, the activation of cilia-mediated autophagy decreased Nrf2 activity and OCT4 and



NANOG expression, thus promoting the neuroectoderm fate (Jang, Wang et al. 2016). Moreover, the interplay between autophagy and the primary cilium is important in the regulation of cell size and volume in the kidney (Orhon, Dupont et al. 2016). The autophagy induced by fluid flow regulates kidney epithelial cell volume. The inhibition of ciliogenesis impairs flow-induced autophagy and consequently the regulation of cell volume. In kidney proximal tubules, primary cilia act as flow sensors and transduce the signals to the LKB1–AMPK–mTOR pathway to activate autophagy (Orhon, Dupont et al. 2016). These studies demonstrated that cilia-mediated autophagy is important in physiological adaptation to stress to maintain tissue homeostasis.

### **3.6 Does Autophagy influences ciliogenesis?**

A large body of experimental evidence now indicate a link between cilia and autophagy and several papers showed that ciliogenesis is regulated by autophagy (Pampliega, Orhon et al. 2013, Tang, Lin et al. 2013, Wang, Livingston et al. 2015). Autophagy has been shown to degrade components essential for ciliogenesis, such as IFT20 and OFD1. However, the data related to the role of autophagy in cilia formation are still controversial. Pampliega et al. showed that autophagy inhibition induces ciliogenesis in mouse embryonic fibroblasts (MEFs) through the accumulation of IFT20 (Pampliega, Orhon et al. 2013). In contrast, Tang et al. showed that ciliogenesis is inhibited in MEFs autophagy-defective cells, due to the accumulation of OFD1 at centriolar satellites (Tang, Lin et al. 2013). The differences in cell confluency and or culturing conditions, which are known to influence ciliogenesis, may underlie the apparent discrepant findings. The regulation of autophagy-mediated ciliogenesis could also be related to the cell type and thus be cell context specific. Genetic and chemical inhibition of autophagy has been shown to attenuate the growth of primary cilia in retinal pigmented epithelium (RPE) cells

(Kim, Shin et al. 2015, Shin, Bae et al. 2015). Conversely, the activation of autophagy negatively regulates primary cilia length in mouse embryo fibroblasts, through decreased expressions of the cilia-associated proteins IFT88, KIF3a and Ac-tubulin (Xu, Liu et al. 2016).

Altogether these data clearly indicate that the relationship between autophagy and primary cilia formation is intriguing but far from being clear and requires further investigations possibly following homogeneous culturing conditions and by comparing results obtained in different cell types.

### **3.7 Autophagy and the centrosome**

In addition to primary cilia, also centrosomes are linked to autophagy through different mechanisms. The number of centrosomes is tightly regulated during the cell cycle and each centriole duplicates to produce two daughter centrioles. The number of centrosomes is regulated not only by the ubiquitin proteasome system, but also by autophagy. Autophagy controls centrosome number by degrading the centrosomal protein of 63 kDa (CEP63) (Watanabe, Honda et al. 2016). Autophagy inhibition causes the presence of supernumerary centrosomes, thus promoting chromosome mis-segregation and genomic instability (Arquint, Gabryjonczyk et al. 2014). As stated above, some Atg proteins are located to centrosomes and ciliary structures. In a recent paper, the authors describe that a pool of the Atg8 ortholog, GABARAP, resides at the centrosome and at the peri-centrosomal region (Joachim, Razi et al. 2017). PCM1, the pericentriolar material 1 protein mentioned at page 10 of this thesis in the introduction section, directly binds GABARAP through a LIR motif and regulates its recruitment at centriolar satellites. In addition, PCM1-GABARAP-positive centriolar satellites colocalize with forming autophagosomes. Loss of PCM1 results in destabilization of GABARAP through proteasomal degradation and enhanced GABARAP-mediated autophagic flux. Conversely, PCM1 has no

significant effect on LC3B-positive autophagosome formation (Joachim, Razi et al. 2017).

PCM1 is a known interactor of OFD1 (Fig. 11) and both proteins colocalize at centriolar satellites (Lopes, Prosser et al. 2011). Moreover, Tang et al. demonstrated that OFD1 interacts with LC3, another Atg8 ortholog (Fig. 11) and specifically colocalize with LC3 at centriolar satellites. Nothing is known so far on how OFD1 binds LC3 although the interaction seems to involve also PCM1 (Tang, Lin et al. 2013). In the same paper the authors also showed that the pool of OFD1 at centriolar satellites is specifically degraded by autophagy upon serum starvation to promote primary cilia biogenesis (Tang, Lin et al. 2013).

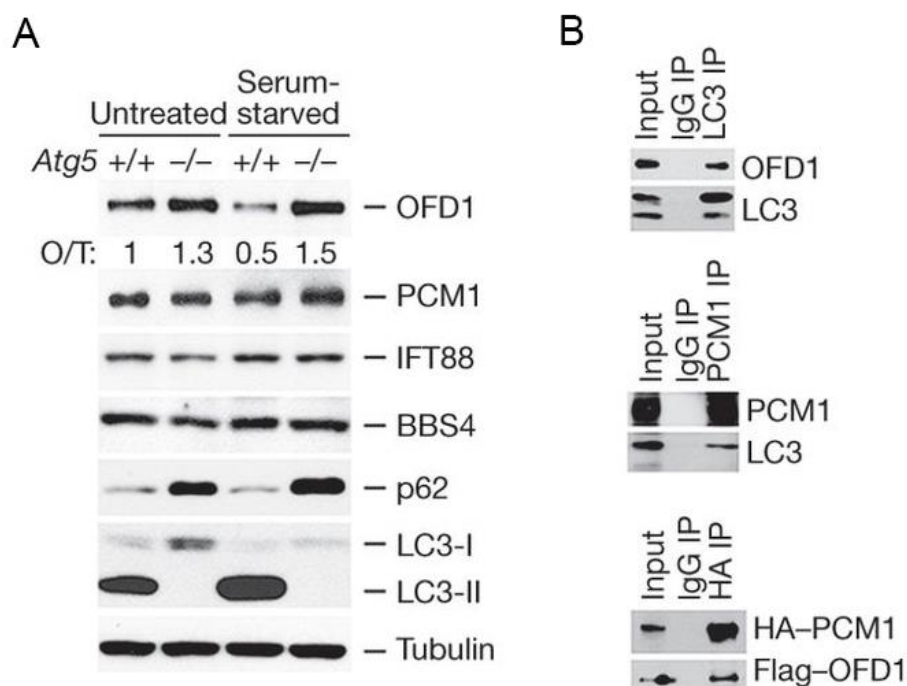


**Figure 11. OFD1 interacts with LC3 and is degraded through autophagy.**

**(A)** Western blotting analysis in mouse embryonic fibroblasts (MEF) KO for Atg5 showed accumulation of OFD1 protein. **(B)** Co-immunoprecipitation (co-IP) of OFD1 with LC3 (top), LC3 with PCM1 (middle), or OFD1 with PCM1 (bottom) in HEK293T cells. Modified from (Tang, Lin et al. 2013).

These observations indicate that the interplay between ciliary structures and autophagy is emerging as a new field which, however, requires future studies. Remains unclear how ciliary and centrosomal proteins participate to autophagy regulation and in general to the different steps of the autophagic processes.

Further studies will be required to better understand the molecular mechanisms involved in this interplay.

### **3.8 The impact of autophagy in kidney function**

As mentioned above, autophagy has already been linked to renal function. Autophagy maintains cellular homeostasis in the kidney, particularly in podocytes and proximal tubular cells by defending the cells from stress stimuli such as ischemia and nephrotoxins (Takabatake, Kimura et al. 2014). Podocytes exhibit an unusually high level of basal autophagy, probably because they have an extremely limited capacity for replacement (Mizushima, Yamamoto et al. 2004). Autophagy is essential for podocyte integrity, in fact podocyte-specific deletion of *Atg5* led to a glomerulopathy phenotype accompanied by accumulation of oxidized and ubiquitinated proteins, ER stress, and proteinuria in aging mice (Hartleben, Godel et al. 2010).

Unlike podocytes, renal tubules display a low level of basal autophagy under normal conditions (Mizushima, Yamamoto et al. 2004), however this level of basal autophagy is important for maintaining homeostasis of renal tubular cells. Mice with *Atg5* deletion in proximal tubules gradually developed deformed mitochondria and accumulation of cytosolic inclusions, leading to proximal tubular cell hypertrophy and eventual degeneration (Kimura, Takabatake et al. 2011). The deletion of *Atg5* in distal tubule cells does not cause a significant alteration in kidney function, while deleting *Atg5* in both distal and proximal tubule cells results in impaired kidney function (Liu, Hartleben et al. 2012). These studies confirm that autophagy is important for maintaining kidney homeostasis and for slowing down kidney aging. Dysregulation of autophagy has been implicated also in polycystic kidney disease (PKD) (Ravichandran and Edelstein 2014). Increased autophagosome formation has been observed in kidneys of rodent models of ADPKD and ARPKD (Belibi, Zafar

et al. 2011). However, the higher number of autophagosomes observed is caused by an impaired autophagic degradation due to a block of autophagosome-lysosome. Whether defective autophagy contribute to the pathogenesis of PKD is not clear based on the data available so far. A recent paper reported that treatment of a zebrafish ADPKD model with autophagy activators attenuated cyst formation (Zhu, Sieben et al. 2017). Additionally, metformin, an AMPK activator, inhibited pronephric cyst formation in a zebrafish model of polycystin-2 deficiency (Chang, Ma et al. 2017). However, other studies showed an enhancement of autophagy in cystic kidneys as for example described in Aquaporin-11 (AQP11) KO mice that display polycystic kidney disease. This study showed in AQP11(-/-) mice increased expression of transcripts encoding autophagy-related genes (e.g. *LC3b*, *SQSTM1*, *BECLIN1* and *ATG5*), suggesting the involvement of autophagy in the development and maintenance/progression of renal cysts (Tanaka, Watari et al. 2016). Moreover, pharmacological targeting of autophagy in an animal model of ARPKD, the PCK rat, was shown to be beneficial for cyst growth in the kidney. In this model, kidney weights, renal cysts and the fibrotic areas decreased by treatment with hydroxychloroquine, an autophagy inhibitor (Masyuk, Masyuk et al. 2017). These studies suggest that the autophagy is a cellular process deregulated in PKD and that autophagy modulation can influence renal cystogenesis. Also in this case, further studies not only in different models of renal cystic disease, but also at different stages of disease progression will be required to understand the link between autophagy and renal cyst formation. The study of early/precystic stages of cystogenesis will inform on the role of autophagy in cyst formation while evaluation of more advanced stages will reveal the impact of autophagy in renal disease progression.

## Results

### 1. OFD1 is required for autophagy inhibition

The involvement of centrosome and primary cilia in autophagy raised different questions about the role of the centrosomal/basal body protein OFD1 in centrosome /primary cilia autophagy related processes. As stated above, OFD1 is an autophagy substrate and interacts with LC3, a critical protein for autophagy (Tang, Lin et al. 2013). However, the role of OFD1 in autophagy regulation is not known. For these reasons, we set up experiments to investigate autophagic processes in *in vitro* and *in vivo* models of OFD type I syndrome.

Given our interest in the renal phenotype, we used human kidney-2 (HK2) cells to study autophagy in OFD1-depleted *in vitro* models. HK2 are immortalized proximal tubule cells derived from normal adult human kidney (Ryan, Johnson et al. 1994). In our laboratory, Knock-Out clones for the OFD1 transcript (KO-OFD1) were generated in HK2 cells by CRISPR-Cas9 technology. KO-OFD1 cells do not express the protein due to a frameshift mutation which causes a premature stop codon (Fig. 12A).

Nutrient depletion by Hanks' Balanced Salt Solution (HBSS) is commonly used to induce autophagy in cell cultures. The amount of LC3-II correlates with the number of autophagosomes, however increased LC3-II levels can be the result of either enhanced autophagosome synthesis or reduced autophagosome turnover (Barth, Glick et al. 2010). For this reason, wt and KO-OFD1 cells were treated with Bafilomycin (Baf) and Chloroquine (Cq) which block the degradation of autophagosome content, including LC3-II (Fig. 12A-B). Lack of increase of LC3-II in the presence of such inhibitors indicates a defect or delay in the autophagic process (Barth, Glick et al. 2010).

KO-OFD1 cells showed increased LC3-II levels both in the presence and in the absence of autophagy inhibitors, suggesting an enhanced synthesis of

autophagosomes (Fig.12A). Consistent with these findings, inactivation of OFD1 obtained through transfection with siRNA directed against the human OFD1 transcript, revealed accumulation of LC3-II in OFD1-depleted and starved cells treated with bafilomycin (Fig. 12B). In addition, KO-OFD1 cells showed increased LC3-II levels also in steady state conditions under Baf treatment, demonstrating that autophagy is enhanced already in basal condition (Fig. 12C). These results suggest that loss of OFD1 enhances autophagy by increasing autophagosomes biogenesis.

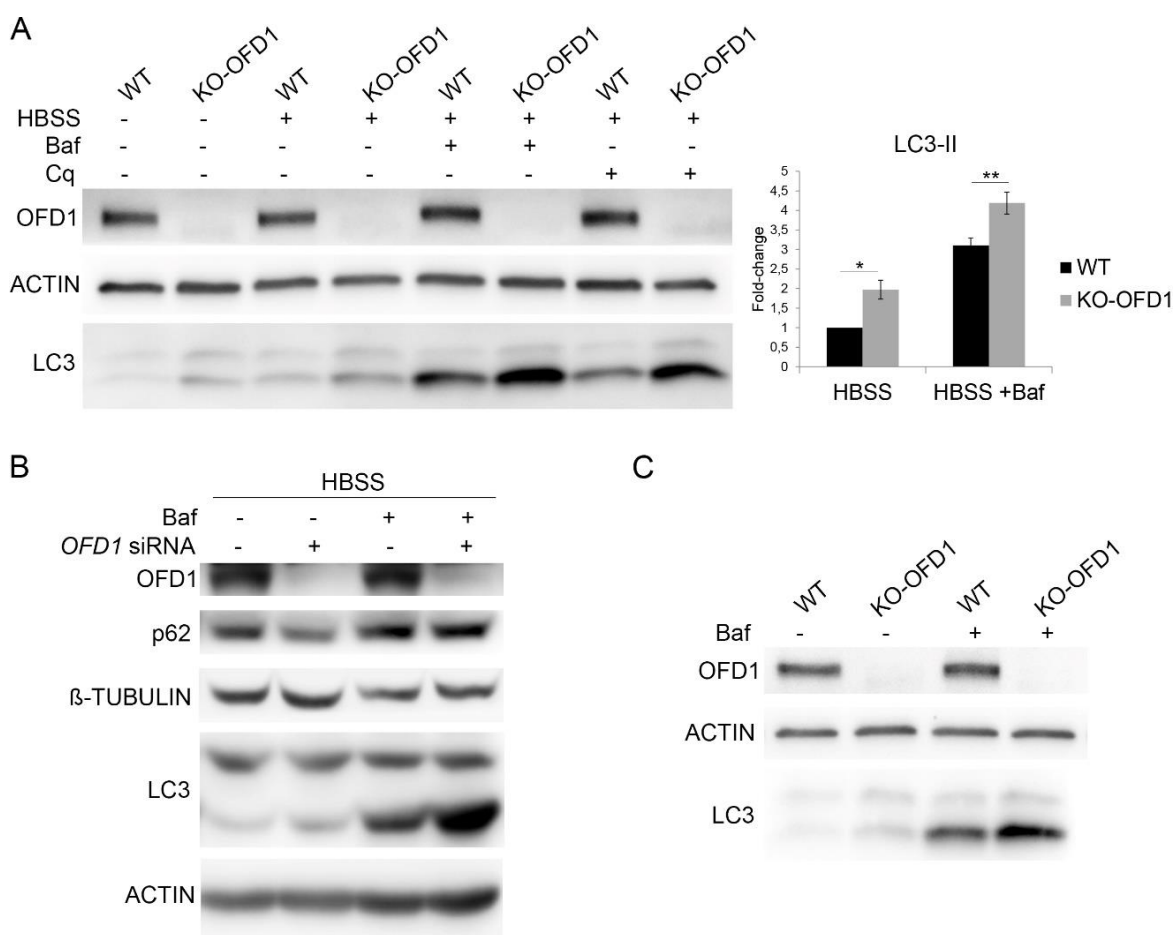


**Figure 12. Loss of OFD1 enhances LC3-II protein levels.**

**(A)** Western blot (WB) analysis of HK2 WT and KO-OFD1 cells treated with Baf (100nM) or Cq (50uM) for two hours in HBSS. Quantification of LC3-II band intensity is represented as fold-change of WT vs KO-OFD1. Bar graphs show standard error mean (SEM). Student's t-test, \*P<0.05; \*\*P<0.01. **(B)** WB analysis of LC3 protein levels in HK2 cells transfected with siRNA against *OFD1* mRNA. 96h after transfection cells were starved with HBSS for 2 hours in the presence of Baf (100nM). **(C)** WB analysis of LC3 protein levels in HK2 WT and KO-OFD1 cells treated with Baf (100nM) at steady state condition (+FBS)

Degradation of p62 is another widely used marker to monitor autophagy. p62 accumulates when autophagy is inhibited, and decreased levels can be observed when autophagy is induced (Bjorkoy, Lamark et al. 2009). OFD1-depleted cells showed reduced p62 levels due to enhanced autophagic degradation, and indeed, in these conditions, Baf treatment restores p62 levels compared to controls (Fig. 12B). The levels of p62 are also decreased in KO-OFD1 cells, whereas in cells treated with the VPS34 inhibitor, SAR405, the levels of p62 are comparable between KO-OFD1 and controls. (Fig 13A). Moreover, our results demonstrate that KO-OFD1 cells showed higher p62 levels in starved condition (under HBSS) after Baf treatment, confirming that p62 is more degraded by autophagy in the absence of OFD1 (Fig. 13B). These results confirm that the impairment of OFD1 causes enhancement of the autophagic flux.

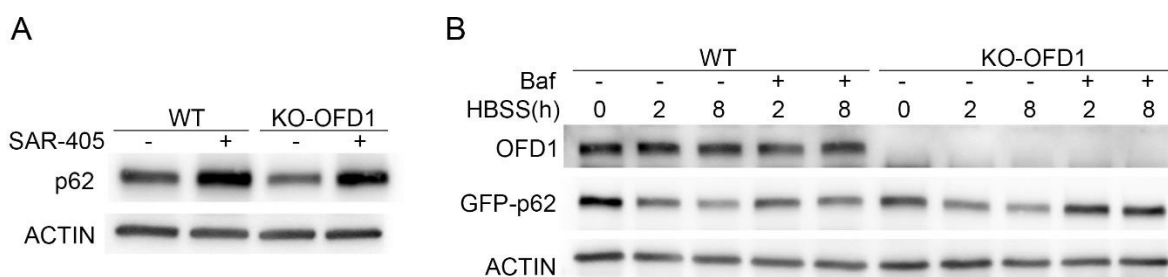


**Figure 13. Loss of OFD1 promotes p62 degradation.**

**(A)** WB analysis of p62 in HK2 KO-OFD1 cells treated with SAR-405 (10 $\mu$ M) for 6 hours. **(B)** WB analysis to analyse time course of degradation of transfected GFP-p62 in HK2 cells after HBSS treatment for the indicated interval (h). Baf (100nM) was used to block GFP-p62 degradation.

To further confirm our results reintroduction of OFD1 in KO-OFD1 cells rescued, as expected, the autophagic flux as cells transfected with the 3xFLAG-OFD1 construct showed reduced LC3-II levels compared to cells transfected with the empty vector (Fig. 14A). In line with this data, overexpression of OFD1 in WT cells also inhibits autophagy (Fig. 14A) confirming that the autophagic phenotype observed is specifically linked to modulation of the OFD1 levels and is OFD1-dependent.



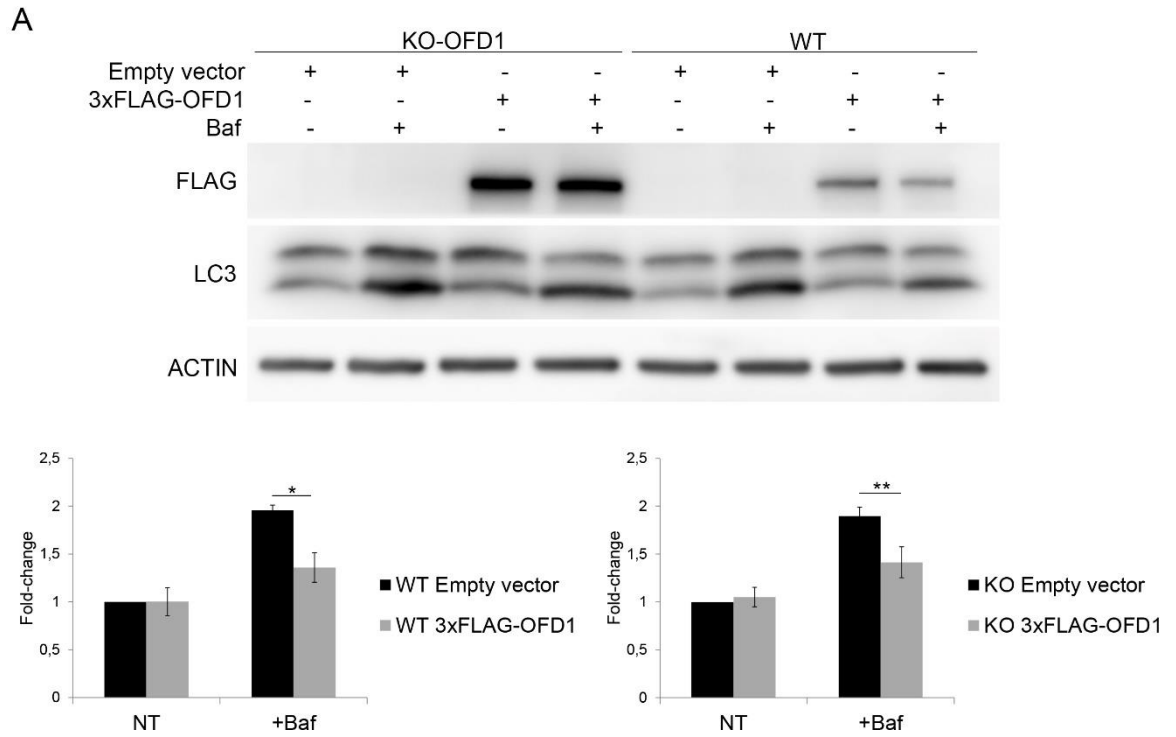


**Figure 14. OFD1 over-expression inhibits autophagy.**

**(A)** WB analysis of LC3 protein levels in HK2 WT and KO-OFD1 cells transfected with 3xFLAG-OFD1 or with the empty vector. Quantification of LC3-II band intensity is represented as Fold-change of Empty vector vs 3xFLAG-OFD1. Error bars show standard error mean (SEM). Student's t-test, \* $P < 0.05$ ; \*\* $P < 0.01$ .

We then tested whether this effect could be observed in a system more physiologically linked to the OFD type I syndrome and we tested the autophagic flux in lymphoblasts from OFD type I patients. The patients analysed have frameshift mutations in *OFD1* gene generating a prematurely truncated protein. Our analysis confirmed the previous results. Cells from OFDI patients were treated with Baf to block LC3 degradation both in steady state and serum-starvation conditions (Fig. 15A). Serum starvation was used to induce autophagy since in our experience HBSS treatment caused excessive cell death of lymphoblasts. Our results indicate that cells from OFDI patients showed accumulation of LC3-II levels compared to control cells after Baf treatment (Fig. 15A). These results further support that impairment of OFD1 results in enhanced autophagy.

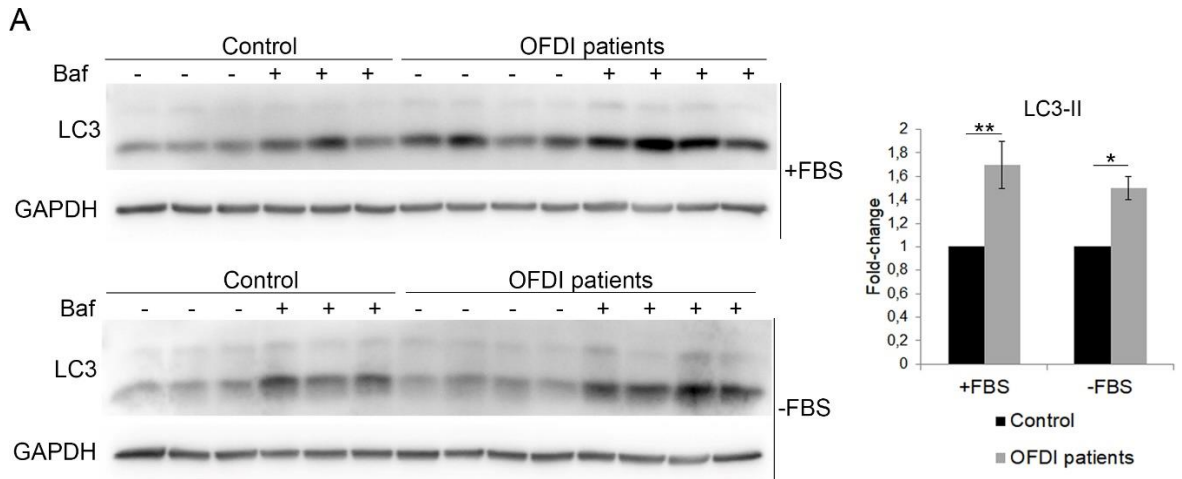


**Figure 15. Increased autophagy in lymphoblasts from OFDI patients.**

**(A)** WB analysis of LC3 in lymphoblasts from controls and OFDI patients. Cells were treated with Baf (100nM) for 2h in steady state and serum-starved (-FBS) conditions. Graphs show the Fold-change of LC3-II band intensity between controls and OFDI patients' cells in the presence of Baf. Error bars show standard error mean (SEM). Student's t-test, \* $P < 0.05$ ; \*\* $P < 0.01$ .

## 2. OFD1 regulates autophagy in a cilia independent manner

As stated above, the absence of OFD1 impairs ciliogenesis *in vivo* and *in vitro* (Ferrante, Zullo et al. 2006, Singla, Romaguera-Ros et al. 2010). We verified if this is true also in our *in vitro* model and indeed, staining for acetylated tubulin in serum-starved KO-OFD1 cells showed no cilia (Fig. 16A). To understand if the enhanced autophagy observed in KO-OFD1 cells is cilium dependent, I analysed the autophagic flux in serum-starved cells at confluent (ciliated cells) and sub-confluent (not ciliated cells) conditions (Fig. 16B). As stated above, ciliogenesis and cell cycle are strictly linked (Plotnikova, Pugacheva et al. 2009), and cell confluence promotes cilia growth. WT cells form primary cilia after serum-starvation in confluent condition, while KO-OFD1 cells do not display primary (Fig 16A). KO-OFD1 cells showed enhanced autophagy in both confluent and sub-confluent conditions, suggesting that the increased autophagy is not dependent on the presence of primary cilia (Fig. 16B). In both conditions (sub-confluent and confluent) LC3-II levels are increased in KO-OFD1 cells treated with Baf compared to WT cells (Fig. 16B).

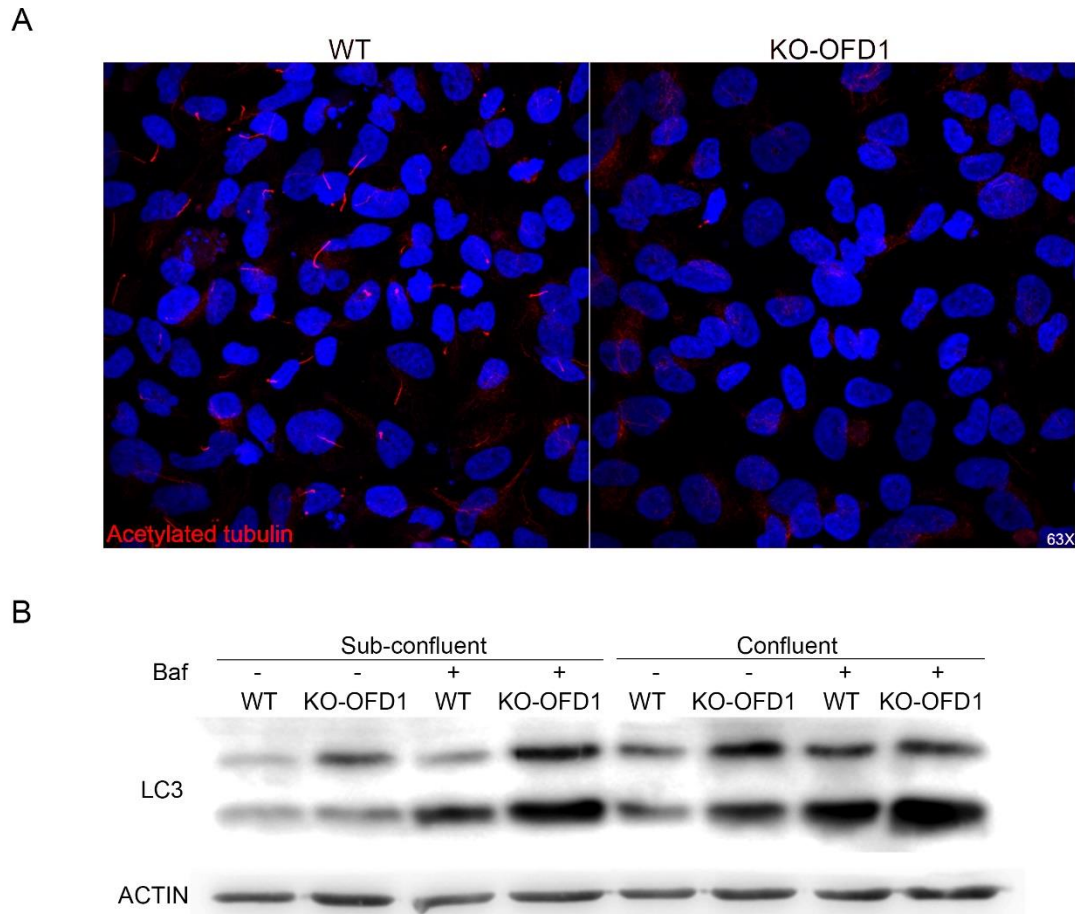


**Figure 16. OFD1 regulates autophagy in a cilia independent manner.**

**(A)** Immunofluorescence staining of primary cilia with an antibody against acetylated tubulin in HK2 cells starved o/n in confluent condition. **(B)** WB analysis of LC3 protein in HK2 KO-OFD1 cells in sub-confluent and confluent conditions starved in serum-free medium for 24h. Cells were treated with Baf (100nM) for 2 hours.

### 3. The role of OFD1 in autophagy is mTOR independent

mTOR is a key regulator of autophagy (Jung, Jun et al. 2009), I thus investigated whether the increased autophagy was associated to mTOR activity downregulation in KO-OFD1 cells. Cells were starved with HBSS and refeeded with complete medium to evaluate mTOR activity in response to nutrients. In these conditions I observed that phosphorylation levels of mTOR targets are comparable or higher in KO-OFD1 cells compared to WT cells (Fig. 17A), suggesting that the increased autophagic flux observed in KO-OFD1 cells is not associated to reduced mTOR activity.

In addition, I also checked the activation of mTOR associated to amino acid stimulus in HK2 cells. I starved cells with amino acids free medium for 1 hour then I refeeded the cells with an amino acids-complete medium to activate mTOR. I observed a stronger mTOR activity in KO-OFD1 cells in the presence of amino acids since the phosphorylation levels of mTOR targets are increased in the absence of OFD1 (Fig. 17B). These results confirmed that impairment of OFD1 leads to increased mTOR activity, as already observed (Zullo, Iaconis et al. 2010). On the basis of these and other results generated in the lab by others we concluded that mTOR up-regulation does not correlate with the increased autophagy observed in KO-OFD1 cells.

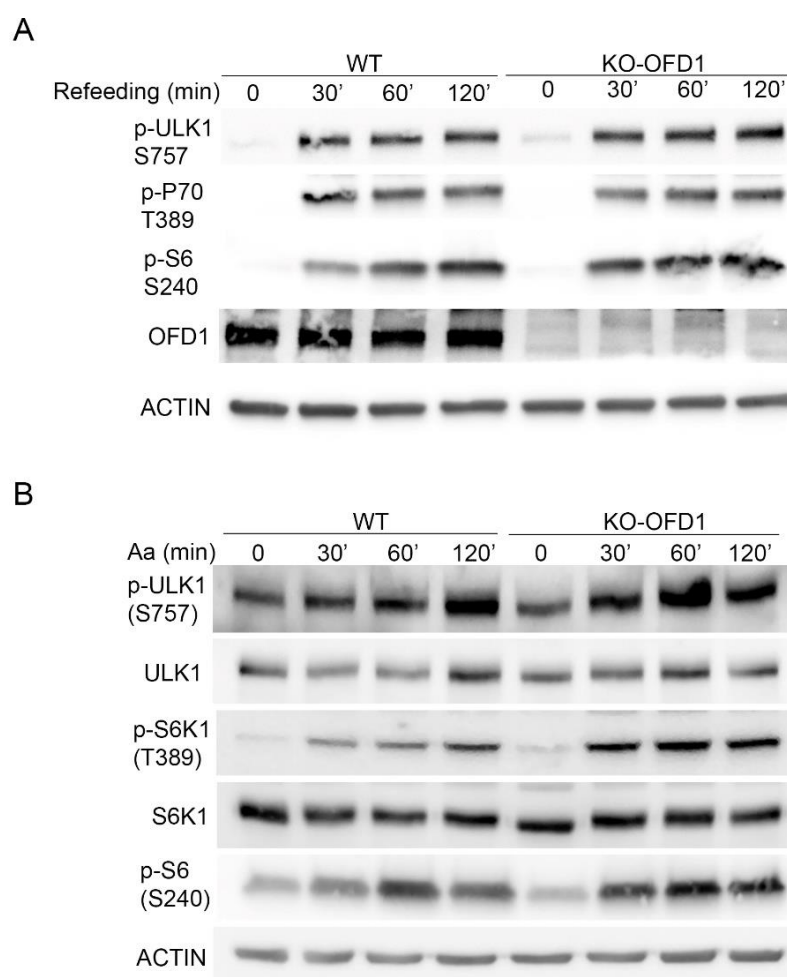


**Figure 17. The role of OFD1 in autophagy is mTOR independent.**

**(A)** WB analysis of mTORC1 substrates phospho-ULK1, phospho-S6K1, and phospho-S6 in WT and KO-OFD1 cells starved with HBSS for 2h (0 time-point) and stimulated with complete medium. **(B)** WB analysis of mTORC1 substrates phospho-ULK1, phospho-S6K1, and phospho-S6 in WT and KO-OFD1 cells starved with RPMI + Glucose 4.5g/L + Dialyzed FBS for 1h (0 time-point) and stimulated with amino acids-complete medium for the indicated time.

#### 4. OFD1 interacts with the ULK1 complex and controls its stability

To investigate the role of OFD1 in autophagy regulation I focused my attention on the putative interactors with a role in autophagy. Mass spectrometry analysis revealed the presence of FIP200, an essential component of the ULK1 complex (Jung, Jun et al. 2009), among the putative interactors (Iaconis, Monti et al. 2017). I first confirmed the interaction between OFD1 and FIP200 by co-immunoprecipitation (co-IP) analysis of the endogenous protein (Fig. 18A). Moreover, I also demonstrated that OFD1 is able to interact with ATG13, another member of the ULK1 complex (Fig. 18B). In particular, the results indicate that OFD1 binds strongly to FIP200 in nutrient independent manner, conversely the interaction of OFD1 with ATG13 is dramatically increased by nutrients deprivation (Fig. 18A-B).

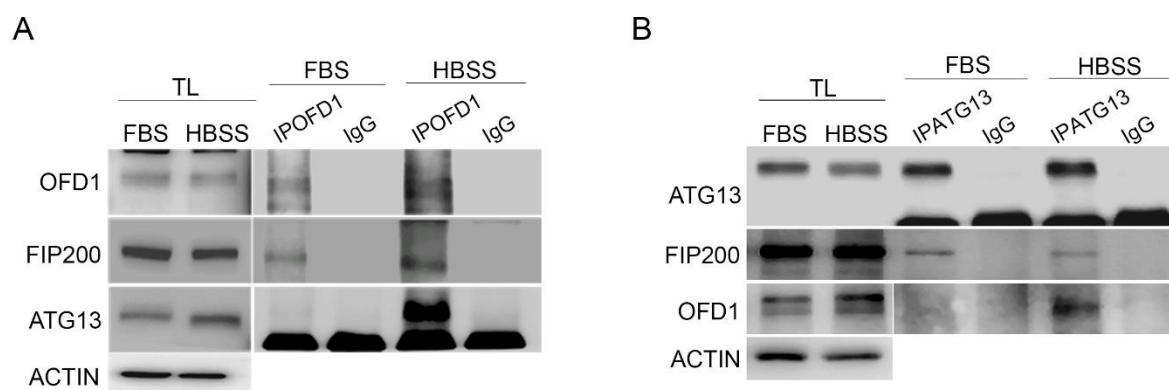


**Figure 18. OFD1 interacts with components of the ULK1 complex.**

**(A)** Immunoprecipitation of endogenous OFD1 in HK2 WT cells. Cells starved 2 hours with HBSS. "TL" indicates Total lysates. **(B)** Immunoprecipitation of endogenous ATG13 in HK2 WT cells. Cells starved 2 hours with HBSS.

ULK1 regulates autophagy by phosphorylating downstream components of the autophagic machinery, including its binding partners FIP200 and ATG13 (Ganley, Lam et al. 2009, Jung, Jun et al. 2009). The low sensitivity of the antibody against phospho-ATG13 did not allow me to look at the ATG13 phosphorylated form. I thus transfected ATG13 and WB analysis showed that the phosphorylation levels of ATG13 in Serine 318, a direct target of ULK1, increased in KO-OFD1 cells

compared to WT cells (Fig. 19A), indicating that ULK1 is more active in OFD1-depleted cells. The enhanced activity of ULK1 in KO-OFD1 cells is confirmed also by the increased phosphorylation of VPS34 in Serine 249, another target of ULK1 (Fig. 19B). Also in this case I transfected VPS34 due to low sensitivity of the antibody. These results confirmed that loss of OFD1 enhances the activity of the ULK1 complex.

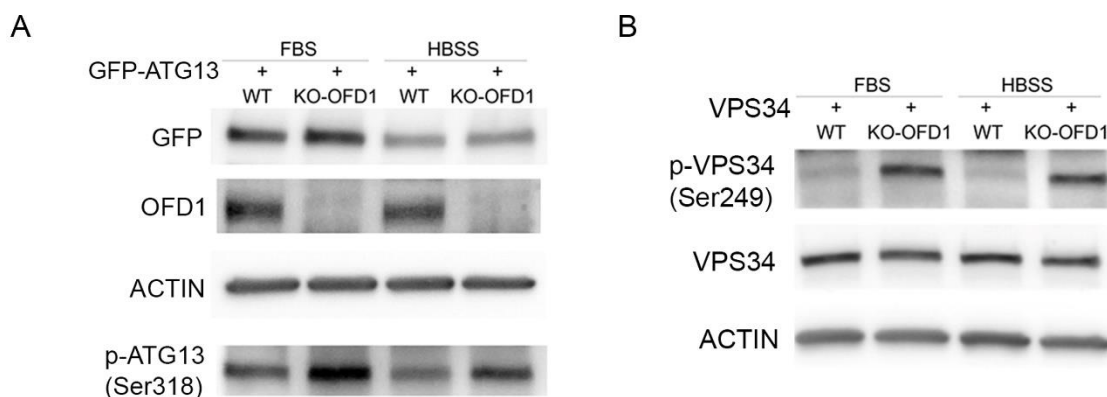


**Figure 19. Loss of OFD1 enhances the ULK1 kinase activity.**

**(A)** WB analysis of phospho-ATG13 (S318) in HK2 WT and KO-OFD1 cells transfected with GFP-ATG13. Cells starved 2 hours with HBSS. **(B)** WB analysis of phospho-VPS34 (S249) in HK2 WT and KO-OFD1 cells transfected with VPS34 and starved 2 hours with HBSS.

Our data suggested that OFD1 regulates the activity of the ULK1 complex, I thus tested whether OFD1 can influence the formation of this complex. One hypothesis could have been that OFD1 could influence the formation of the complex by competing with ULK1 for the binding of FIP200 and ATG13. Therefore, to test this hypothesis, I immunoprecipitated ATG13 in WT and KO-OFD1 cells but I found that the interaction of ATG13 with FIP200 and ULK1 is comparable to OFD1 depleted cells with that observed in WT cells (Fig. 20A). I confirmed the result also in HEK-293 cells silenced for *OFD1*. OFD1 reduction does not influence the interaction between FIP200 and ULK1 (Fig. 20B). However, in both experiments KO-OFD1 and *OFD1*-silenced cells showed increased protein levels of FIP200, ULK1 and ATG13 (Fig. 20A-B).

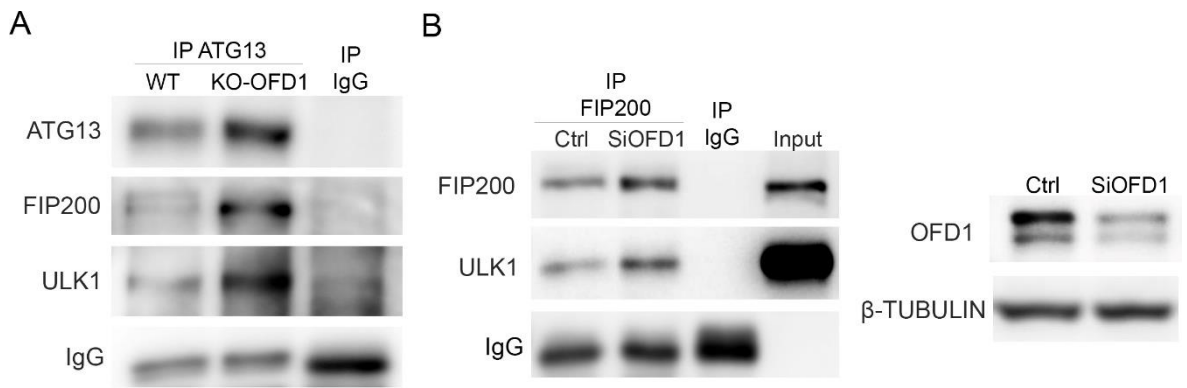


**Figure 20. OFD1 does not influence ULK1 complex formation.**

**(A)** IP of ATG13 in HK2 WT and KO-OFD1 cells **(B)** IP of FIP200 in HK2 cells transfected with siRNA against *OFD1* mRNA. Cells were analysed 96h after transfection.

At this point I evaluated the protein levels of components of the ULK1 complex in normal conditions and after nutrients depletion. Interestingly, I observed that ULK1 and ATG13 proteins are degraded in WT cells during starvation, while their protein levels remain stable in KO-OFD1 cells (Fig. 21). As stated above, the degradation of ULK1 and other autophagic components during starvation is important to restrain autophagy amplitude and duration (Liu, Lin et al. 2016). The impaired degradation of ULK1 and ATG13 observed in KO-OFD1 cells could be related to the deregulated autophagy induction in these cells. Conversely, FIP200 protein levels are not significantly changed in KO-OFD1 cells. This could be explained by the higher stability of this protein compared to ULK1 and ATG13 (Jung, Jun et al. 2009, Liu, Lin et al. 2016).

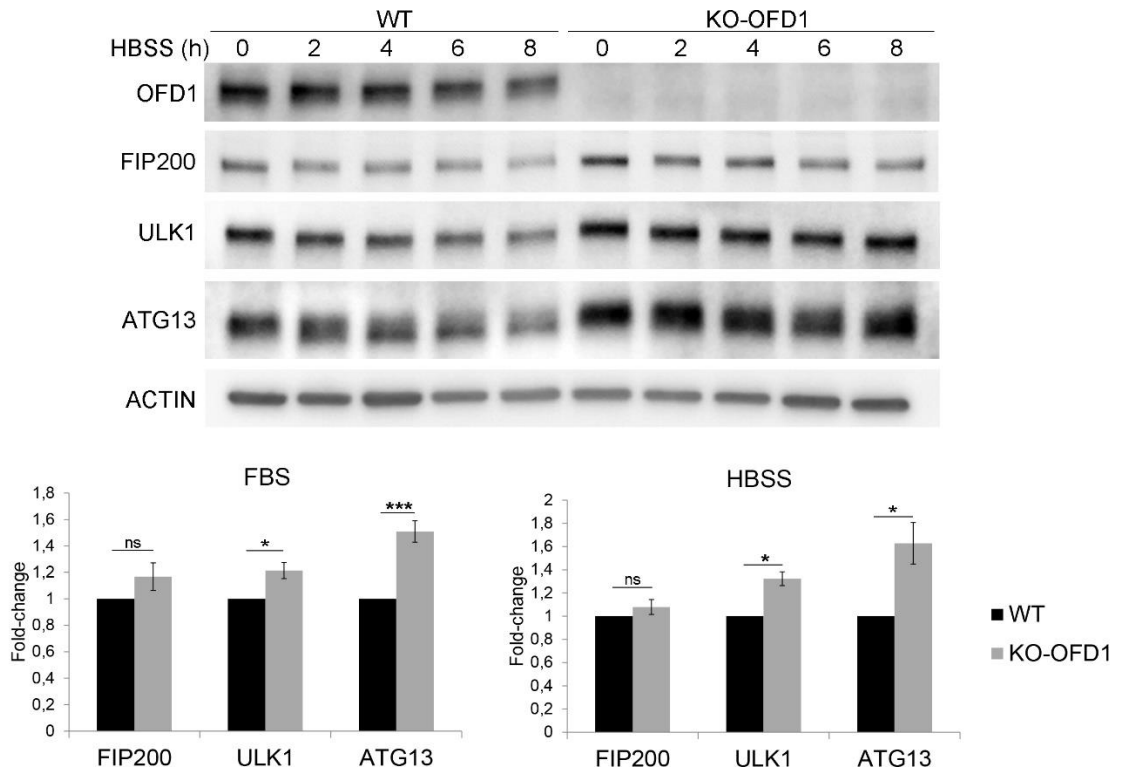


**Figure 21. Impaired degradation of ULK1 and ATG13 in KO-OFD1 cells.**

WB analysis of ULK1 complex components in HK2 WT and KO-OFD1 cells treated for indicated times with HBSS. Quantification of band intensities is represented as Fold-change of WT vs KO-OFD1. Bar graphs show standard error mean (SEM). Student's t-test, \*P<0.05; \*\*P<0.01; \*\*\*P<0.001.

The differences in protein levels between WT and KO-OFD1 are not related to transcriptional regulation, as shown by quantitative RT-PCR analysis that demonstrates comparable gene expression levels of FIP200, ULK1 and ATG13 between KO-OFD1 and WT cells (Fig. 22).

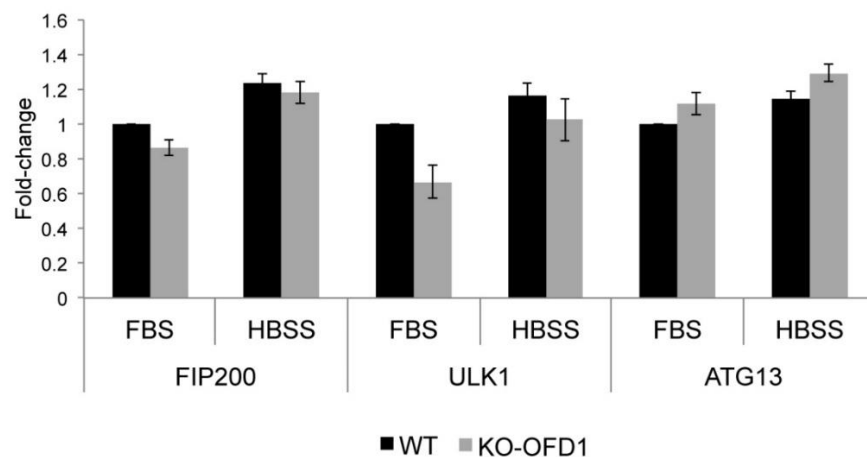


**Figure 22. FIP200, ULK1 and ATG13 transcripts are not regulated by OFD1.**

Real-time PCR analysis of FIP200, ULK1 and ATG13 transcripts in HK2 KO-OFD1 cells. Cells starved 2 hours with HBSS. The data are represented as Fold-change of WT vs KO-OFD1  $\pm$ SEM.



Moreover, when I treated cells with cycloheximide, a potent inhibitor of protein synthesis (Ennis and Lubin 1964), the protein levels of FIP200, ULK1 and ATG13 decreased in WT cells while remained more stable in KO-OFD1 cells (Fig. 23A), confirming that loss of OFD1 results in impaired degradation of ULK1 complex components. On the same line, overexpression of 3xFLAG-OFD1 in KO-OFD1 cells reduced protein levels of FIP200, ULK1 and ATG13 compared to cells transfected with the empty vector (Fig. 23B), demonstrating that OFD1 regulates the stability of ULK1 complex components by promoting their degradation. Altogether, these results indicated that OFD1 acts as inhibitor of autophagy, by controlling the stability of the ULK1 autophagosome initiation complex.

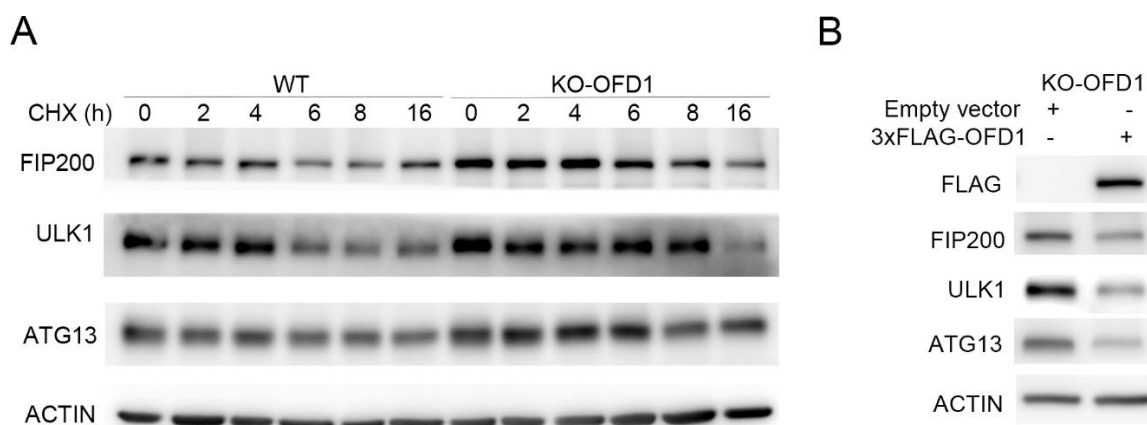


**Figure 23. OFD1 promotes ULK1 and ATG13 degradation.**

**(A)** WB analysis of ULK1 complex components in HK2 cells treated at indicated time-points with cycloheximide (CHX) (50ug/ml) to block protein synthesis. **(B)** WB analysis of ULK1 complex components in HK2 KO-OFD1 cells transfected with 3xFLAG-OFD1 or empty vector.

## **5. Analysis of ULK1 and ATG13 ubiquitination in KO-OFD1 cells**

Ubiquitination represents one of most important post-translational modification for protein stability. ULK1 and ATG13 are more stable in KO-OFD1 cells, we thus hypothesized that OFD1 could regulate their ubiquitination. To analyse the ubiquitination of ULK1 I immunoprecipitated the protein in WT and KO-OFD1 cells overexpressing MYC-ULK1 and HA-UBIQUITIN (Fig. 24A). As showed previously, ULK1 levels are increased in KO-OFD1 cells (Fig. 24A). Unfortunately, I was not able to detect UBIQUITIN signal on immunoprecipitated samples, although the ULK1 protein has been appropriately immunoprecipitated (Fig. 24A). I repeated this experiment six times and I always obtained the same results. The reasons for this problem are not clear. The absence of UBIQUITIN signal could be related to technical problems or to a very low ubiquitination level of ULK1 in HK2 cells. We decided to concentrate on a different aspect and not to pursue the ubiquitination at this time.

Moreover, I analysed the ubiquitination of ATG13 in the absence of OFD1. I immunoprecipitated ATG13 in WT and KO-OFD1 cells overexpressing GFP-ATG13 and HA-UBIQUITIN (Fig. 24B). GFP-ATG13 does not show different polyubiquitination levels between WT and KO-OFD1 cells, however the presence of a single band at 110 kDa suggests mono-ubiquitination of the protein which is more abundant in KO-OFD1 cells (Fig. 24B). There is no evidence in the scientific literature about mono-ubiquitination of ATG13. Further studies will be required to demonstrate the existence of the mono-ubiquitination and the role of this modification in the process.

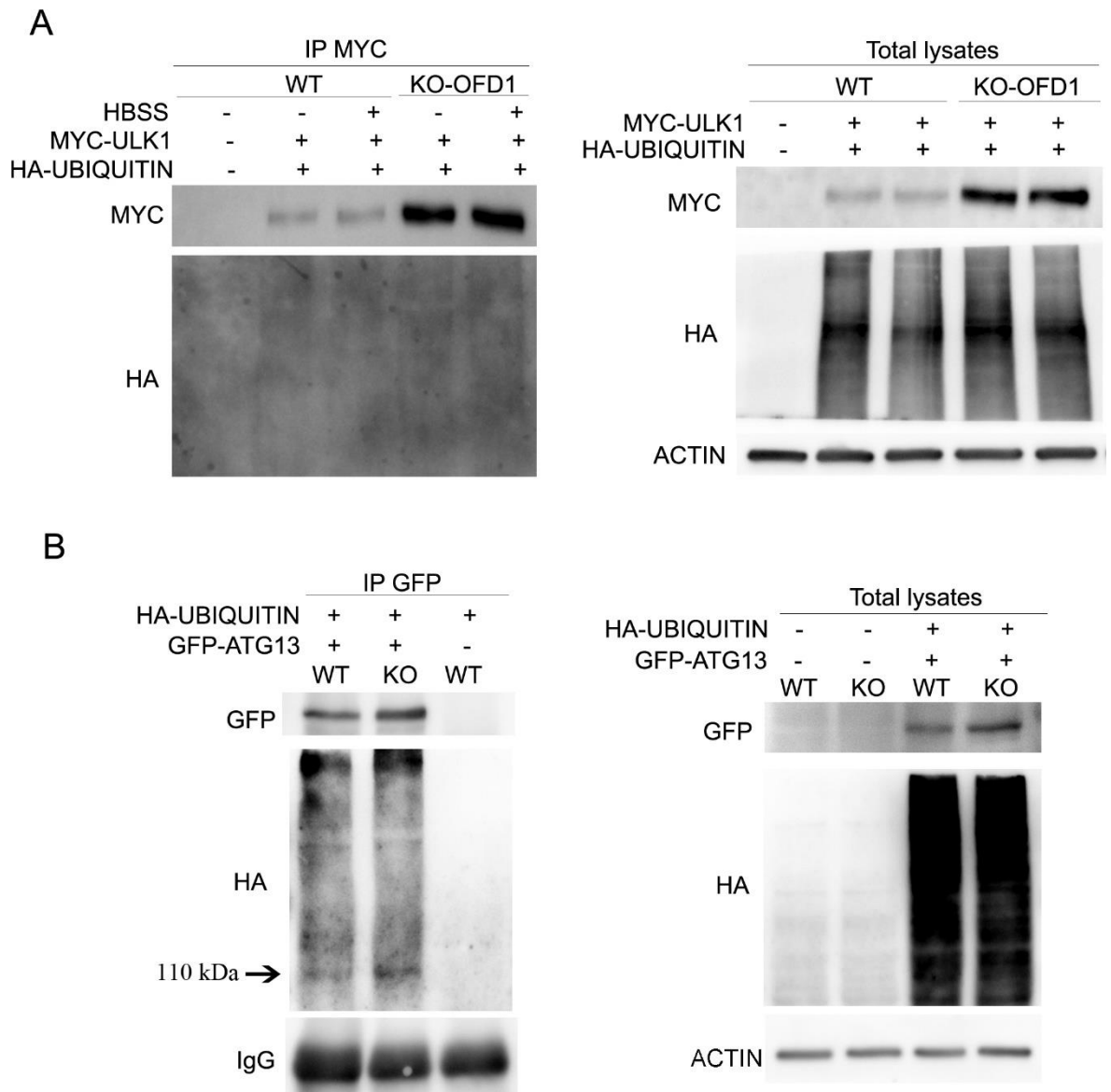


**Figure 24. Analysis of ULK1 and ATG13 ubiquitination levels.**

**(A)** IP of ULK1 in HK2 WT and KO-OFD1 cells transfected with MYC-ULK1 and HA-UBIQUITIN (left). WB analysis on total lysates (right). **(B)** IP of ATG13 in HK2 WT and KO-OFD1 cells transfected with GFP-ATG13 and HA-UBIQUITIN (left). WB analysis on total lysates (right).

As stated above, the regulation of ULK1 through post-translational modifications is critical for autophagy modulation. After autophagy induction ULK1 is ubiquitinated and degraded to restrain the amplitude and the duration of autophagy. Liu and co-authors demonstrated that the Cul3-KLHL20 complex is responsible for ubiquitination and degradation of ULK1 during starvation (Liu, Lin et al. 2016). Since my results showed that OFD1 promotes the degradation of ULK1, I wondered whether this process could be mediated by KLHL20. I performed co-immunoprecipitation of OFD1 and KLHL20 and I surprisingly found that OFD1 is

able to interact with KLHL20 (Fig. 25A). However, the role of this interaction is not clear, because I was not able to reproduce the results described in Liu et al. 2016. In their paper they demonstrated in HeLa cells that KLHL20 promotes ULK1 degradation, whereas the inactivation of KLHL20 induces the stabilization of ULK1. Conversely, when I silenced KLHL20 in HK2 cells I observed, unexpectedly, a decrease of ULK1 protein levels (Fig. 25B). Our data seem to indicate that KLHL20 has an opposite effect on ULK1 protein levels in HK2 cells (Fig. 25B). The cause of this discrepancy is not clear right now. KLHL20 is an adaptor protein, and its role could be different in our cellular model due to different interacting proteins. Since KLHL20 does not promote ULK1 degradation in HK2 cells, we decided to abandon this hypothesis and to analyse the mechanisms involved in the degradation of ULK1 and ATG13 in our cellular model.

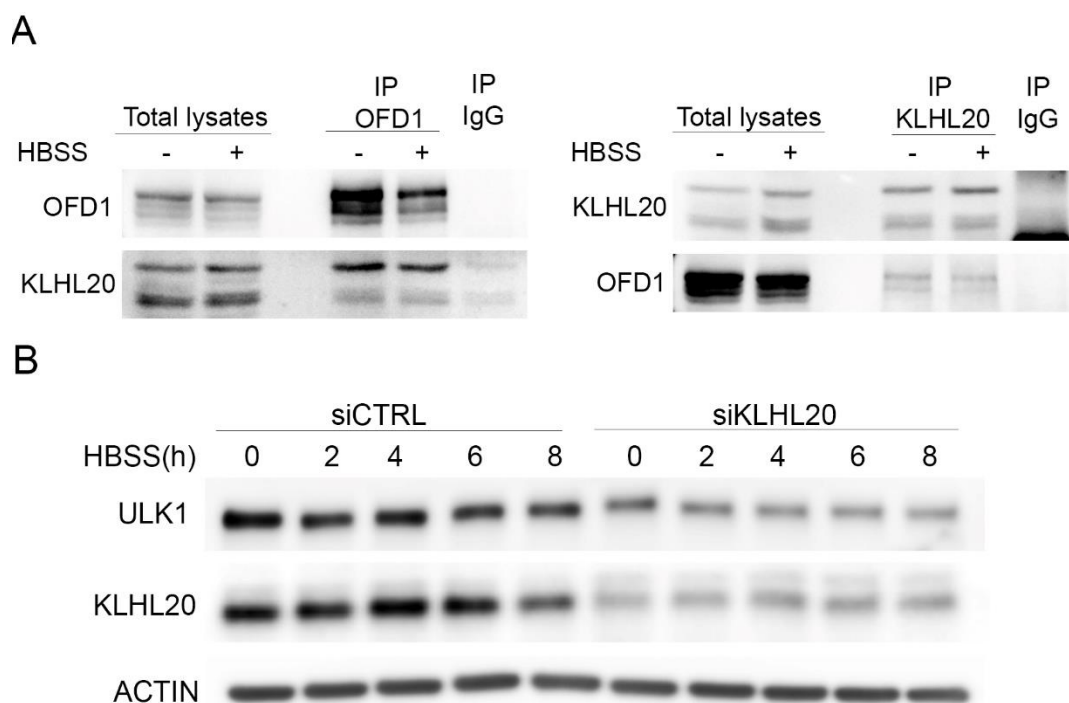


**Figure 25. OFD1 interacts with KLHL20.**

**(A)** Co-IP of endogenous OFD1 and KLHL20 in HEK-293 cells. Left panel shows the IP of endogenous OFD1 protein. Right panel shows the IP of endogenous KLHL20 protein. **(B)** WB analysis in HK2 cells transfected with siRNA against KLHL20 transcript. Cells were treated with HBSS for indicated times to induce ULK1 degradation.

## 6. ULK1 and ATG13 are degraded through different mechanisms

To understand how OFD1 could control the degradation of ULK1 and ATG13, I analysed whether they are degraded by autophagy or proteasome, the two main degradative pathways. I induced degradation of ULK1 and ATG13 through nutrient-depletion and I blocked proteasomal activity through Bortezomib, an inhibitor of the catalytic site of the 26S proteasome (Fig. 26A). Inhibition of proteasome reduces the degradation of ULK1 during starvation, but do not have any effects on ATG13 levels (Fig. 26A). Treatments with Bortezomib or MG-132, another proteasome inhibitor, upregulate ULK1 levels also in steady-state conditions, while do not affect ATG13 protein levels (Fig. 26B). These results demonstrate that ULK1 is mainly degraded by the proteasome, as already shown (Liu, Lin et al. 2016, Nazio, Carinci et al. 2016) while ATG13 is not influenced by proteasomal degradation.

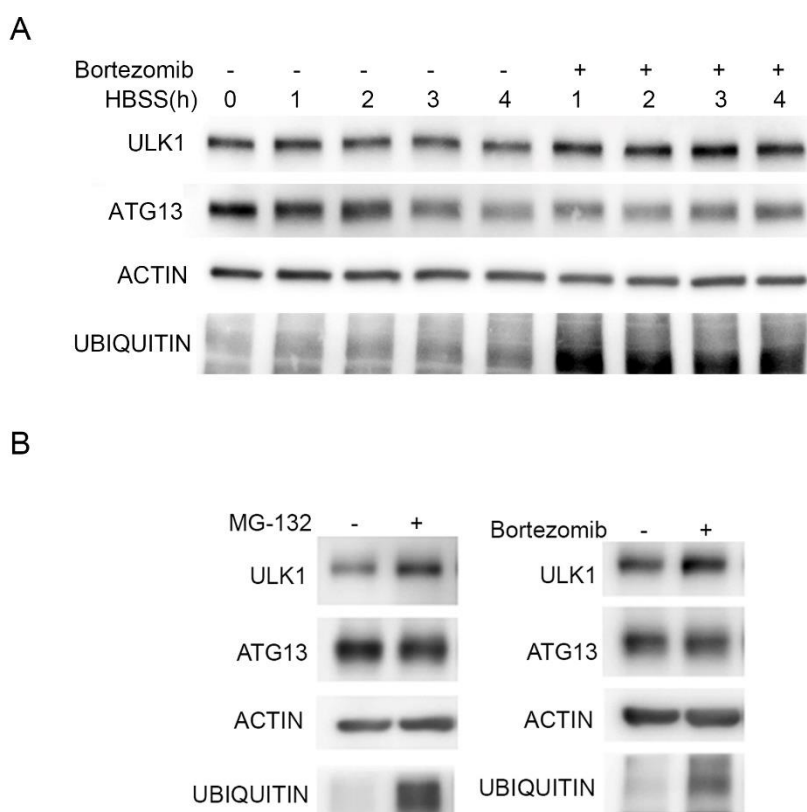


**Figure 26. ULK1 is mainly degraded by proteasome.**

**(A)** WB analysis of ULK1 and ATG13 degradation in HK2 cells treated with HBSS and Bortezomib (100nM) for the indicated times. **(B)** WB analysis in HK2 cells treated with MG-132 (10uM) or Bortezomib (100nM) for 2 hours.

At this point I analysed the effect of autophagy inhibition on the degradation of ULK1 and ATG13. I used KO-ATG9 autophagy-deficient cells treated with HBSS or cycloheximide to induce degradation of such proteins. The accumulation of p62 confirmed autophagy impairment in KO-ATG9 cells (Fig. 27A-B). Consistent with previous findings, ULK1 is normally degraded in autophagy-deficient cells, confirming that it is mainly degraded by the proteasome (Fig. 27A-B). In contrast, KO-ATG9 cells showed impaired degradation of ATG13, suggesting that, indeed, ATG13 is degraded by autophagy (Fig. 27A-B).

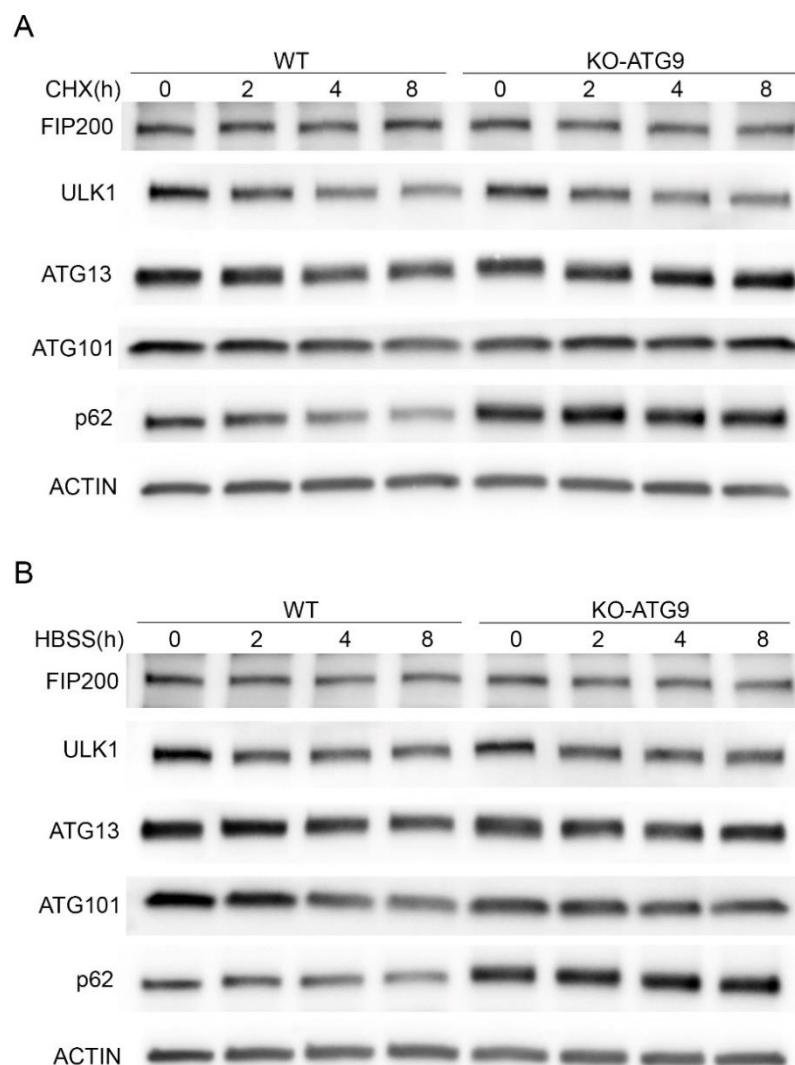


**Figure 27. ATG13 degradation is impaired in autophagy-deficient cells.**

**(A)** WB analysis in SAOS cells WT and KO-ATG9 treated with CHX (50ug/ml) for indicated times.

**(B)** WB analysis in SAOS cells WT and KO-ATG9 treated with HBSS for indicated times.

Treatment with autophagy inhibitors, SAR-405 and Baf, upregulate ATG13 protein levels, confirming this hypothesis (Fig. 28A-B). Interestingly, both ATG13 and OFD1 are increased by autophagy inhibition (Fig. 28A-B), suggesting that they are both autophagy substrates.

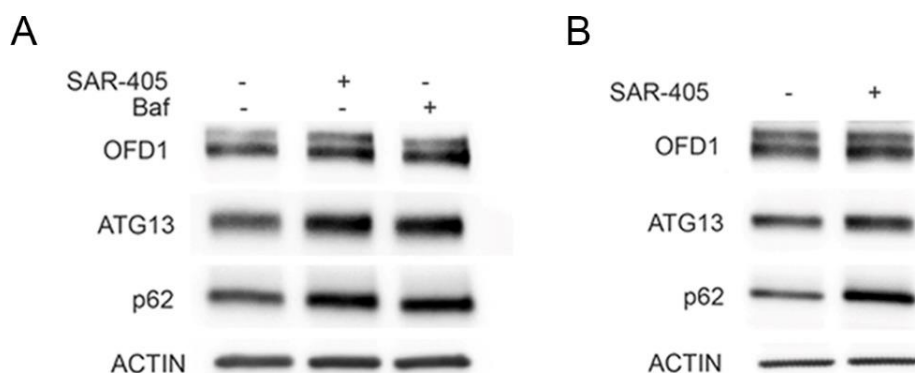


**Figure 28. Autophagy inhibition upregulates ATG13 and OFD1.**

**(A)** WB analysis in SAOS cells treated with SAR-405 (10uM) and Baf (100nM) for 6 hours. **(B)** WB analysis in HK2 cells treated with SAR-405 (10uM) for 6 hours.

## 7. Is OFD1 a novel selective autophagy receptor?

OFD1 binds LC3 and is an autophagy substrate (Tang, Lin et al. 2013). However, the interaction between OFD1 and LC3 has not been well-characterized. Analysis of the OFD1 protein sequence by using the iLIR server (<https://ilir.warwick.ac.uk/>) (Kalvari, Tsompanis et al. 2014) revealed the presence of six potential LIR motifs (Fig. 29). Further bioinformatics analysis and alignment of homologous proteins in *Homo sapiens*, *Mus musculus*, *Rattus norvegicus*, *Gallus gallus* and *Macaca mulatta* revealed that three of them (LIR1, LIR3 and LIR6) display high conservation across species (Fig. 29).

LIR motif (ADEFGLPRSK)(DEGMSTV)(**WFY**)(DEILQTV)(ADEFHIKLPSTV)(**ILV**)

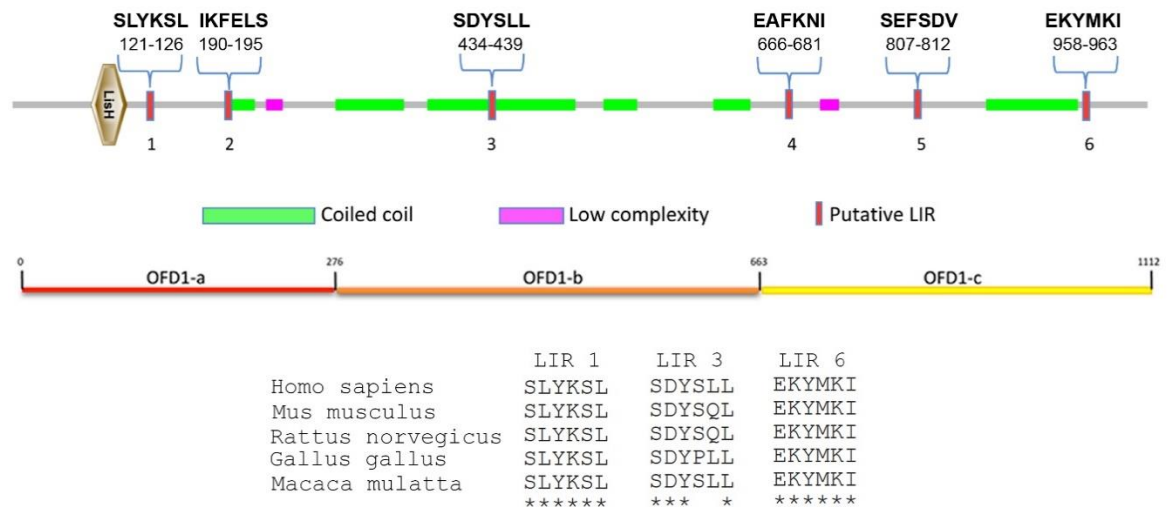


**Figure 29. OFD1 protein contains putative LIR motifs.**

Putative LIR sequences identified in the OFD1 protein sequence. Conservation of three representative LIRs across species is depicted in the lower panel.

As stated above, LIR motifs are characteristic of selective autophagy receptors, which promote the autophagic degradation of specific cargoes through the interaction with Atg8-family proteins (e.g. LC3 and GABARAP). Since OFD1 interacts with ATG13 and promotes its degradation, I hypothesized that OFD1 may functions as a selective autophagy receptor for ATG13.

First, I confirmed the interaction between LC3 and OFD1 through co-IP analysis and glutathione S-transferase (GST) pulldown assay. GFP-LC3 co-immunoprecipitated with 3xFLAG-OFD1 in HEK-293T transfected with both constructs (Fig. 30A). Accordingly, the 3xFLAG-OFD1 protein was pulled-down by the GST-LC3B protein bound to the glutathione sepharose 4B resin (Fig. 30B).



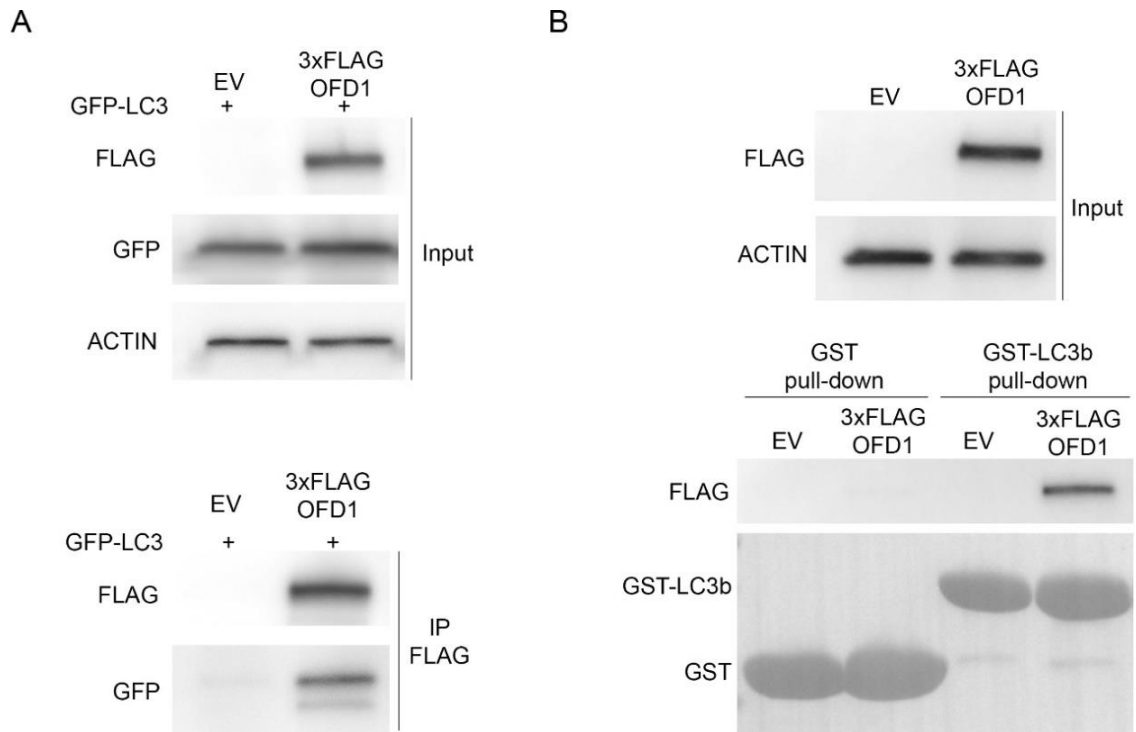


**Figure 30. OFD1 interacts with LC3.**

**(A)** FLAG immunoprecipitation in HEK-293T transfected with 3xFLAG-OFD1 and GFP-LC3. **(B)** GST pull-down of lysates from HEK-293T transfected with empty vector or 3-FLAG-OFD1.

Therefore, we started to mutagenize the putative LIRs identified in the OFD1 protein to demonstrate their functionality. The approach consists in the substitution of the two hydrophobic amino acids (positions 3 and 6 of the LIR sequence) into Alanine. Previous reports demonstrated that these mutations are sufficient to ablate the interaction with LC3 (Birgisdottir, Lamark et al. 2013).

Furthermore, to understand which portion of the OFD1 protein is able to interact with LC3, I used three fragments of the OFD1 proteins, already described (Giorgio, Alfieri et al. 2007), corresponding respectively to the N-terminal (A), central (B) and C-terminal regions (C) of OFD1 protein (Fig. 29-31). The results of these experiments demonstrated that only the A and C fragments are pulled-down by the GST-LC3B protein (Fig. 31), suggesting that these are the regions containing putative functional LIRs. Further experiments are currently ongoing in the laboratory to understand whether OFD1 is a novel autophagy receptor and whether the OFD1-LC3 binding is essential and/or necessary for ATG13 degradation.

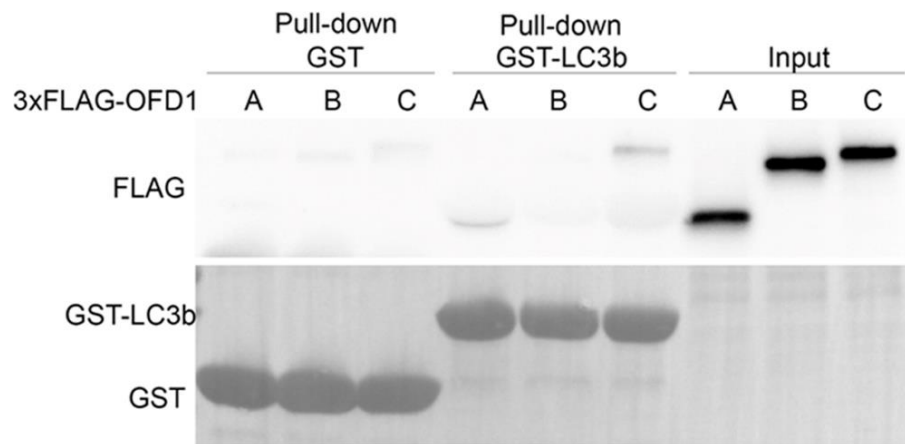


**Figure 31. OFD1 binds LC3 through the N-terminal and C-terminal regions of the protein.**

GST pull-down of lysates from HEK-293T cells transfected with the A, B and C portions of 3xFLAG-OFD1 protein.

## 8. Loss of *Ofd1* enhances autophagy *in vivo*

To test the physiological relevance of our observations I moved to *in vivo* models reproducing the features observed in OFDI syndrome. I analysed two different *Ofd1* murine models: the inducible model (*Ofd1*-IND) and the *Cre<sup>Ksp</sup>;Ofd1* conditional model. First, we set up conditions to study the autophagic flux in kidneys and treated fasted (6 hours) P7 wt pups by intraperitoneal injection of leupeptin, which is a lysosomal protease inhibitor. The results demonstrated that leupeptin is capable to reach the kidney and to block the renal autophagic flux as demonstrated by the specific increase of the LC3-II band observed in leupeptin treated animals compared to DMSO-only treated mice (Fig. 32A). We then moved to our models and in the *Ofd1*-IND model we demonstrated that *Ofd1* leupeptin-treated mutant kidneys showed increased levels of LC3-II compared to treated controls, demonstrating that loss of *Ofd1* causes increased autophagy *in vivo*, in kidneys at pre-cystic stages (Fig. 32B). This result indicate that enhanced autophagy is present before renal cyst formation and raised the question whether autophagy may contribute to the pathogenesis of the disease from the early phases of renal cysts formation.

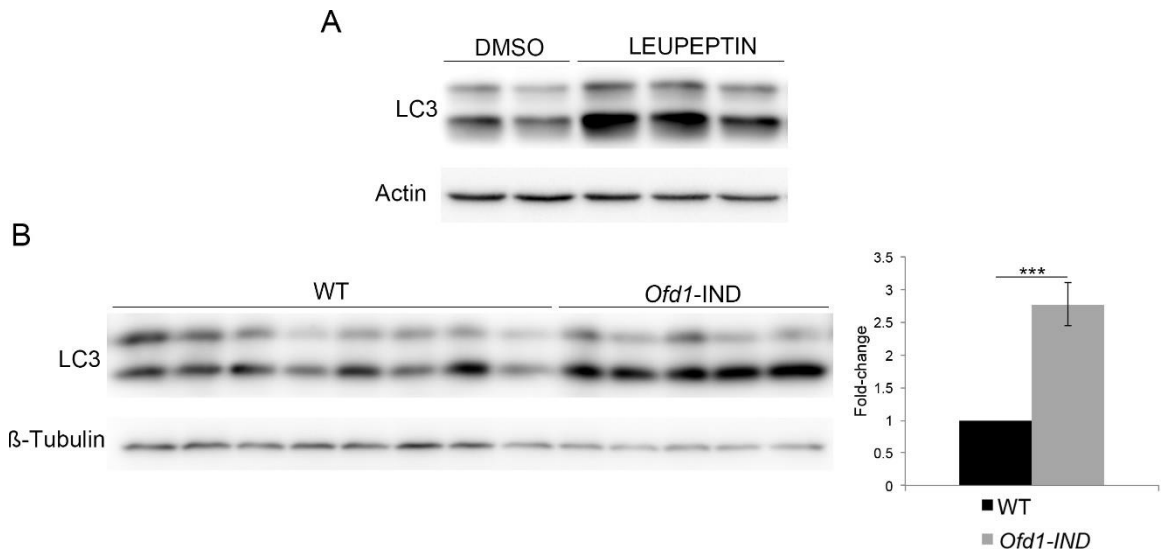


**Figure 32. Kidneys from *Ofd1*-IND mice showed increased autophagy.**

(A) WB analysis of LC3 protein in renal lysates from WT mice starved (6h) and treated with leupeptin. (B) WB analysis of LC3 protein in renal lysates from *Ofd1*-IND mice at P8. All mice have been starved (6h) and treated with leupeptin. Quantification of LC3-II band intensity represented as Fold-change of WT vs *Ofd1*-IND. Error bars show standard error mean (SEM). Student's t-test, \*\*\*P<0.001.

I confirmed these results also in the *Cre<sup>Ksp</sup>;Ofd1* conditional model, in which the *Ofd1* gene is specifically inactivated in the kidney (Zullo, Iaconis et al. 2010). Also in this case as described above mice were fasted and treated with leupeptin to block the autophagic flux. Also Kidneys from *Cre<sup>Ksp</sup>;Ofd1* treated mice showed increased LC3-II levels compared to treated WT mice (Fig. 33) from early cystic stages, confirming the enhancement of autophagy in two different *Ofd1* mutant models.

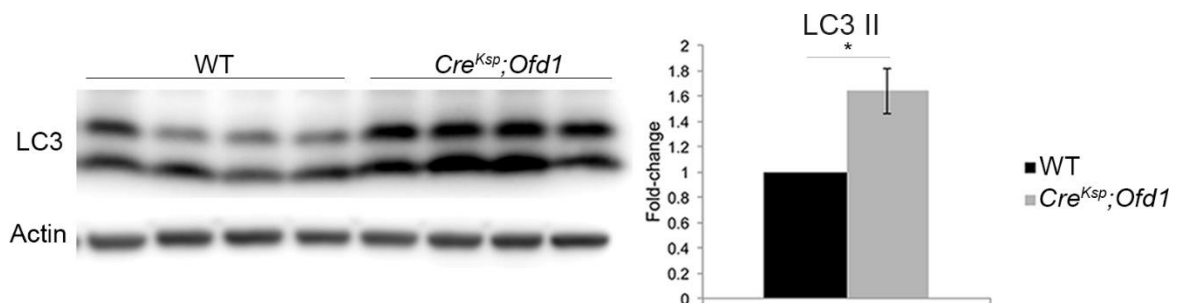


**Figure 33. Kidneys from *Cre<sup>Ksp</sup>;Ofd1* mice showed increased autophagy.**

WB analysis of LC3 protein in renal lysates from *Cre<sup>Ksp</sup>;Ofd1* mice at P13 (early cystic stage). All mice have been starved and treated with leupeptin. Quantification of LC3 II band intensity represented as Fold-change of WT vs *Cre<sup>Ksp</sup>;Ofd1*. Error bars show standard error mean (SEM). Student's t-test, \*P<0.05.

In line with data obtained *in vitro*, ATG13 protein levels were increased in kidneys from  $Cre^{Ksp};Ofd1$  mice both at pre-cystic and cystic stages (Fig.34).

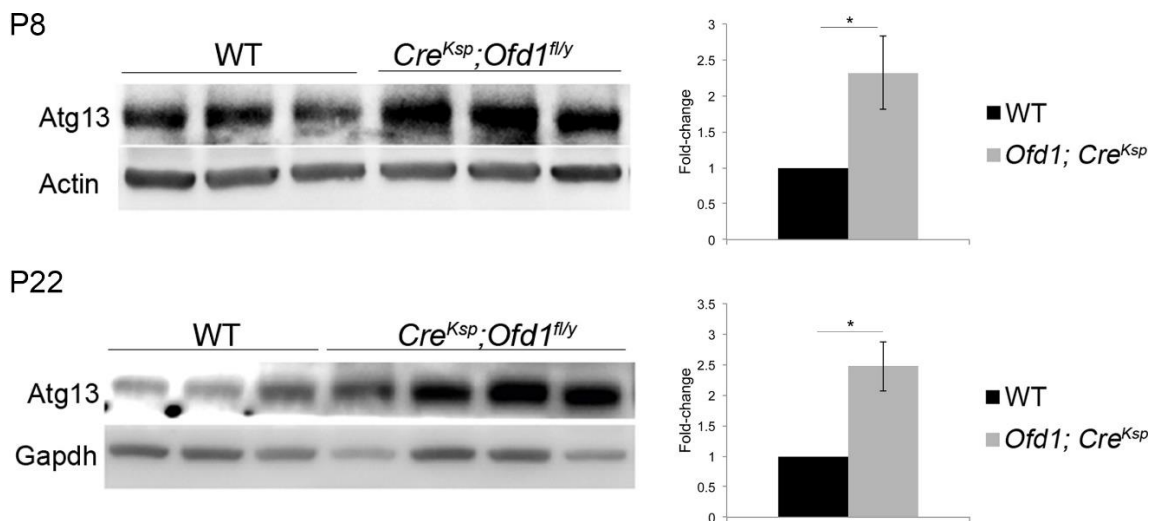


**Figure 34. ATG13 is increased in  $Cre^{Ksp};Ofd1$  mice.**

WB analysis of ATG13 protein in renal lysates from  $Cre^{Ksp};Ofd1$  mice at P8 (top, precystic stage) and P22 (bottom, cystic stage). Quantification of ATG13 band intensity represented as fold-change of WT vs  $Cre^{Ksp};Ofd1$  mice. Error bars show standard error mean (SEM). Student's t-test, \*P<0.05.

## 9. Inhibition of autophagy reduces renal cysts formation in *Ofd1* mutant mice

To understand if autophagy could contribute to the renal cystic phenotype observed in OFD type I syndrome, we crossed mice carrying *Ofd1* floxed alleles with *Atg7* deficient mice that were previously characterized and reported to display impaired starvation-induced and constitutive autophagy (Komatsu, Waguri et al. 2005). Kidneys derived from *Atg7* deficient mice appeared normal and without any evident morphological alterations (Fig. 35A).  $Cre^{Ksp};Ofd1^{-/y};Atg7^{fl/fl}$  mice showed decreased number of renal cysts compared to  $Cre^{Ksp};Ofd1^{-/y}$  mice (Fig. 35B-C) demonstrating that inactivation of ATG7 in these mice attenuates cysts formation. These data suggest that the increased autophagy observed in *Ofd1* mutant kidneys may contribute to the pathogenesis of renal cystic disease.

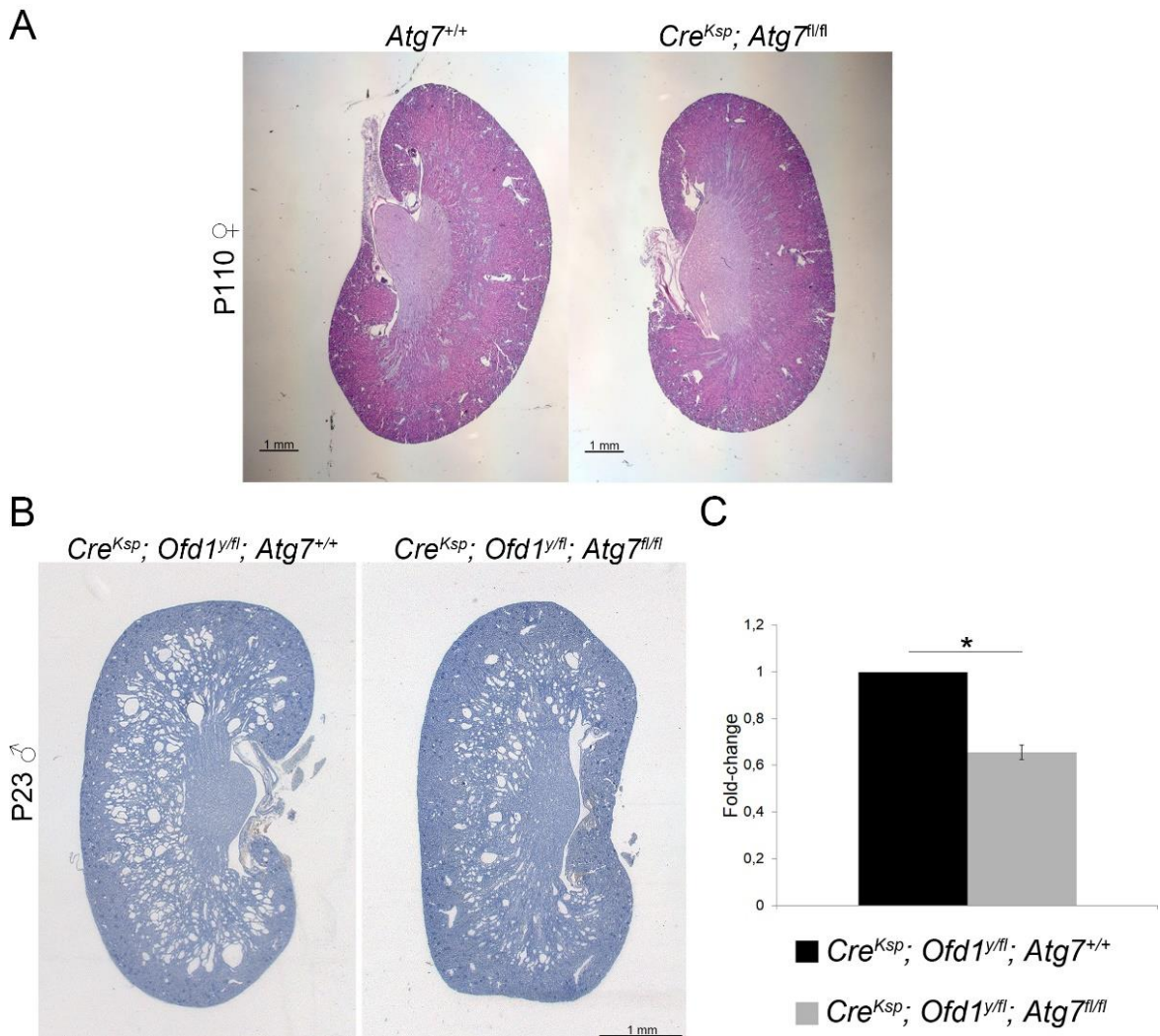


**Figure 35. Inhibition of autophagy reduces renal cysts formation in *Ofd1* mutant mice.** (A) Haematoxylin/Eosin staining of renal sections from  $Cre^{Ksp}; Atg7^{fl/fl}$  mice at P110. (B) Haematoxylin/Eosin staining of renal sections from  $Cre^{Ksp}; Ofd1^{-y}; Atg7^{fl/fl}$  male mice at P23. (C) Quantification of cysts number of kidneys from  $Cre^{Ksp}; Ofd1^{-y}; Atg7^{fl/fl}$  mice compared to their control mice. Values are expressed as fold-change considering  $Cre^{Ksp}; Ofd1^{-y}; Atg7^{fl/fl}$  as 1. Error bars show standard error mean. Student's t-test, \* $P < 0.05$ .

Based on the data described above, we hypothesize that inhibition of autophagy may represent a strategy to ameliorate the renal cystic phenotype. We thus treated  $Cre^{Ksp}; Ofd1$  with the autophagy inhibitor CQ and compared the results with  $Cre^{Ksp}; Ofd1$  mice treated with vehicle only. Histological evaluation of the kidneys revealed that also CQ treatment lead to reduction in the number of renal cysts (Fig.36).

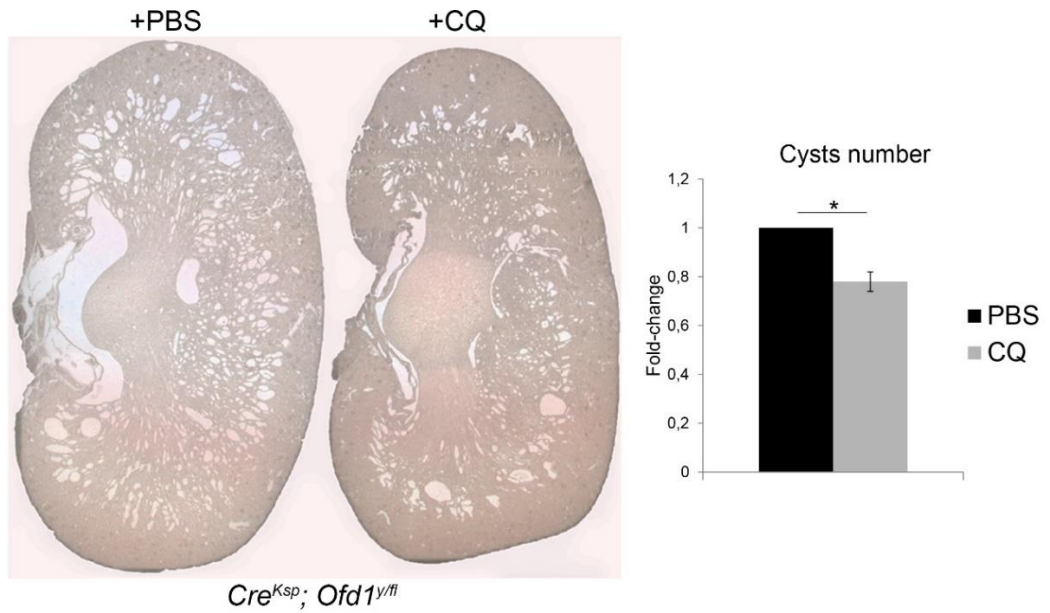


**Figure 36. Chloroquine reduces cysts number in kidneys from *Ofd1* mutant mice.** Histological analysis of renal sections from *Cre<sup>Ksp</sup>;Ofd1<sup>y/fl</sup>* mice at P23 treated with PBS or CQ. Graph shows the fold-change of cysts number of PBS vs CQ treated mice  $\pm$ SEM. Student's t-test, \*P<0.05.

These results suggest that autophagy inhibition could be a new promising therapy to inhibit cyst formation in cystic kidney disease. This pharmacological approach could be associated with other drugs to slow down the progression of the disease.

## Discussion

Primary cilia are sensory organelles that allow cells to sense different stimuli thus activating various signaling pathways. As such, disruption of the primary cilium causes deregulation of different cellular processes (Satir, Pedersen et al. 2010). Recent studies showed that primary cilia are important also for autophagy activation. Cells with compromised cilia are not able to efficiently induce autophagy through a still undefined mechanism (Pampliega, Orhon et al. 2013). Deregulation of cilia-mediated signaling pathways such as mTOR and/or the Hh signaling have been involved in autophagy inhibition in cilia-depleted cells (Pampliega, Orhon et al. 2013, Wang, Livingston et al. 2015). However, other ciliary signaling could be involved in cilia-mediated autophagy and further studies are required to understand this relationship. During the PhD training, my project involved the investigation of the role of the centrosomal/basal body protein OFD1 in autophagy. OFD1 is required for primary cilium formation and in fact OFD1-depleted cells do not form primary cilia. In contrast with previous studies, my results showed that loss of OFD1 results in impaired cilia formation and enhanced autophagy, suggesting that ciliary dysfunction is not always associated with autophagy deficiency. Another example comes from studies of pancreatic ductal adenocarcinoma (PDAC) cells, in which loss of primary cilia is associated to increased autophagy (Seeley, Carrière et al. 2009, Perera, Stoykova et al. 2015). Therefore, ciliary proteins may have different roles in autophagy regulation depending on the pathway or the cell type involved. Moreover, I found that OFD1 modulates autophagic processes independently from the presence of primary cilia, suggesting that OFD1 is directly involved in autophagy regulation and does not need cilia to exert this role. We also analyzed mTOR, a key regulator of autophagy. When active, mTORC1 promotes anabolic processes such as protein, lipid and nucleotide synthesis, and represses catabolic processes, such as autophagy. Our study demonstrates that OFD1-depleted cells show increased

autophagy although they display higher mTOR activity, suggesting that OFD1 could act downstream the mTOR pathway and that mTOR is not responsible for the enhanced autophagy observed in OFD1 depleted models.

Numerous experimental evidences obtained by others in our laboratory reveal that OFD1 is localized on autophagosome forming sites supporting a direct role for this ciliary protein in the control of autophagosome biogenesis. This hypothesis is confirmed by the interaction of OFD1 with the ULK1 complex which represents the first step in autophagy induction.

It has been shown that contrary to what demonstrated in yeast, the formation of the ULK1 complex in mammals is not influenced by nutrients (Jung, Jun et al. 2009, Zachari and Ganley 2017). Here we show that although the OFD1-ATG13 interaction seems to be nutrient dependent, FIP200, ULK1 and ATG13 interact with each other and regularly form the complex in the absence of OFD1 suggesting that OFD1 is not necessary for the formation of the complex.

However, my results demonstrate that OFD1 modulates the activity of the ULK1 complex by regulating the stability of its components. Different studies revealed that stability of the ULK1 complex is affected by the protein levels of its components. Depletion of ATG13 or FIP200 leads to decreased stability of ULK1 (Ganley, Lam et al. 2009, Jung, Jun et al. 2009). My results indicate that in the absence of OFD1, ULK1 and ATG13 are more stable, thus promoting the kinase activity of the complex and subsequently enhancing autophagy in KO-OFD1 cells. Conversely, over-expression of OFD1 promotes degradation of ULK1 and ATG13, causing autophagy inhibition.

Which are the mechanisms through which OFD1 regulates degradation of ULK1 and ATG13? This is still an open question and is currently under investigation in our laboratory. Several post-translational modifications can modulate the stability of ULK1 or ATG13 (Fig. 9). The presence of mono-ubiquitination of ATG13 in KO-



OFD1 cells (Fig. 24) could have an important role on its stability or function. However, additional experiments are required to prove or disprove this hypothesis. During the investigation of the mechanisms involved in the degradation of the ULK1 complex, I found that both OFD1 and ATG13 are degraded through autophagy. Moreover, preliminary results showed that ATG13 is not degraded by OFD1 when autophagy is inhibited, suggesting that OFD1 promotes degradation of ATG13 through the autophagic process.

The identification of putative LIR domains in the OFD1 protein sequence supported this hypothesis and we hypothesize that OFD1 may function as a selective autophagy receptor for ATG13. To understand whether the interaction between OFD1 and LC3 could be responsible for ATG13 degradation, we decided to mutagenize the putative LIRs identified in OFD1. According to my hypothesis, the OFD1 protein mutated in the functional LIR region should not induce autophagic degradation of ATG13, therefore, it should not inhibit autophagy. According to this hypothesis OFD1 may be a new selective autophagy receptor, responsible for the degradation of a core autophagy protein (ATG13) to restrain ULK1 activity and consequently autophagy activation. This could represent an important feedback mechanism for the control of autophagy activation during starvation. The experiments are still ongoing and, to date, I don't have a definite answer.

The presence of functional LIR domains in OFD1 could highlight new possible cellular functions for this already versatile protein. The OFD1 protein sequence is characterized by many coiled coil domains important for protein-protein interactions. OFD1 may act as scaffold for different cargoes and mediate their autophagic degradation through LC3. Different ciliary proteins are degraded by autophagy, and OFD1 may be an important mediator of this process, referred to as ciliophagy (Cloonan, Lam et al. 2014). The modulation of ciliary protein levels through autophagy might influence primary cilia formation and resorption. The elucidation of

the role of OFD1 in autophagy and the definition of the selective processes in which OFD1 is involved could shed new light towards understanding the complicate link between autophagy and ciliogenesis.

As mentioned above, the OFD1 protein is located at centrosome. The involvement of this centrosomal protein in autophagy highlights the link between centrosomes and autophagy. These organelles have been described as important signaling centers for GABARAP-mediated autophagy (Joachim, Razi et al. 2017). The centrosomal protein PCM1, a known interactor of OFD1, interacts with GABARAP through a LIR domain (Joachim, Razi et al. 2017). OFD1 presents many interesting similarities with PCM1, such as the binding with an Atg8 family protein (LC3) and the localization at centriolar satellites. Considering the similarity between the two proteins, OFD1 and PCM1 may collaborate in autophagy regulation. Also in this case, additional studies are required to understand their roles and how they connect the centrosome to autophagy.

The results illustrated in this thesis clearly show that OFD1 impairment results in enhanced autophagy both in *in vitro* and *in vivo* models of OFD type I syndrome and I also demonstrated the same in lymphoblastoid cell lines obtained from OFDI patients. The autophagy deregulation observed could contribute to the different clinical manifestations observed in the disease. As stated above, autophagy has an essential role during development, thus it could be involved in some of the developmental abnormalities observed in OFDI patients. Similarly to what described for other inherited disorders associated to ciliary dysfunction, OFDI patients display neurological abnormalities (Del Giudice, Macca et al. 2014) and it has been demonstrated that OFD1 plays a crucial role in forebrain development and in early corticogenesis (D'Angelo, De Angelis et al. 2012). It is tempting to speculate that autophagy regulation may be involved in the role of OFD1 in brain development.

Moreover, most of the OFDI patients display skeletal abnormalities (Macca and Franco 2009) and conditional inactivation of *Ofd1* in early limb buds results in mineralization defects during endochondral bone formation (Bimonte, De Angelis et al. 2011). Autophagy has been shown to play an important role in mineralization and bone homeostasis (Nollet, Santucci-Darmanin et al. 2014), thus it may be involved in the skeletal defects observed in OFDI syndrome. In both cases specifically designed experiments will give the answers to these questions.

Since autophagy has been mainly proposed as a protective mechanism, the harmful effects of increased autophagy are not widely described in the scientific literature.

Autophagy has been clearly linked to cancer (White 2015). In cancer cells, increased autophagy can provide substrates for high-level metabolism and promote cell proliferation (White 2015). Renal cystic disease, one of the hallmarks of ciliopathies and OFD type I syndrome, shares important traits with cancer, such as higher proliferation rate and altered metabolism (Seeger-Nukpezah, Geynisman et al. 2015). Increased autophagy could cause cyst-lining cells to change metabolism and to hyper-proliferate, contributing to the progression of the renal disease.

Another effect of excessive autophagy is cell death (Shi, Weng et al. 2012). The increased apoptosis contributes to cystogenesis in polycystic kidneys and is associated with progressive loss of normal nephrons (Goilav 2011). Increased autophagy could cause excessive apoptosis in cystic kidneys of OFDI patients promoting the progression of the renal disease. Staining with the anti-cleaved Caspase-3 antibody in kidneys from *Cre<sup>Ksp</sup>;Ofd1* mice confirmed a moderate increase in apoptotic cells in the epithelial layer lining the cysts in the dilated renal tubules (Zullo, Iaconis et al. 2010).

Finally, increased autophagy could cause excessive degradation of specific proteins involved in the pathogenesis of the disease. For example, the Polycystin 1 (PC1) protein, codified by PKD1, one of the transcripts responsible for ADPKD, is

degraded by autophagy (Pema, Drusian et al. 2016) and its dosage is strictly connected with disease severity (Hopp, Ward et al. 2012). The enhanced autophagic degradation of PC1 in *Ofd1* mutant mice may cause and/or contribute to renal cystogenesis. For this reason, autophagy inhibition may ameliorate the cystic phenotype blocking PC1 degradation. Crossing *Ofd1* mutant mice with *Pkd1* mice could clarify the role of PC1 dosage in OFD type I syndrome.

Recent studies showed a beneficial effect of metformin in zebrafish and mouse models of ADPKD (Takiar, Nishio et al. 2011, Chang, Ma et al. 2017). Metformin is a pharmacological activator of AMPK and is widely used in clinics. AMPK stimulation results in mTOR inhibition and consequently autophagy enhancement. The authors suggested that autophagy activation could have therapeutic potential for ADPKD treatment (Takiar, Nishio et al. 2011, Chang, Ma et al. 2017). However, the involvement of autophagy in the beneficial effect of metformin is not clear. Metformin inhibits the cystic fibrosis transmembrane conductance regulator (CFTR), which is responsible for the fluid secretion in cyst lumen (Takiar, Nishio et al. 2011). Moreover, metformin-mediated inhibition of mTOR signaling slows the proliferation of cystic epithelial cells (Takiar, Nishio et al. 2011). The modulation of these pathways could play a major role on the therapeutic effect of metformin in ADPKD models.

Another recent paper revealed that treatment with autophagy activators attenuates cyst formation in a zebrafish model of ADPKD (Zhu, Sieben et al. 2017). This supports the hypothesis that autophagy modulation could be a modifying event for cystogenesis. However, the role of autophagy in renal cystic disease is controversial: we demonstrated that in OFDI animal models autophagy is enhanced while it has been shown that autophagy is inhibited in ADPKD models.

As discussed above, an increasing number of ciliary/centrosomal proteins involved in autophagy are being discovered. In contrast to what shown for other ciliary

proteins, my results demonstrated that loss of OFD1 results in increased autophagy. It is plausible that cilioproteins play different roles in autophagy and only detailed and specific studies analyzing the autophagic profile of a significant number of cilioproteins will clarify this issue. Different experimental evidence indicates a link between autophagy and renal cystic disease and I propose that the protein imbalance caused by autophagy deregulation could be involved in ciliopathy-associated conditions, including renal cystic disease. Therefore, modulation of autophagy could have a therapeutic value in ciliopathies. The recognition of a role for autophagy in the pathogenesis of PKD is of high clinical relevance. Our data indicate autophagy deregulation in the early phases of renal cysts formation and we believe that dissection of the molecular mechanisms underlying the initial phases of renal cyst formation will allow designing therapeutic approaches that could prevent cysts formation and/or slow down progression of renal cystic disease thus disclosing new therapeutic avenues for renal cystic disease.

## **Materials & Methods**

### **Cell culture, treatments and transfection**

Human Kidney 2 (HK-2) cells were grown in DMEM/F12 medium (Gibco 11330057) supplemented with 5% FBS, 1mM glutamine, 1X Insulin-transferrin-sodium selenite (Sigma I1884) and 1X Penicillin/Streptomycin (ECB3001D). Sarcoma osteogenic cells (SAOS) KO-ATG9 were a gift of Carmine Settembre and are still unpublished. SAOS cells were grown in McCoy's 5a Medium Modified (Gibco 16600082) supplemented with 15% FBS, 1mM glutamine, 1X Penicillin/Streptomycin. Cells were grown at 37 °C with 5% CO<sub>2</sub>. To induce ciliogenesis, HK2 cells were starved for 16h with DMEM/F12 without FBS. To induce autophagy, cells have been starved with HBSS (HEPES 10 mM). Bafilomycin (Sigma B1793) was used at 100nM to block the autophagic flux. Chloroquine (Sigma H0915) was used at 50 uM and SAR-405 (ApexBIO A8883) at 10uM. Proteasome inhibition was performed using Bortezomib (100nM) and MG-132 (10uM).

For amino acid starvation and stimulation experiments, the cell culture medium was amino acid-free RPMI 1640 (US Biological) supplemented with 10% dialyzed FBS (Invitrogen, Thermo Fisher Scientific). After 1 hour of starvation, a complete amino acid RPMI 1640 medium was added back to the cells.

Cells were transfected with TransIT®-LT1 Transfection Reagent (Mirus MIR 2304) according to the manufacturer's instructions and harvested after 48h. Transfection of siRNA was performed using Interferin (Polyplus 409). Cells were harvested after 96h for the WB analysis.

### **Plasmids and siRNAs**

The construct 3xFLAG-OFD1 codifies for the OFD1 protein with a 3xFLAG tag in N-terminal region and was already described (Giorgio, Alfieri et al. 2007, Iaconis, Monti et al. 2017). The plasmids expressing the 3 portions of OFD1 protein (3xFLAG-

OFD1A, 3xFLAG-OFD1B, 3xFLAG-OFD1C) were already described (Giorgio, Alfieri et al. 2007). The empty vector is the p3xFLAG-CMV<sup>TM</sup>-10 Expression Vector (E7658 Sigma). GFP-LC3 and GFP-p62 plasmids were provided by Dr. Carmine Settembre (Cinque, Forrester et al. 2015). FLAG-VPS34 was a gift from Ruey-Hwa Chen (Liu, Lin et al. 2016). HA-Ubiquitin construct was provided by Dr. Lucia Di Marcotullio (Di Marcotullio, Ferretti et al. 2006). GST-LC3b and GST plasmids were a gift from Dr. Paolo Grumati (Grumati, Morozzi et al. 2017). pMXs-IP-EGFP-hAtg13 was a gift from Noboru Mizushima (Addgene plasmid #38191). myc-hULK1 was a gift from Do-Hyung Kim (Addgene plasmid #31961).

*OFD1* and *KLHL20* silencing were performed with ON-TARGETplus siRNA SMARTpool (Dharmacon) against *OFD1* and *KLHL20* transcripts respectively.

### **Western blot and co-immunoprecipitation**

Total protein extracts from cells and tissues were obtained by using RIPA buffer (150 mM NaCl, 1.0% IGEPAL® CA-630, 0.5% sodium deoxycholate, 0.1% SDS, 50 mM Tris, pH 8.0) completed with a mix of inhibitors of proteases (P8340 Sigma) and phosphatases (PHOSS-RO Roche). Mouse kidneys were disrupted using the Qiagen TissueLyser. The extracted proteins were separated by SDS-PAGE and then transferred onto Immobilon-P PVDF membrane (IPVH00010). Membranes were blocked with BSA or 5% non-fat milk and then incubated with the respective antibodies. Cells for co-Immunoprecipitation were lysed in lysis buffer (50 mM Tris-HCl, 1 mM EDTA, 10 mM MgCl<sub>2</sub>, 5 mM EGTA, 0.5% Triton X-100, pH 7.28), 1 mg of lysate was incubated with specific antibodies and IgG, as control. Co-IP was performed using Protein A/G PLUS-Agarose (Santa Cruz sc-2003), the immunoprecipitated beads were washed three times with lysis buffer and then eluted with the Laemmli sample buffer. Band intensities were quantified by ImageJ and fold-change between two groups was calculated. Western blot quantifications

showed the mean of fold-changes calculated in at least three different experiments. Error bars represent the standard error of the mean (SEM). The significance of the results was calculated by Student's t-test and reported as p-value. Symbol meaning: \* P<0,05; \*\* P<0,01; \*\*\* P<0,001.

## Antibodies

The antibody anti-OFD1 was generated against the human full-length OFD1 protein and was used for WB analyses (Ferrante, Zullo et al. 2006, Giorgio, Alfieri et al. 2007). All other antibodies used in this study are commercially available and are listed below.

Antigen	Company	Catalog Number	Application
ACETYL-TUBULIN	SIGMA	AT7451	IF
ACTIN	SIGMA	A5316	WB
ATG13	CELL SIGNALING	13273	WB; IP
ATG101	CELL SIGNALING	13492	WB
BETA-TUBULIN	SIGMA	T4026	WB
FIP200	PROTEINTECH	17250-1-AP	WB; IP
FLAG	SIGMA	F1804	WB; IP
GAPDH	SANTA CRUZ	SC-32233	WB
GFP	ABCAM	AB290	WB; IP
HA	BIOLEGEND	901502	WB
KLHL20	SANTA CRUZ	SC-515381	WB; IP
LC3B	NOVUS BIO	NB100-2220	WB
MYC	MILLIPORE	05-724	WB; IP
OFD1	SIGMA	HPA031103	IP
P62	ABNOVA	H00008878	WB



p-ATG13 (S318)	ROCKLAND	600-401-C49	WB
p-S6 (S240)	CELL SIGNALING	2215	WB
p-S6K1 (T389)	CELL SIGNALING	9205	WB
p-ULK1 (S757)	CELL SIGNALING	6888	WB
p-VPS34 (S249)	CELL SIGNALING	13857	WB
S6	CELL SIGNALING	2217	WB
S6K1	CELL SIGNALING	9202	WB
UBIQUITIN	SANTA CRUZ	SC-8017	WB
ULK1	CELL SIGNALING	8054	WB
VPS34	SANTA CRUZ	SC-365404	WB

### **Ubiquitination assays**

The analysis of ULK1 and ATG13 ubiquitination was performed transfecting HEK-293T cells with respective constructs and HA-ubiquitin. Cells were treated with MG132 for 16 hr or subjected to starvation (HBSS) for reported time periods. Cells were lysed with RIPA lysis buffer, and lysates were used for immunoprecipitation with anti-MYC or anti-GFP and followed by western blot with anti-HA to detect UBIQUITIN signal.

### **GST pull-down assay**

GST and GST-LC3B plasmids were expressed in Escherichia coli BL21 (DE3) cells. Expression was induced by addition of 0.5 mM IPTG in LB medium and cells were incubated at 37°C for 5 hours. Harvested cells were lysed using sonication in a lysis buffer (20 mM Tris-HCl pH 7.5, 10 mM EDTA, 5 mM EGTA, 150 mM NaCl) and GST fused proteins were immuno-precipitated using Glutathione Sepharose 4B beads (GE Healthcare). Fusion protein-bound beads were used directly in GST pull down assays. HEK293T cells were transfected with indicated constructs and cell lysates

were mixed with GST fusion protein-loaded beads and incubated over-night at 4°C. Beads were then washed five times in lysis buffer, resuspended in Laemmli buffer and boiled. Supernatants were loaded on SDS-PAGE.

### **Histological and immunofluorescence analysis**

For immunofluorescence experiments, cells were fixed in PFA 4%. Blocking was performed in PBS 0.05% Saponin, 0,5% BSA. The primary antibodies used was anti-acetylated tubulin antibody (cat. no. T6793, Sigma-Aldrich). Analysis at the microscopy was performed with a LEICA SPE confocal microscope with a 63x oil objective.

For histological assay, isolated kidneys were fixed in 4% paraformaldehyde in PBS buffer at 4°C overnight. After fixation, the tissue was dehydrated with increasing concentrations of ethanol, cleared with xylene and embedded in paraffin. The tissue was sectioned using a microtome and hematoxylin–eosin staining was performed on paraffin sections. Representative images of hematoxylin–eosin-stained kidneys were acquired. Cysts number was counted manually with ImageJ software in at least 5 different sections of each sample.

### **Real-time PCR and Primers**

RNA was extracted from cells using the RNeasy Mini Kit from QIAGEN (74106). cDNA was obtained with QuantiTect Reverse Transcription Kit from QIAGEN. The LightCycler® 480 SYBR Green I Master Mix (04707516001) was used for all samples for Real-time PCR. The  $\Delta\Delta CT$  method was used for statistical analysis to determine gene expression levels. Primers that amplify the *ACTIN* transcript were used as internal reference. Primers used for real-time PCR are listed below.

*hFIP200*-FW (5'-GGATCTCAAACCAGGTGAGGG-3')

*hFIP200*-REV (5'-GTGCCTTTTTGGCTTGACAGT-3')

*hULK1-FW* (5'-CTGGTCCTCTTGCTTCCGTC-3')

*hULK1-REV* (5'-ACACCAGCCCAACAATTCC-3')

*hATG13-FW* (5'-GACCTTCTATCGGGAGTTTCAG-3')

*hATG13-REV* (5'-GGGTTTCCACAAAGGCATCAAAC-3')

*hACTIN-FW* (5'-AGAGCTACGAGCTGCCTGAC-3')

*hACTIN-REV* (5'-AGCACTGTGTTGGCGTACAG-3')

### **Animal models**

The generation of *Ofd1* floxed mice was previously described (Ferrante, Zullo et al. 2006). *Ofd1-IND* mice (Iaconis, Monti et al. 2017) were obtained crossing *Ofd1<sup>fl/+</sup>* females with CAGGCre-ER<sup>TM</sup> mice, a transgenic mouse line in which Cre-ER<sup>TM</sup> is ubiquitously expressed to permit, temporally regulated, Cre-mediated recombination in diverse tissues of the mouse (Hayashi and McMahon 2002). For induction of Cre activity at birth in the inducible model, tamoxifen administration was performed once at E18.5 in the pregnant mother *Ofd1<sup>fl/fl</sup>* crossed with CAGGCre-ER<sup>TM</sup> male. *Ofd1-IND* male mice are viable and develop kidney cysts starting from P10. *Cre<sup>Ksp</sup>;Ofd* mice are characterized by kidney-specific inactivation of *Ofd1* (Zullo, Iaconis et al. 2010). They were obtained by crossing females *Ofd1<sup>fl/+</sup>* with the *Cre<sup>Ksp</sup>* transgenic line in which Cre recombinase is specifically expressed in renal tubular epithelial cells and the developing genitourinary tract under the control of the *Ksp-cadherin* (*Cdh16*) gene promoter (Zullo, Iaconis et al. 2010). To block autophagic degradation mice were starved and injected intra-peritoneally with leupeptin (50 mg/kg) for 6h. *Atg7<sup>fl/fl</sup>* mice were previously described, they are characterized by impairment of starvation-induced and constitutive autophagy (Komatsu, Waguri et al. 2005). *Cre<sup>Ksp</sup>;Atg7<sup>fl/+</sup>* mice, with renal specific inactivation of *Atg7*, were obtained crossing *Cre<sup>Ksp</sup>* mice with *Atg7<sup>fl/fl</sup>* mice. *Cre<sup>Ksp</sup>;Atg7<sup>fl/+</sup>* were crossed with *Ofd1<sup>fl/fl</sup>;Atg7<sup>fl/fl</sup>* mice to obtain *Cre<sup>Ksp</sup>;Ofd<sup>fl/+</sup>;Atg7<sup>fl/fl</sup>* and

$Cre^{Ksp};Ofd^{fl/y};Atg7^{fl/fl}$  mice. These mice are viable and are characterized by the inactivation of both *Atg7* and *Ofd1* in the kidney.

To block autophagic degradation, mice were starved and treated by intraperitoneal injection of leupeptin (50 mg/kg). The animals were sacrificed 6 hours after the treatment. To address the effect of autophagy blockade on cysts formation, mice were treated with either vehicle alone or chloroquine (50mg/kg) (Sigma H0915) by daily intraperitoneal injection from P8 to P23.

## **Contributions**

Elvira Damiano generated the KO-OFD1 HK2 cells used in this thesis using CRISPR/Cas9 technology. Serena Maione performed WB analysis of LC3 in kidneys from  $Cre^{Ksp};Ofd1$  mice illustrated in Fig 33. Daniela Iaconis generated the  $Cre^{Ksp};Ofd1^{fl};Atg7^{fl}$  mice and performed all the treatments in mice used to generate the data illustrated in Fig 32-33-36.

## References

- Abada, A. and Z. Elazar (2014). "Getting ready for building: signaling and autophagosome biogenesis." EMBO Rep **15**(8): 839-852.
- Alemu, E. A., T. Lamark, K. M. Torgersen, A. B. Birgisdottir, K. B. Larsen, A. Jain, H. Olsvik, A. Øvervatn, V. Kirkin and T. Johansen (2012). "ATG8 Family Proteins Act as Scaffolds for Assembly of the ULK Complex: SEQUENCE REQUIREMENTS FOR LC3-INTERACTING REGION (LIR) MOTIFS." Journal of Biological Chemistry **287**(47): 39275-39290.
- Arquint, C., A.-M. Gabryjonczyk and E. A. Nigg (2014). "Centrosomes as signalling centres." Philosophical Transactions of the Royal Society B: Biological Sciences **369**(1650): 20130464.
- Avasthi, P., R. L. Maser and P. V. Tran (2017). "Primary Cilia in Cystic Kidney Disease." Results Probl Cell Differ **60**: 281-321.
- Axe, E. L., S. A. Walker, M. Manifava, P. Chandra, H. L. Roderick, A. Habermann, G. Griffiths and N. T. Ktistakis (2008). "Autophagosome formation from membrane compartments enriched in phosphatidylinositol 3-phosphate and dynamically connected to the endoplasmic reticulum." The Journal of Cell Biology **182**(4): 685-701.
- Barker, A. R., R. Thomas and H. R. Dawe (2014). "Meckel-Gruber syndrome and the role of primary cilia in kidney, skeleton, and central nervous system development." Organogenesis **10**(1): 96-107.
- Barth, S., D. Glick and K. F. Macleod (2010). "Autophagy: assays and artifacts." The Journal of pathology **221**(2): 117-124.
- Belibi, F., I. Zafar, K. Ravichandran, A. B. Segvic, A. Jani, D. G. Ljubanovic and C. L. Edelstein (2011). "Hypoxia-inducible factor-1alpha (HIF-1alpha) and autophagy in polycystic kidney disease (PKD)." Am J Physiol Renal Physiol **300**(5): F1235-1243.
- Bimonte, S., A. De Angelis, L. Quagliata, F. Giusti, R. Tammara, R. Dallai, M. G. Ascenzi, G. Diez-Roux and B. Franco (2011). "Ofd1 is required in limb bud patterning and endochondral bone development." Dev Biol **349**(2): 179-191.
- Birgisdottir, Å. B., T. Lamark and T. Johansen (2013). "The LIR motif – crucial for selective autophagy." Journal of Cell Science **126**(15): 3237-3247.
- Bisschoff, I. J., C. Zeschning, D. Horn, B. Wellek, A. Rieß, M. Wessels, P. Willems, P. Jensen, A. Busche, J. Bekkebraten, M. Chopra, H. D. Hove, C. Evers, K. Heimdal, A.-S. Kaiser, E. Kunstmann, K. L. Robinson, M. Linné, P. Martin, J. McGrath, W. Pradel, T. E. Prescott, B. Roesler, G. Rudolf, U. Siebers-Renelt, N. Tyshchenko, D. Wiczorek, G. Wolff, W. B. Dobyns and D. J. Morris-Rosendahl (2013). "Novel mutations including deletions of the entire OFD1 gene in 30 families with type I orofacioidigital syndrome: a study of the extensive clinical variability." Human mutation **34**(1): 237-247.

- Bjorkoy, G., T. Lamark, S. Pankiv, A. Overvatn, A. Brech and T. Johansen (2009). "Monitoring autophagic degradation of p62/SQSTM1." Methods Enzymol **452**: 181-197.
- Boehlke, C., F. Kotsis, V. Patel, S. Braeg, H. Voelker, S. Brecht, T. Beyer, H. Janusch, C. Hamann, M. Godel, K. Muller, M. Herbst, M. Hornung, M. Doerken, M. Kottgen, R. Nitschke, P. Igarashi, G. Walz and E. W. Kuehn (2010). "Primary cilia regulate mTORC1 activity and cell size through Lkb1." Nat Cell Biol **12**(11): 1115-1122.
- Bruel, A. L., B. Franco, Y. Duffourd, J. Thevenon, L. Jego, E. Lopez, J. F. Deleuze, D. Doummar, R. H. Giles, C. A. Johnson, M. A. Huynen, V. Chevrier, L. Burglen, M. Morleo, I. Desguerrès, G. Pierquin, B. Doray, B. Gilbert-Dussardier, B. Reversade, E. Steichen-Gersdorf, C. Baumann, I. Panigrahi, A. Fargeot-Espaliat, A. Dieux, A. David, A. Goldenberg, E. Bongers, D. Gaillard, J. Argente, B. Aral, N. Gigot, J. St-Onge, D. Birnbaum, S. R. Phadke, V. Cormier-Daire, T. Eguether, G. J. Pazour, V. Herranz-Perez, J. S. Goldstein, L. Pasquier, P. Loget, S. Saunier, A. Megarbane, O. Rosnet, M. R. Leroux, J. B. Wallingford, O. E. Blacque, M. V. Nachury, T. Attie-Bitach, J. B. Riviere, L. Faivre and C. Thauvin-Robinet (2017). "Fifteen years of research on oral-facial-digital syndromes: from 1 to 16 causal genes." J Med Genet **54**(6): 371-380.
- Budny, B., W. Chen, H. Omran, M. Fliegauf, A. Tzschach, M. Wisniewska, L. R. Jensen, M. Raynaud, S. A. Shoichet, M. Badura, S. Lenzner, A. Latos-Bielenska and H. H. Ropers (2006). "A novel X-linked recessive mental retardation syndrome comprising macrocephaly and ciliary dysfunction is allelic to oral-facial-digital type I syndrome." Hum Genet **120**(2): 171-178.
- Cardenas-Rodriguez, M. and J. L. Badano (2009). "Ciliary biology: understanding the cellular and genetic basis of human ciliopathies." Am J Med Genet C Semin Med Genet **151c**(4): 263-280.
- Chang, M.-Y., T.-L. Ma, C.-C. Hung, Y.-C. Tian, Y.-C. Chen, C.-W. Yang and Y.-C. Cheng (2017). "Metformin Inhibits Cyst Formation in a Zebrafish Model of Polycystin-2 Deficiency." Scientific Reports **7**: 7161.
- Chen, Y., S. Yue, L. Xie, X.-h. Pu, T. Jin and S. Y. Cheng (2011). "Dual Phosphorylation of Suppressor of Fused (Sufu) by PKA and GSK3 $\beta$  Regulates Its Stability and Localization in the Primary Cilium." Journal of Biological Chemistry **286**(15): 13502-13511.
- Christensen, S. T., I. R. Veland, A. Schwab, M. Cammer and P. Satir (2013). "Analysis of primary cilia in directional cell migration in fibroblasts." Methods Enzymol **525**: 45-58.
- Cinque, L., A. Forrester, R. Bartolomeo, M. Svelto, R. Venditti, S. Montefusco, E. Polishchuk, E. Nusco, A. Rossi, D. L. Medina, R. Polishchuk, M. A. De Matteis and C. Settembre (2015). "FGF signalling regulates bone growth through autophagy." Nature **528**: 272.
- Clement, C. A., S. G. Kristensen, K. Møllgård, G. J. Pazour, B. K. Yoder, L. A. Larsen and S. T. Christensen (2009). "The primary cilium coordinates early cardiogenesis and hedgehog signaling in cardiomyocyte differentiation." Journal of Cell Science **122**(17): 3070-3082.

- Cloonan, S. M., H. C. Lam, S. W. Ryter and A. M. Choi (2014). "Ciliophagy": The consumption of cilia components by autophagy." Autophagy **10**(3): 532-534.
- Cookson, M. R. (2012). "Parkinsonism Due to Mutations in PINK1, Parkin, and DJ-1 and Oxidative Stress and Mitochondrial Pathways." Cold Spring Harbor Perspectives in Medicine **2**(9): a009415.
- Czarnecki, P. G. and J. V. Shah (2012). "The ciliary transition zone: from morphology and molecules to medicine." Trends Cell Biol **22**(4): 201-210.
- D'Angelo, A., A. De Angelis, B. Avallone, I. Piscopo, R. Tammaro, M. Studer and B. Franco (2012). "Ofd1 controls dorso-ventral patterning and axoneme elongation during embryonic brain development." PLoS One **7**(12): e52937.
- de Conciliis, L., A. Marchitello, M. C. Wapenaar, G. Borsani, S. Giglio, M. Mariani, G. G. Consalez, O. Zuffardi, B. Franco, A. Ballabio and S. Banfi (1998). "Characterization of Cxorf5 (71-7A), a novel human cDNA mapping to Xp22 and encoding a protein containing coiled-coil alpha-helical domains." Genomics **51**(2): 243-250.
- Debnath, J., E. H. Baehrecke and G. Kroemer (2005). "Does autophagy contribute to cell death?" Autophagy **1**(2): 66-74.
- Del Giudice, E., M. Macca, F. Imperati, A. D'Amico, P. Parent, L. Pasquier, V. Layet, S. Lyonnet, V. Stamboul-Darmency, C. Thauvin-Robinet and B. Franco (2014). "CNS involvement in OFD1 syndrome: a clinical, molecular, and neuroimaging study." Orphanet Journal of Rare Diseases **9**: 74-74.
- Di Bartolomeo, S., M. Corazzari, F. Nazio, S. Oliverio, G. Lisi, M. Antonioli, V. Pagliarini, S. Matteoni, C. Fuoco, L. Giunta, M. D'Amelio, R. Nardacci, A. Romagnoli, M. Piacentini, F. Cecconi and G. M. Fimia (2010). "The dynamic interaction of AMBRA1 with the dynein motor complex regulates mammalian autophagy." The Journal of Cell Biology **191**(1): 155-168.
- Di Gioia, S. A., S. J. Letteboer, C. Kostic, D. Bandah-Rozenfeld, L. Hetterschijt, D. Sharon, Y. Arsenijevic, R. Roepman and C. Rivolta (2012). "FAM161A, associated with retinitis pigmentosa, is a component of the cilia-basal body complex and interacts with proteins involved in ciliopathies." Hum Mol Genet **21**(23): 5174-5184.
- Di Marcotullio, L., E. Ferretti, A. Greco, E. De Smaele, A. Po, M. A. Sico, M. Alimandi, G. Giannini, M. Maroder, I. Screpanti and A. Gulino (2006). "Numb is a suppressor of Hedgehog signalling and targets Gli1 for Itch-dependent ubiquitination." Nat Cell Biol **8**(12): 1415-1423.
- Dikic, I. and Z. Elazar (2018). "Mechanism and medical implications of mammalian autophagy." Nature Reviews Molecular Cell Biology **19**(6): 349-364.
- Doherty, D. (2009). "Joubert syndrome: insights into brain development, cilium biology and complex disease." Seminars in pediatric neurology **16**(3): 143-154.
- Dooley, Hannah C., M. Razi, Hannah E. J. Polson, Stephen E. Girardin, Michael I. Wilson and Sharon A. Tooze (2014). "WIPI2 Links LC3 Conjugation with PI3P, Autophagosome Formation, and Pathogen Clearance by Recruiting Atg12-5-16L1." Molecular Cell **55**(2): 238-252.

- Doyon, Y. and J. Cote (2004). "The highly conserved and multifunctional NuA4 HAT complex." Curr Opin Genet Dev **14**(2): 147-154.
- Egan, D. F., M. G. Chun, M. Vamos, H. Zou, J. Rong, C. J. Miller, H. J. Lou, D. Raveendra-Panickar, C. C. Yang, D. J. Sheffler, P. Teriete, J. M. Asara, B. E. Turk, N. D. Cosford and R. J. Shaw (2015). "Small Molecule Inhibition of the Autophagy Kinase ULK1 and Identification of ULK1 Substrates." Mol Cell **59**(2): 285-297.
- Egan, D. F., D. B. Shackelford, M. M. Mihaylova, S. Gelino, R. A. Kohnz, W. Mair, D. S. Vasquez, A. Joshi, D. M. Gwinn, R. Taylor, J. M. Asara, J. Fitzpatrick, A. Dillin, B. Viollet, M. Kundu, M. Hansen and R. J. Shaw (2011). "Phosphorylation of ULK1 (hATG1) by AMP-Activated Protein Kinase Connects Energy Sensing to Mitophagy." Science **331**(6016): 456-461.
- Emes, R. D. and C. P. Ponting (2001). "A new sequence motif linking lissencephaly, Treacher Collins and oral-facial-digital type 1 syndromes, microtubule dynamics and cell migration." Hum Mol Genet **10**(24): 2813-2820.
- Ennis, H. L. and M. Lubin (1964). "Cycloheximide: Aspects of Inhibition of Protein Synthesis in Mammalian Cells." Science **146**(3650): 1474-1476.
- Feather, S. A., P. J. Winyard, S. Dodd and A. S. Woolf (1997). "Oral-facial-digital syndrome type 1 is another dominant polycystic kidney disease: clinical, radiological and histopathological features of a new kindred." Nephrol Dial Transplant **12**(7): 1354-1361.
- Feather, S. A., A. S. Woolf, D. Donnai, S. Malcolm and R. M. Winter (1997). "The oral-facial-digital syndrome type 1 (OFD1), a cause of polycystic kidney disease and associated malformations, maps to Xp22.2-Xp22.3." Hum Mol Genet **6**(7): 1163-1167.
- Feng, Y. and D. J. Klionsky (2017). "Autophagic membrane delivery through ATG9." Cell Research **27**: 161.
- Ferrante, M. I., A. Barra, J. P. Truong, S. Banfi, C. M. Disteché and B. Franco (2003). "Characterization of the OFD1/Ofd1 genes on the human and mouse sex chromosomes and exclusion of Ofd1 for the Xpl mouse mutant." Genomics **81**(6): 560-569.
- Ferrante, M. I., S. A. Feather, A. Bulfone, V. Wright, M. Ghiani, A. Selicorni, L. Gammara, F. Scolari, A. S. Woolf, O. Sylvie, L. M. Bernard, S. Malcolm, R. Winter, A. Ballabio, G. Giorgio and B. Franco (2001). "Identification of the Gene for Oral-Facial-Digital Type I Syndrome." The American Journal of Human Genetics **68**(3): 569-576.
- Ferrante, M. I., A. Zullo, A. Barra, S. Bimonte, N. Messaddeq, M. Studer, P. Dolle and B. Franco (2006). "Oral-facial-digital type I protein is required for primary cilia formation and left-right axis specification." Nat Genet **38**(1): 112-117.
- Franco, B. and C. Thauvin-Robinet (2016). "Update on oral-facial-digital syndromes (OFDS)." Cilia **5**: 12.



- Ganley, I. G., D. H. Lam, J. Wang, X. Ding, S. Chen and X. Jiang (2009). "ULK1-ATG13-FIP200 Complex Mediates mTOR Signaling and Is Essential for Autophagy." Journal of Biological Chemistry **284**(18): 12297-12305.
- Gao, C., W. Cao, L. Bao, W. Zuo, G. Xie, T. Cai, W. Fu, J. Zhang, W. Wu, X. Zhang and Y.-G. Chen (2010). "Autophagy negatively regulates Wnt signalling by promoting Dishevelled degradation." Nature Cell Biology **12**: 781.
- Gerlitz, G., E. Darhin, G. Giorgio, B. Franco and O. Reiner (2005). "Novel Functional Features of the LIS-H Domain: Role in Protein Dimerization, Half-Life and Cellular Localization." Cell Cycle **4**(11): 1632-1640.
- Giorgio, G., M. Alfieri, C. Prattichizzo, A. Zullo, S. Cairo and B. Franco (2007). "Functional Characterization of the OFD1 Protein Reveals a Nuclear Localization and Physical Interaction with Subunits of a Chromatin Remodeling Complex." Molecular Biology of the Cell **18**(11): 4397-4404.
- Goetz, S. C. and K. V. Anderson (2010). "The Primary Cilium: A Signaling Center During Vertebrate Development." Nature reviews. Genetics **11**(5): 331-344.
- Goilav, B. (2011). "Apoptosis in polycystic kidney disease." Biochim Biophys Acta **1812**(10): 1272-1280.
- Gong, C., C. Bauvy, G. Tonelli, W. Yue, C. Deloménie, V. Nicolas, Y. Zhu, V. Domergue, V. Marin-Esteban, H. Tharinger, L. Delbos, H. Gary-Gouy, A. P. Morel, S. Ghavami, E. Song, P. Codogno and M. Mehrpour (2012). "Beclin 1 and autophagy are required for the tumorigenicity of breast cancer stem-like/progenitor cells." Oncogene **32**: 2261.
- Grumati, P., G. Morozzi, S. Hölper, M. Mari, M.-L. I. E. Harwardt, R. Yan, S. Müller, F. Reggiori, M. Heilemann and I. Dikic (2017). "Full length RTN3 regulates turnover of tubular endoplasmic reticulum via selective autophagy." eLife **6**: e25555.
- Hamasaki, M., N. Furuta, A. Matsuda, A. Nezu, A. Yamamoto, N. Fujita, H. Oomori, T. Noda, T. Haraguchi, Y. Hiraoka, A. Amano and T. Yoshimori (2013). "Autophagosomes form at ER-mitochondria contact sites." Nature **495**(7441): 389-393.
- Hara, T., A. Takamura, C. Kishi, S.-i. Iemura, T. Natsume, J.-L. Guan and N. Mizushima (2008). "FIP200, a ULK-interacting protein, is required for autophagosome formation in mammalian cells." The Journal of Cell Biology **181**(3): 497-510.
- Harris, P. C. and V. E. Torres (2009). "Polycystic kidney disease." Annu Rev Med **60**: 321-337.
- Hartleben, B., M. Godel, C. Meyer-Schwesinger, S. Liu, T. Ulrich, S. Kobler, T. Wiech, F. Grahammer, S. J. Arnold, M. T. Lindenmeyer, C. D. Cohen, H. Pavenstadt, D. Kerjaschki, N. Mizushima, A. S. Shaw, G. Walz and T. B. Huber (2010). "Autophagy influences glomerular disease susceptibility and maintains podocyte homeostasis in aging mice." J Clin Invest **120**(4): 1084-1096.

- Hayashi, S. and A. P. McMahon (2002). "Efficient recombination in diverse tissues by a tamoxifen-inducible form of Cre: a tool for temporally regulated gene activation/inactivation in the mouse." Dev Biol **244**(2): 305-318.
- Hernandez-Hernandez, V., P. Pravincumar, A. Diaz-Font, H. May-Simera, D. Jenkins, M. Knight and P. L. Beales (2013). "Bardet–Biedl syndrome proteins control the cilia length through regulation of actin polymerization." Human Molecular Genetics **22**(19): 3858-3868.
- Hildebrandt, F., M. Attanasio and E. Otto (2009). "Nephronophthisis: Disease Mechanisms of a Ciliopathy." Journal of the American Society of Nephrology : JASN **20**(1): 23-35.
- Hopp, K., C. J. Ward, C. J. Hommerding, S. H. Nasr, H. F. Tuan, V. G. Gainullin, S. Rossetti, V. E. Torres and P. C. Harris (2012). "Functional polycystin-1 dosage governs autosomal dominant polycystic kidney disease severity." J Clin Invest **122**(11): 4257-4273.
- Hosokawa, N., T. Hara, T. Kaizuka, C. Kishi, A. Takamura, Y. Miura, S.-i. Iemura, T. Natsume, K. Takehana, N. Yamada, J.-L. Guan, N. Oshiro and N. Mizushima (2009). "Nutrient-dependent mTORC1 Association with the ULK1–Atg13–FIP200 Complex Required for Autophagy." Molecular Biology of the Cell **20**(7): 1981-1991.
- Hosokawa, N., T. Sasaki, S.-i. Iemura, T. Natsume, T. Hara and N. Mizushima (2009). "Atg101, a novel mammalian autophagy protein interacting with Atg13." Autophagy **5**(7): 973-979.
- Iaconis, D., M. Monti, M. Renda, A. van Koppen, R. Tammaro, M. Chiaravalli, F. Cozzolino, P. Pignata, C. Crina, P. Pucci, A. Boletta, V. Belcastro, R. H. Giles, E. M. Surace, S. Gallo, M. Pende and B. Franco (2017). "The centrosomal OFD1 protein interacts with the translation machinery and regulates the synthesis of specific targets." Scientific Reports **7**(1): 1224.
- Ichimura, Y., T. Kirisako, T. Takao, Y. Satomi, Y. Shimonishi, N. Ishihara, N. Mizushima, I. Tanida, E. Kominami, M. Ohsumi, T. Noda and Y. Ohsumi (2000). "A ubiquitin-like system mediates protein lipidation." Nature **408**(6811): 488-492.
- Irigoín, F. and J. L. Badano (2011). "Keeping the Balance Between Proliferation and Differentiation: The Primary Cilium." Current Genomics **12**(4): 285-297.
- Itakura, E., C. Kishi, K. Inoue and N. Mizushima (2008). "Beclin 1 forms two distinct phosphatidylinositol 3-kinase complexes with mammalian Atg14 and UVRAG." Mol Biol Cell **19**(12): 5360-5372.
- Jackson, P. K. (2018). "EZH2 Inactivates Primary Cilia to Activate Wnt and Drive Melanoma." Cancer Cell **34**(1): 3-5.
- Jacomin, A.-C., S. Samavedam, V. Promponas and I. P. Nezis (2016). "iLIR database: A web resource for LIR motif-containing proteins in eukaryotes." Autophagy **12**(10): 1945-1953.
- Jang, J., Y. Wang, Matthew A. Lalli, E. Guzman, Sirie E. Godshalk, H. Zhou and Kenneth S. Kosik (2016). "Primary Cilium–Autophagy–Nrf2 (PAN) Axis Activation Commits Human Embryonic Stem Cells to a Neuroectoderm Fate." Cell **165**(2): 410-420.

- Janke, C. and M. Kneussel (2010). "Tubulin post-translational modifications: encoding functions on the neuronal microtubule cytoskeleton." Trends Neurosci **33**(8): 362-372.
- Jerman, S., H. H. Ward, R. Lee, C. A. M. Lopes, A. M. Fry, M. MacDougall and A. Wandinger-Ness (2014). "OFD1 and Flotillins Are Integral Components of a Ciliary Signaling Protein Complex Organized by Polycystins in Renal Epithelia and Odontoblasts." PLoS ONE **9**(9): e106330.
- Joachim, J., M. Razi, D. Judith, M. Wirth, E. Calamita, V. Encheva, B. D. Dynlacht, A. P. Snijders, N. O'Reilly, H. B. J. Jefferies and S. A. Tooze (2017). "Centriolar Satellites Control GABARAP Ubiquitination and GABARAP-Mediated Autophagy." Current Biology **27**(14): 2123-2136.e2127.
- Jones, C. and P. Chen (2008). "Primary Cilia in Planar Cell Polarity Regulation of the Inner Ear." Current topics in developmental biology **85**: 197-224.
- Jung, C. H., C. B. Jun, S.-H. Ro, Y.-M. Kim, N. M. Otto, J. Cao, M. Kundu and D.-H. Kim (2009). "ULK-Atg13-FIP200 Complexes Mediate mTOR Signaling to the Autophagy Machinery." Molecular Biology of the Cell **20**(7): 1992-2003.
- Jung, C. H., S.-H. Ro, J. Cao, N. M. Otto and D.-H. Kim (2010). "mTOR regulation of autophagy." FEBS letters **584**(7): 1287-1295.
- Kalvari, I., S. Tsompanis, N. C. Mulakkal, R. Osgood, T. Johansen, I. P. Nezis and V. J. Promponas (2014). "iLIR: A web resource for prediction of Atg8-family interacting proteins." Autophagy **10**(5): 913-925.
- Kamada, Y., T. Funakoshi, T. Shintani, K. Nagano, M. Ohsumi and Y. Ohsumi (2000). "Tor-Mediated Induction of Autophagy via an Apg1 Protein Kinase Complex." The Journal of Cell Biology **150**(6): 1507-1513.
- Karanasios, E., E. Stapleton, M. Manifava, T. Kaizuka, N. Mizushima, S. A. Walker and N. T. Ktistakis (2013). "Dynamic association of the ULK1 complex with omegasomes during autophagy induction." Journal of Cell Science **126**(22): 5224-5238.
- Karantza-Wadsworth, V., S. Patel, O. Kravchuk, G. Chen, R. Mathew, S. Jin and E. White (2007). "Autophagy mitigates metabolic stress and genome damage in mammary tumorigenesis." Genes & Development **21**(13): 1621-1635.
- Kennedy, S. M., Y. Hashida and J. J. Malatack (1991). "Polycystic kidneys, pancreatic cysts, and cystadenomatous bile ducts in the oral-facial-digital syndrome type I." Arch Pathol Lab Med **115**(5): 519-523.
- Kim, E. S., J. H. Shin, S. J. Park, Y. K. Jo, J. S. Kim, I. H. Kang, J. B. Nam, D. Y. Chung, Y. Cho, E. H. Lee, J. W. Chang and D. H. Cho (2015). "Inhibition of autophagy suppresses sertraline-mediated primary ciliogenesis in retinal pigment epithelium cells." PLoS One **10**(2): e0118190.
- Kim, J., M. Kundu, B. Viollet and K. L. Guan (2011). "AMPK and mTOR regulate autophagy through direct phosphorylation of Ulk1." Nat Cell Biol **13**(2): 132-141.
- Kim, S. and B. D. Dynlacht (2013). "Assembling a primary cilium." Current opinion in cell biology **25**(4): 506-511.

- Kim, Y. M., C. H. Jung, M. Seo, E. K. Kim, J. M. Park, S. S. Bae and D. H. Kim (2015). "mTORC1 phosphorylates UVRAG to negatively regulate autophagosome and endosome maturation." Mol Cell **57**(2): 207-218.
- Kimura, T., Y. Takabatake, A. Takahashi, J. Y. Kaimori, I. Matsui, T. Namba, H. Kitamura, F. Niimura, T. Matsusaka, T. Soga, H. Rakugi and Y. Isaka (2011). "Autophagy protects the proximal tubule from degeneration and acute ischemic injury." J Am Soc Nephrol **22**(5): 902-913.
- Komatsu, M., S. Waguri, T. Ueno, J. Iwata, S. Murata, I. Tanida, J. Ezaki, N. Mizushima, Y. Ohsumi, Y. Uchiyama, E. Kominami, K. Tanaka and T. Chiba (2005). "Impairment of starvation-induced and constitutive autophagy in *Atg7*-deficient mice." The Journal of Cell Biology **169**(3): 425-434.
- Kuma, A., M. Hatano, M. Matsui, A. Yamamoto, H. Nakaya, T. Yoshimori, Y. Ohsumi, T. Tokuhiya and N. Mizushima (2004). "The role of autophagy during the early neonatal starvation period." Nature **432**(7020): 1032-1036.
- Lamark, T., V. Kirkin, I. Dikic and T. Johansen (2009). "NBR1 and p62 as cargo receptors for selective autophagy of ubiquitinated targets." Cell Cycle **8**(13): 1986-1990.
- Lehtreck, K. F. (2015). "IFT-Cargo Interactions and Protein Transport in Cilia." Trends Biochem Sci **40**(12): 765-778.
- Lee, K. L., M. D. Guevarra, A. M. Nguyen, M. C. Chua, Y. Wang and C. R. Jacobs (2015). "The primary cilium functions as a mechanical and calcium signaling nexus." Cilia **4**: 7.
- Lee, S. H. and S. Somlo (2014). "Cyst growth, polycystins, and primary cilia in autosomal dominant polycystic kidney disease." Kidney Research and Clinical Practice **33**(2): 73-78.
- Levine, B. and V. Deretic (2007). "Unveiling the roles of autophagy in innate and adaptive immunity." Nature Reviews Immunology **7**: 767.
- Liu, C.-C., Y.-C. Lin, Y.-H. Chen, C.-M. Chen, L.-Y. Pang, H.-A. Chen, P.-R. Wu, M.-Y. Lin, S.-T. Jiang, T.-F. Tsai and R.-H. Chen (2016). "Cul3-KLHL20 Ubiquitin Ligase Governs the Turnover of ULK1 and VPS34 Complexes to Control Autophagy Termination." Molecular Cell **61**(1): 84-97.
- Liu, S., B. Hartleben, O. Kretz, T. Wiech, P. Igarashi, N. Mizushima, G. Walz and T. B. Huber (2012). "Autophagy plays a critical role in kidney tubule maintenance, aging and ischemia-reperfusion injury." Autophagy **8**(5): 826-837.
- Lopes, C. A., S. L. Prosser, L. Romio, R. A. Hirst, C. O'Callaghan, A. S. Woolf and A. M. Fry (2011). "Centriolar satellites are assembly points for proteins implicated in human ciliopathies, including oral-facial-digital syndrome 1." J Cell Sci **124**(Pt 4): 600-612.
- Lopes, C. A. M., S. L. Prosser, L. Romio, R. A. Hirst, C. O'Callaghan, A. S. Woolf and A. M. Fry (2011). "Centriolar satellites are assembly points for proteins implicated in human ciliopathies, including oral-facial-digital syndrome 1." Journal of Cell Science **124**(4): 600-612.

Lu, Z., R. Z. Luo, Y. Lu, X. Zhang, Q. Yu, S. Khare, S. Kondo, Y. Kondo, Y. Yu, G. B. Mills, W. S. Liao and R. C. Bast, Jr. (2008). "The tumor suppressor gene ARHI regulates autophagy and tumor dormancy in human ovarian cancer cells." J Clin Invest **118**(12): 3917-3929.

Macca, M. and B. Franco (2009). "The molecular basis of oral-facial-digital syndrome, type 1." Am J Med Genet C Semin Med Genet **151c**(4): 318-325.

Masyuk, A. I., T. V. Masyuk, M. J. Lorenzo Pisarello, J. Ding, L. Loarca, B. Q. Huang and N. F. LaRusso (2017). "Cholangiocyte autophagy contributes to hepatic cystogenesis in polycystic liver disease and represents a potential therapeutic target." Hepatology **67**(3): 1088-1108.

Matsunaga, K., E. Morita, T. Saitoh, S. Akira, N. T. Ktistakis, T. Izumi, T. Noda and T. Yoshimori (2010). "Autophagy requires endoplasmic reticulum targeting of the PI3-kinase complex via Atg14L." J Cell Biol **190**(4): 511-521.

Mayor, T., P. Meraldi, Y. D. Stierhof, E. A. Nigg and A. M. Fry (1999). "Protein kinases in control of the centrosome cycle." FEBS Lett **452**(1-2): 92-95.

Mizushima, N. (2005). "The pleiotropic role of autophagy: from protein metabolism to bactericide." Cell Death And Differentiation **12**: 1535.

Mizushima, N. (2007). "Autophagy: process and function." Genes Dev **21**(22): 2861-2873.

Mizushima, N., A. Yamamoto, M. Matsui, T. Yoshimori and Y. Ohsumi (2004). "In Vivo Analysis of Autophagy in Response to Nutrient Starvation Using Transgenic Mice Expressing a Fluorescent Autophagosome Marker." Molecular Biology of the Cell **15**(3): 1101-1111.

Moreau, K., S. Luo and D. C. Rubinsztein (2010). "Cytoprotective roles for autophagy." Current Opinion in Cell Biology **22**(2): 206-211.

Morleo, M. and B. Franco (2008). "Dosage compensation of the mammalian X chromosome influences the phenotypic variability of X-linked dominant male-lethal disorders." J Med Genet **45**(7): 401-408.

Murdoch, J. N. and A. J. Copp (2010). "The relationship between sonic Hedgehog signaling, cilia, and neural tube defects." Birth Defects Res A Clin Mol Teratol **88**(8): 633-652.

Nagy, A. (2000). "Cre recombinase: the universal reagent for genome tailoring." Genesis **26**(2): 99-109.

Nair, U., W.-L. Yen, M. Mari, Y. Cao, Z. Xie, M. Baba, F. Reggiori and D. J. Klionsky (2012). "A role for Atg8-PE deconjugation in autophagosome biogenesis." Autophagy **8**(5): 780-793.

Nakai, A., O. Yamaguchi, T. Takeda, Y. Higuchi, S. Hikoso, M. Taniike, S. Omiya, I. Mizote, Y. Matsumura, M. Asahi, K. Nishida, M. Hori, N. Mizushima and K. Otsu (2007). "The role of autophagy in cardiomyocytes in the basal state and in response to hemodynamic stress." Nature Medicine **13**: 619.

Nascimbeni, A. C., F. Giordano, N. Dupont, D. Grasso, M. I. Vaccaro, P. Codogno and E. Morel (2017). "ER-plasma membrane contact sites contribute to autophagosome biogenesis by regulation of local PI3P synthesis." Embo j **36**(14): 2018-2033.

Nauli, S. M., F. J. Alenghat, Y. Luo, E. Williams, P. Vassilev, X. Li, A. E. Elia, W. Lu, E. M. Brown, S. J. Quinn, D. E. Ingber and J. Zhou (2003). "Polycystins 1 and 2 mediate mechanosensation in the primary cilium of kidney cells." Nat Genet **33**(2): 129-137.

Nazio, F., M. Carinci, C. Valacca, P. Bielli, F. Strappazon, M. Antonioli, F. Ciccocanti, C. Rodolfo, S. Campello, G. M. Fimia, C. Sette, P. Bonaldo and F. Cecconi (2016). "Fine-tuning of ULK1 mRNA and protein levels is required for autophagy oscillation." The Journal of Cell Biology **215**(6): 841-856.

Nazio, F., F. Strappazon, M. Antonioli, P. Bielli, V. Cianfanelli, M. Bordi, C. Gretzmeier, J. Dengjel, M. Piacentini, G. M. Fimia and F. Cecconi (2013). "mTOR inhibits autophagy by controlling ULK1 ubiquitylation, self-association and function through AMBRA1 and TRAF6." Nature Cell Biology **15**: 406.

Nigg, E. A. and T. Stearns (2011). "The centrosome cycle: Centriole biogenesis, duplication and inherent asymmetries." Nat Cell Biol **13**(10): 1154-1160.

Noda, K., M. Kitami, K. Kitami, M. Kaku and Y. Komatsu (2016). "Canonical and noncanonical intraflagellar transport regulates craniofacial skeletal development." Proceedings of the National Academy of Sciences of the United States of America **113**(19): E2589-E2597.

Nollet, M., S. Santucci-Darmanin, V. Breuil, R. Al-Sahlane, C. Cros, M. Topi, D. Momier, M. Samson, S. Pagnotta, L. Cailleateau, S. Battaglia, D. Farlay, R. Dacquin, N. Barois, P. Jurdic, G. Boivin, D. Heymann, F. Lafont, S. S. Lu, D. W. Dempster, G. F. Carle and V. Pierrefite-Carle (2014). "Autophagy in osteoblasts is involved in mineralization and bone homeostasis." Autophagy **10**(11): 1965-1977.

O'Toole, J. F., Y. Liu, E. E. Davis, C. J. Westlake, M. Attanasio, E. A. Otto, D. Seelow, G. Nurnberg, C. Becker, M. Nuutinen, M. Kärppä, J. Ignatius, J. Uusimaa, S. Pakanen, E. Jaakkola, L. P. van den Heuvel, H. Fehrenbach, R. Wiggins, M. Goyal, W. Zhou, M. T. F. Wolf, E. Wise, J. Helou, S. J. Allen, C. A. Murga-Zamalloa, S. Ashraf, M. Chaki, S. Heeringa, G. Chernin, B. E. Hoskins, H. Chaib, J. Gleeson, T. Kusakabe, T. Suzuki, R. E. Isaac, L. M. Quarmby, B. Tennant, H. Fujioka, H. Tuominen, I. Hassinen, H. Lohi, J. L. van Houten, A. Rotig, J. A. Sayer, B. Rolinski, P. Freisinger, S. M. Madhavan, M. Herzer, F. Madignier, H. Prokisch, P. Nurnberg, P. Jackson, H. Khanna, N. Katsanis and F. Hildebrandt (2010). "Individuals with mutations in XPNPEP3, which encodes a mitochondrial protein, develop a nephronophthisis-like nephropathy." The Journal of Clinical Investigation **120**(3): 791-802.

Ohsumi, Y. and N. Mizushima (2004). "Two ubiquitin-like conjugation systems essential for autophagy." Seminars in Cell & Developmental Biology **15**(2): 231-236.

Ong, A. C. M. and R. Sandford (2016). Autosomal dominant polycystic kidney diseases: overview. Oxford Textbook of Clinical Nephrology. N. Turner, N. Lameire, D. J. Goldsmith et al. Oxford, Oxford University Press. **3**: 2625-2626.

- Orhon, I., N. Dupont, M. Zaidan, V. Boitez, M. Burtin, A. Schmitt, T. Capiod, A. Viau, I. Beau, E. W. Kuehn, G. Friedlander, F. Terzi and P. Codogno (2016). "Primary-cilium-dependent autophagy controls epithelial cell volume in response to fluid flow." Nature Cell Biology **18**: 657.
- Pampliega, O., I. Orhon, B. Patel, S. Sridhar, A. Diaz-Carretero, I. Beau, P. Codogno, B. H. Satir, P. Satir and A. M. Cuervo (2013). "Functional interaction between autophagy and ciliogenesis." Nature **502**(7470): 194-200.
- Pampliega, O., I. Orhon, B. Patel, S. Sridhar, A. Díaz-Carretero, I. Beau, P. Codogno, B. H. Satir, P. Satir and A. M. Cuervo (2013). "Functional interaction between autophagy and ciliogenesis." Nature **502**: 194.
- Pema, M., L. Drusian, M. Chiaravalli, M. Castelli, Q. Yao, S. Ricciardi, S. Somlo, F. Qian, S. Biffo and A. Boletta (2016). "mTORC1-mediated inhibition of polycystin-1 expression drives renal cyst formation in tuberous sclerosis complex." Nature Communications **7**: 10786.
- Perera, R. M., S. Stoykova, B. N. Nicolay, K. N. Ross, J. Fitamant, M. Boukhali, J. Lengrand, V. Deshpande, M. K. Selig, C. R. Ferrone, J. Settleman, G. Stephanopoulos, N. J. Dyson, R. Zoncu, S. Ramaswamy, W. Haas and N. Bardeesy (2015). "Transcriptional control of autophagy-lysosome function drives pancreatic cancer metabolism." Nature **524**(7565): 361-365.
- Pitaval, A., Q. Tseng, M. Bornens and M. Théry (2010). "Cell shape and contractility regulate ciliogenesis in cell cycle–arrested cells." The Journal of Cell Biology **191**(2): 303-312.
- Plotnikova, O. V., E. N. Pugacheva and E. A. Golemis (2009). "Primary Cilia and the Cell Cycle." Methods in cell biology **94**: 137-160.
- Prattichizzo, C., M. Macca, V. Novelli, G. Giorgio, A. Barra, B. Franco and I. C. G. Oral-Facial-Digital Type (2008). "Mutational spectrum of the oral-facial-digital type I syndrome: a study on a large collection of patients." Human mutation **29**(10): 1237-1246.
- Praveen, K., E. E. Davis and N. Katsanis (2015). "Unique among ciliopathies: primary ciliary dyskinesia, a motile cilia disorder." F1000Prime Reports **7**: 36.
- Prodromou, N. V., C. L. Thompson, D. P. Osborn, K. F. Cogger, R. Ashworth, M. M. Knight, P. L. Beales and J. P. Chapple (2012). "Heat shock induces rapid resorption of primary cilia." J Cell Sci **125**(Pt 18): 4297-4305.
- Qi, S., Do J. Kim, G. Stjepanovic and James H. Hurley (2015). "Structure of the Human Atg13-Atg101 HORMA Heterodimer: an Interaction Hub within the ULK1 Complex." Structure **23**(10): 1848-1857.
- Rautou, P.-E., A. Mansouri, D. Lebecq, F. Durand, D. Valla and R. Moreau (2010). "Autophagy in liver diseases." Journal of Hepatology **53**(6): 1123-1134.
- Ravichandran, K. and C. L. Edelstein (2014). "Polycystic Kidney Disease: A Case of Suppressed Autophagy?" Seminars in Nephrology **34**(1): 27-33.

- Ravikumar, B., R. Duden and D. C. Rubinsztein (2002). "Aggregate-prone proteins with polyglutamine and polyalanine expansions are degraded by autophagy." Human Molecular Genetics **11**(9): 1107-1117.
- Reiter, J. F. and M. R. Leroux (2017). "Genes and molecular pathways underpinning ciliopathies." Nat Rev Mol Cell Biol **18**(9): 533-547.
- Reiter, J. F. and M. R. Leroux (2017). "Genes and molecular pathways underpinning ciliopathies." Nature Reviews Molecular Cell Biology **18**: 533.
- Rohatgi, R. and W. J. Snell (2010). "The ciliary membrane." Curr Opin Cell Biol **22**(4): 541-546.
- Romio, L., A. M. Fry, P. J. Winyard, S. Malcolm, A. S. Woolf and S. A. Feather (2004). "OFD1 is a centrosomal/basal body protein expressed during mesenchymal-epithelial transition in human nephrogenesis." J Am Soc Nephrol **15**(10): 2556-2568.
- Roy, S. (2009). "The motile cilium in development and disease: emerging new insights." Bioessays **31**(7): 694-699.
- Rui, Y. N., Z. Xu, B. Patel, Z. Chen, D. Chen, A. Tito, G. David, Y. Sun, E. F. Stimming, H. J. Bellen, A. M. Cuervo and S. Zhang (2015). "Huntingtin functions as a scaffold for selective macroautophagy." Nat Cell Biol **17**(3): 262-275.
- Russell, R. C., Y. Tian, H. Yuan, H. W. Park, Y.-Y. Chang, J. Kim, H. Kim, T. P. Neufeld, A. Dillin and K.-L. Guan (2013). "ULK1 induces autophagy by phosphorylating Beclin-1 and activating VPS34 lipid kinase." Nature Cell Biology **15**: 741.
- Ryan, M. J., G. Johnson, J. Kirk, S. M. Fuerstenberg, R. A. Zager and B. Torok-Storb (1994). "HK-2: an immortalized proximal tubule epithelial cell line from normal adult human kidney." Kidney Int **45**(1): 48-57.
- Satir, P. and S. T. Christensen (2007). "Overview of structure and function of mammalian cilia." Annu Rev Physiol **69**: 377-400.
- Satir, P., L. B. Pedersen and S. T. Christensen (2010). "The primary cilium at a glance." J Cell Sci **123**(Pt 4): 499-503.
- Seeger-Nukpezah, T., D. M. Geynisman, A. S. Nikonova, T. Benzing and E. A. Golemis (2015). "The hallmarks of cancer: relevance to the pathogenesis of polycystic kidney disease." Nat Rev Nephrol **11**(9): 515-534.
- Seeley, E. S., C. Carrière, T. Goetze, D. S. Longnecker and M. Korc (2009). "Pancreatic Cancer and Precursor PanIN Lesions Are Devoid of Primary Cilia." Cancer research **69**(2): 422-430.
- Serra, A. L., D. Poster, A. D. Kistler, F. Krauer, S. Raina, J. Young, K. M. Rentsch, K. S. Spanaus, O. Senn, P. Kristanto, H. Scheffel, D. Weishaupt and R. P. Wuthrich (2010). "Sirolimus and kidney growth in autosomal dominant polycystic kidney disease." N Engl J Med **363**(9): 820-829.



- Shi, R., J. Weng, L. Zhao, X.-M. Li, T.-M. Gao and J. Kong (2012). "Excessive Autophagy Contributes to Neuron Death in Cerebral Ischemia." CNS Neuroscience & Therapeutics **18**(3): 250-260.
- Shin, J. H., D. J. Bae, E. S. Kim, H. B. Kim, S. J. Park, Y. K. Jo, D. S. Jo, D. G. Jo, S. Y. Kim and D. H. Cho (2015). "Autophagy Regulates Formation of Primary Cilia in Mefloquine-Treated Cells." Biomol Ther (Seoul) **23**(4): 327-332.
- Singla, V. and J. F. Reiter (2006). "The primary cilium as the cell's antenna: signaling at a sensory organelle." Science **313**(5787): 629-633.
- Singla, V., M. Romaguera-Ros, J. M. Garcia-Verdugo and J. F. Reiter (2010). "Ofd1, a human disease gene, regulates the length and distal structure of centrioles." Developmental cell **18**(3): 410-424.
- Stannard, W. and C. O'Callaghan (2006). "Ciliary function and the role of cilia in clearance." J Aerosol Med **19**(1): 110-115.
- Struchtrup, A., A. Wiegering, B. Stork, U. Rütger and C. Gerhardt (2018). "The ciliary protein RPGRIP1L governs autophagy independently of its proteasome-regulating function at the ciliary base in mouse embryonic fibroblasts." Autophagy **14**(4): 567-583.
- Takabatake, Y., T. Kimura, A. Takahashi and Y. Isaka (2014). "Autophagy and the kidney: health and disease." Nephrology Dialysis Transplantation **29**(9): 1639-1647.
- Takiar, V., S. Nishio, P. Seo-Mayer, J. D. King, H. Li, L. Zhang, A. Karihaloo, K. R. Hallows, S. Somlo and M. J. Caplan (2011). "Activating AMP-activated protein kinase (AMPK) slows renal cystogenesis." Proceedings of the National Academy of Sciences **108**(6): 2462-2467.
- Tanaka, Y., M. Watari, T. Saito, Y. Morishita and K. Ishibashi (2016). "Enhanced Autophagy in Polycystic Kidneys of AQP11 Null Mice." Int J Mol Sci **17**(12).
- Tang, Z., M. G. Lin, T. R. Stowe, S. Chen, M. Zhu, T. Stearns, B. Franco and Q. Zhong (2013). "Autophagy Promotes Primary Ciliogenesis by Removing OFD1 from Centriolar Satellites." Nature **502**(7470): 254-257.
- Thauvin-Robinet, C., S. Thomas, M. Sinico, B. Aral, L. Burglen, N. Gigot, H. Dollfus, S. Rossignol, M. Raynaud, C. Philippe, C. Badens, R. Touraine, C. Gomes, B. Franco, E. Lopez, N. Elkhartoufi, L. Faivre, A. Munnich, N. Boddaert, L. Van Maldergem, F. Encha-Razavi, S. Lyonnet, M. Vekemans, E. Escudier and T. Attie-Bitach (2013). "OFD1 mutations in males: phenotypic spectrum and ciliary basal body docking impairment." Clin Genet **84**(1): 86-90.
- Thauvin-Robinet, C., M. Cossée, V. Cormier-Daire, L. Van Maldergem, A. Toutain, Y. Alembik, E. Bieth, V. Layet, P. Parent, A. David, A. Goldenberg, G. Mortier, D. Héron, P. Sagot, A. M. Bouvier, F. Huet, V. Cusin, A. Donzel, D. Devys and J. R. Teyssier (2006). "Clinical, molecular, and genotype–phenotype correlation studies from 25 cases of oral–facial–digital syndrome type 1: a French and Belgian collaborative study." Journal of Medical Genetics **43**(1): 54-61.

Toprak, O., A. Uzum, M. Cirit, E. Esi, A. Inci, R. Ersoy, M. Tanrisev, E. Ok and B. Franco (2006). "Oral–facial–digital syndrome type 1, Caroli's disease and cystic renal disease." Nephrology Dialysis Transplantation **21**(6): 1705-1709.

Torres, V. E., A. Boletta, A. Chapman, V. Gattone, Y. Pei, Q. Qian, D. P. Wallace, T. Weimbs and R. P. Wüthrich (2010). "Prospects for mTOR Inhibitor Use in Patients with Polycystic Kidney Disease and Hamartomatous Diseases." Clinical journal of the American Society of Nephrology : CJASN **5**(7): 1312-1329.

Truebestein, L. and T. A. Leonard (2016). "Coiled-coils: The long and short of it." Bioessays **38**(9): 903-916.

Verani, R. R. and F. G. Silva (1988). "Histogenesis of the renal cysts in adult (autosomal dominant) polycystic kidney disease: a histochemical study." Mod Pathol **1**(6): 457-463.

Vora, S. M. and B. T. Phillips (2016). "The benefits of local depletion: The centrosome as a scaffold for ubiquitin-proteasome-mediated degradation." Cell Cycle **15**(16): 2124-2134.

Walz, G., K. Budde, M. Mannaa, J. Nürnberger, C. Wanner, C. Sommerer, U. Kunzendorf, B. Banas, W. H. Hörl, N. Obermüller, W. Arns, H. Pavenstädt, J. Gaedeke, M. Büchert, C. May, H. Gschaidmeier, S. Kramer and K.-U. Eckardt (2010). "Everolimus in Patients with Autosomal Dominant Polycystic Kidney Disease." New England Journal of Medicine **363**(9): 830-840.

Wang, S., M. J. Livingston, Y. Su and Z. Dong (2015). "Reciprocal regulation of cilia and autophagy via the MTOR and proteasome pathways." Autophagy **11**(4): 607-616.

Ward, C. J., D. Yuan, T. V. Masyuk, X. Wang, R. Punyashtiti, S. Whelan, R. Bacallao, R. Torra, N. F. LaRusso, V. E. Torres and P. C. Harris (2003). "Cellular and subcellular localization of the ARPKD protein; fibrocystin is expressed on primary cilia." Hum Mol Genet **12**(20): 2703-2710.

Watanabe, Y., S. Honda, A. Konishi, S. Arakawa, M. Murohashi, H. Yamaguchi, S. Torii, M. Tanabe, S. Tanaka, E. Warabi and S. Shimizu (2016). "Autophagy controls centrosome number by degrading Cep63." Nature Communications **7**: 13508.

Waters, A. M. and P. L. Beales (2011). "Ciliopathies: an expanding disease spectrum." Pediatric Nephrology (Berlin, Germany) **26**(7): 1039-1056.

Webb, T. R., D. A. Parfitt, J. C. Gardner, A. Martinez, D. Bevilacqua, A. E. Davidson, I. Zito, D. L. Thiselton, J. H. C. Ressa, M. Aperi, N. Schwarz, N. Kanuga, M. Michaelides, M. E. Cheetham, M. B. Gorin and A. J. Hardcastle (2012). "Deep intronic mutation in OFD1, identified by targeted genomic next-generation sequencing, causes a severe form of X-linked retinitis pigmentosa (RP23)." Human Molecular Genetics **21**(16): 3647-3654.

Wei, Q., K. Ling and J. Hu (2015). "The essential roles of transition fibers in the context of cilia." Current opinion in cell biology **35**: 98-105.

Wentzensen, I. M., J. J. Johnston, J. H. Patton, J. M. Graham, J. C. Sapp and L. G. Biesecker (2016). "Exome sequencing identifies a mutation in OFD1 in a male

with Joubert syndrome, orofacioidigital spectrum anomalies and complex polydactyly." Hum Genome Var **3**: 15069.

White, E. (2015). "The role for autophagy in cancer." The Journal of Clinical Investigation **125**(1): 42-46.

Wikipedia. (2018). "Centriole." Retrieved 21 August 2018, from <https://en.wikipedia.org/w/index.php?title=Centriole&oldid=848459916>.

Winyard, P. and D. Jenkins (2011). "Putative roles of cilia in polycystic kidney disease." Biochim Biophys Acta **1812**(10): 1256-1262.

Wojcik, E. J., D. M. Glover and T. S. Hays (2000). "The SCF ubiquitin ligase protein slimb regulates centrosome duplication in Drosophila." Curr Biol **10**(18): 1131-1134.

Wong, E. and A. M. Cuervo (2010). "Autophagy gone awry in neurodegenerative diseases." Nature neuroscience **13**(7): 805-811.

Wu, Y., S. Cheng, H. Zhao, W. Zou, S. Yoshina, S. Mitani, H. Zhang and X. Wang (2014). "PI3P phosphatase activity is required for autophagosome maturation and autolysosome formation." EMBO Rep **15**(9): 973-981.

Xu, Q., W. Liu, X. Liu, W. Liu, H. Wang, G. Yao, L. Zang, T. Hayashi, S. Tashiro, S. Onodera and T. Ikejima (2016). "Silibinin negatively contributes to primary cilia length via autophagy regulated by histone deacetylase 6 in confluent mouse embryo fibroblast 3T3-L1 cells." Mol Cell Biochem **420**(1-2): 53-63.

Ye, H., X. Wang, M. M. Constans, C. R. Sussman, F. T. Chebib, M. V. Irazabal, W. F. Young, Jr., P. C. Harris, L. S. Kirschner and V. E. Torres (2017). "The regulatory 1alpha subunit of protein kinase A modulates renal cystogenesis." Am J Physiol Renal Physiol **313**(3): F677-f686.

Yildiz, O. and H. Khanna (2012). "CILINARY SIGNALING CASCADES IN PHOTORECEPTORS." Vision research **75**: 112-116.

Zachari, M. and Ian G. Ganley (2017). "The mammalian ULK1 complex and autophagy initiation." Essays In Biochemistry **61**(6): 585-596.

Zaffagnini, G. and S. Martens (2016). "Mechanisms of Selective Autophagy." Journal of Molecular Biology **428**(9Part A): 1714-1724.

Zhu, P., C. J. Sieben, X. Xu, P. C. Harris and X. Lin (2017). "Autophagy activators suppress cystogenesis in an autosomal dominant polycystic kidney disease model." Human Molecular Genetics **26**(1): 158-172.

Zullo, A., D. Iaconis, A. Barra, A. Cantone, N. Messaddeq, G. Capasso, P. Dolle, P. Igarashi and B. Franco (2010). "Kidney-specific inactivation of *Ofd1* leads to renal cystic disease associated with upregulation of the mTOR pathway." Hum Mol Genet **19**(14): 2792-2803.